Spring 2017

Mechanisms and prevention of SUDEP in Dravet Syndrome

YuJaung Kim
University of Iowa

MECHANISMS AND PREVENTION OF SUDEP IN DRAVET SYNDROME

by

YuJaung Kim

A thesis submitted in partial fulfillment
of the requirements for the Doctor of Philosophy
degree in Biomedical Engineering in the
Graduate College of
The University of Iowa

May 2017

Thesis Supervisor: Professor George B. Richerson

Graduate College
The University of Iowa
Iowa City, Iowa

CERTIFICATE OF APPROVAL

_____

PH.D. THESIS

_____

This is to certify that the Ph.D. thesis of

YuJaung Kim

has been approved by the Examining Committee for
the thesis requirement for the Doctor of Philosophy degree
in Biomedical Engineering at the May 2017 graduation.

Thesis Committee: _____
George B. Richerson, Thesis Supervisor

_____
Jose Assouline

_____
Gordon F. Buchanan

_____
Edwin L. Dove

_____
Brian K. Gehlbach

_____
Amy Lee

_____
Joseph M. Reinhardt

To my parents, SunBin Kim and HeeJaung La, for unconditional support and love. I will always remember all the efforts you have put in as my guardians and caretakers especially for last 2 years. I would like to thank to Susie's family in Cleveland, SoHee Kim, Booki Min, and Susie Min, for sharing the long journey with me and always encouraging my scientific passion. To my previous roommates, EunYoung and PaRang & Ryan, for all the time we have spent in the Rushmore place. You guys are much more than roommates during my Iowa life.

ACKNOWLEDGEMENTS

I would like to express the deepest appreciation to my thesis advisor, Dr. George Richerson, for guiding me into the interdisciplinary study. All his guidance and mentorship during my PhD project have trained me to be a better scientist.

I would like to thank my thesis committee members – Drs. Joss Assouline, Gordon Buchanan, Edwin Dove, Brian Gehlbach, Amy Lee, and Joseph Reinhardt – for encouraging all the way and making me have interest in learning through the Iowa SUDEP meeting and an individual Investigations course.

Many thanks to current and former members of the Richerson laboratory for sharing all the time in the lab for last five years. I especially want to thank Lori Smith-Mellecker, our lab manager, for her assistance for my experiments and paperwork. I appreciate Dr. Eduardo Bravo for sharing his thoughts and experiences that improves my work. I also thank Xiu Zhou for her time and effort to maintain our animal colony and genotype the numerous mice I used in my study.

And finally, last but not least, also I thank to my collaborators in the Univ. of Iowa, Dr. Toshi Kitamoto, Junko Kasuya, and Dr. YoungCho Kim for their assistance and for their collaboration during my PhD research.

ABSTRACT

Sudden unexpected death in epilepsy (SUDEP) is the most common cause of death in chronic refractory epilepsy patients. Dravet Syndrome (DS) is an infantile-onset epilepsy with severe seizures commonly due to mutations of the sodium channel gene SCN1A. DS patients have a high risk of SUDEP, but the mechanisms of death are not well defined. The principal risk factor for SUDEP is a high frequency of seizures. The recent MORTality in Epilepsy Monitoring Unit Study (MORTEMUS) reported the largest series of SUDEP cases while in Epilepsy Monitoring Units (EMUs). Most cases occurred after a generalized seizure, and were associated with both cardiac and respiratory dysfunction. None of the SUDEP cases in the MORTEMUS study had direct measurements of breathing, but visual analysis of video recording suggested that apnea occurred early in the sequence of events preceding death. Since SUDEP is always identified after death and is impossible to predict its incidence, it is not possible to run clinical trials in patients. Therefore, developing animal models of SUDEP is beneficial. In a DS mouse model with an $Scn1a^{R1407X/+}$ mutation, death occurs after spontaneous and induced seizures. This post-ictal death is likely to be relevant to the mechanisms of SUDEP in DS patients. In a previous study, electrocardiogram (EKG) recordings from DS mice have shown that post-ictal death after heat-induced seizures is due to progressive bradycardia and asystole. However, post-ictal breathing has not been measured during experiments studying post-ictal death in these mice, so it is unknown if respiratory dysfunction, such as central apnea, contributes to post-ictal death.

The first goal of this dissertation is to design and develop a mouse EMU that monitored electroencephalogram (EEG), nuchal electromyography (EMG), EKG, video,

whole body plethysmography (breathing), body temperature, room temperature, and humidity from mice until the occurrence of post-ictal death. Using a mouse EMU we sought to evaluate the primary cause of death in multiple mouse strains with seizure-induced death, and to determine whether they have a common final pathway of death. We induced seizures acutely in multiple non-epileptic mouse strains that are prone to sudden death in response to seizures: 1) maximal electroshock (MES)-induced seizures in *Lmx1b*$^{f/f/p}$ mice, 2) MES-induced seizures in C57Bl6 mice, and 3) audiogenic seizures in DBA/1 mice. These seizures caused immediate and permanent respiratory arrest (terminal apnea) in all 3 strains of mice. In each strain, EKG activity continued for 3 to 5 minutes after terminal apnea. We interpret these data as indicating that the primary cause of post-ictal death was central apnea, and the resulting hypoxia then caused bradycardia and asystole.

The second goal of this dissertation is to understand the mechanism(s) of SUDEP in DS. Here we found that DS patients have frequent post-ictal respiratory dysfunction, while cardiac activity was normal. One of these patients who had severe post-ictal hypoventilation later died of SUDEP. Also, we studied mice with an *Scn1a*$^{R1407X/+}$ mutation to determine the role of respiratory dysfunction in post-ictal death after spontaneous and acutely induced seizures. In DS mice, death occurred after spontaneous, heat-induced, and MES seizures while monitoring in a mouse EMU. Death always occurred after a severe seizure with tonic extension. We found that both non-epileptic and epileptic mice have consistently died by the same primary mechanisms of central apnea. Death could be prevented after heat-induced and MES seizures by mechanical ventilation. We conclude that the primary cause of post-ictal death was central apnea that

began during the seizures and induced secondarily bradycardia due to the hypoxia, ultimately leading to terminal asystole.

The final goal of this dissertation is to propose a new alternative dietary therapy for DS patients. Some epilepsy children with refractory seizures, especially DS patients, have been able to reduce their seizures by following a strict high-fat and low-carbohydrate ketogenic diet (KD). Although the exact anti-epileptic mechanisms of KD diet are unknown, producing ketone bodies and creating ketosis have been widely believed to contribute to the anti-epileptic effects. Our collaborator (Toshi Kitamoto, PhD, Univ. of Iowa) has found that a diet containing milk whey was able to prevent seizures in Drosophila with an orthologous sodium channel mutation. Here we tested the effect of both KD and milk whey supplementation on DS mice. Two types of KD (with and without milk additives), KD with glucose water to eliminate ketone formation, milk whey supplementation, and standard diet were administered to growing DS mice age from P16 to P60. Compared to a standard diet, all KDs, an addition of glucose water to a KD, and milk whey supplementation had beneficial effects on seizure control and prevention of post-ictal death. Compared to a standard diet, all KDs greatly elevated ketone body levels (β-hydroxybutyrate) and mice consistently weighed less, whereas the milk whey diet had no effect on ketosis or weight. The diet of addition of glucose water to the KD did not produce high ketone levels, but mice weighed less. These results demonstrate that ketone bodies are not the main reason for the anti-epileptic property of ketogenic diets.

Taken together, these data indicate it is important to obtain data on both cardiac and respiratory function to make conclusions about the mechanisms of SUDEP in both

humans and animals. Data in this dissertation show that severe post-ictal respiratory dysfunction in DS patients may play a major role in causing SUDEP, and may be a biomarker for those at highest risk. Death in DS mice with spontaneous seizures may be directly related to the mechanism of SUDEP in humans. Defining the specific mechanisms of post-ictal apnea may help to identify methods for prevention of SUDEP. We propose a SUDEP prevention strategy in DS through a new alternative diet supplemented with a milk whey compound. Milk whey supplementation of diet has a great potential to prevent post-ictal death in an economical and non-invasive manner without detrimental metabolic outcomes, such as ketosis and weight reduction. Milk whey supplementation of diet may be a new treatment to prevent SUDEP in DS patients.

PUBLIC ABSTRACT

Seizures occur when there is abnormal electrical activity in the brain, and that cause changes in attention or behavior. A single seizure can occur with any healthy person due to head injury, drugs, toxins, high fever, or lack of oxygen. Epilepsy is a chronic common neurological disorder involved with repetitive seizures. Epilepsy may occur as a result of a genetic disorder an acquired brain injury, such as tumors, trauma, infection, or stroke. 65-70% of epilepsy patients become seizure free with medications and in some cases by surgery or dietary changes, but the remaining 30-35% patients are often refractory to treatment and continue to have seizures. Most epilepsy patients live a full life span, but some these refractory epilepsy patients die suddenly without warning or other apparent medical cause. Sudden unexpected death in epilepsy (SUDEP) is the most common cause of death in chronic refractory epilepsy patients. No cause of death can be found in SUDEP, because most cases occur at night without witnesses and recordings of physiological data have rarely been obtained at the time of death. Dravet syndrome is a rare, lifelong form of epilepsy that begins in the first year of life with frequent and severe seizures. DS patients have high risk of SUDEP.

The overall goal of this thesis is to provide better understanding of the SUDEP mechanism(s) in Dravet Syndrome (DS) mice and propose a prevention strategy for SUDEP through an alternative diet composed of a milk whey compound.

TABLE OF CONTENTS

LIST OF TABLES

LIST OF FIGURES

CHAPTER 1: BACKGROUND AND SIGNIFICANCE

Introduction

Epilepsy is the fourth most common neurological disorder with a chronic condition of repeated seizures. Most epilepsy patients live a full life span, but some epilepsy patients die suddenly without warning or other apparent medical cause. Sudden unexpected death in epilepsy (SUDEP) is the most common cause of death in chronic refractory epilepsy patients. Dravet Syndrome (DS) is a severe, infantile-onset epilepsy syndrome and DS patients have a high risk of SUDEP. The principle risk factor for SUDEP is a high frequency of seizures. Therefore, SUDEP is probably a seizure-related event. No cause of death can be found in SUDEP, because most cases occur at night without witnesses and recordings of physiological data have rarely been obtained at the time of death. It is well known that seizures induce changes in respiratory and cardiac activity that can be severe, and often cause prolonged alterations of consciousness. However, a major unknown issue is whether the primary mechanism of death is cardiac or respiratory. Understanding the mechanisms underlying SUDEP from seizure to death is essential to developing effective preventive strategies. This chapter reviews the theoretical background, literatures and existing knowledge in the field of epilepsy relevant to SUDEP.

General background and literature reviews

Seizures, Epilepsy and SUDEP

Seizures are episodes of abnormal increased neuronal activity in the brain that cause abnormal sensory or motor manifestations (Kandel et al., 2000). A single seizure can occur with any healthy person under certain circumstances, such as head injury, drugs, toxins, high fever, or lack of oxygen. Usually a single seizure lasts less than 3 minutes and is not considered as epilepsy (Fisher et al., 2005). Seizures are classified according to whether the seizure origination is in part of the brain (focal seizures) or in the entire brain (primary generalized seizures). A focal seizure may spread throughout the brain, becoming a generalized seizure called a secondarily generalized seizure. Generalized seizures induce loss of consciousness and these can affect the body differently. Tonic-clonic seizures are the most common type of generalized seizures that exhibit violent body movement, first with intension whole body muscle contraction, and then alternating extension and flexion of the limbs. Myoclonic seizures are sudden, involuntary whole body muscle twitching. Atonic seizures cause sudden falling due to loss of muscle tone. Absence seizures are characterized by brief seizure activity accompanied by loss of awareness, more common in children than in adults (Bear et al., 2001; Kandel et al., 2000).

Some epilepsy patients have identifiable causes such as tumors, trauma, infection, stroke, and hereditary diseases. However, the causes of epilepsy in many patients remain unidentified (Fisher et al., 2005; Kandel et al., 2000). Epilepsy affects around 1% of the population, and about 65-70% of epilepsy patients become seizure free with antiepileptic

drugs (AED), but the remaining 30-35% are often refractory to treatment and continue to have seizures (Kwan & Sander, 2004).

SUDEP is defined as "the sudden, unexpected, witnessed or unwitnessed, non-traumatic, and non-drowning death of a patient with epilepsy patients with or without evidence of a seizure, excluding documented status epilepticus, and in which postmortem examination does not reveal a structural or toxicological cause of death" (Nashef, 1997). Epilepsy patients have a significant risk of SUDEP and it is a great concern for the epilepsy community (Devinsky et al., 2016). In patients with refractory epilepsy, SUDEP has been determined as a leading cause of death, accounting for 10-50% of all deaths (Shorvon & Tomson, 2011). The principal risk factor for SUDEP is a high frequency of seizures (Hesdorffer et al., 2011). The underlying mechanisms of SUDEP are unknown, but it is believed that most deaths occur immediately after a seizure (Ryvlin et al., 2013).

Recent research in SUDEP seems to be gaining traction around the world. A total of 796 SUDEP studies have been published in the last two decades. 668 SUDEP materials have been published in the present decade (from 2006 to 2016) (Figure 1; published materials searched in *PubMed* from 1993 to 2016; 'sudden unexpected death in epilepsy', 'SUDEP'). This increased awareness of SUDEP has ramped up efforts to identify preventative strategies for SUDEP. There are also ongoing investigations of SUDEP mechanisms by basic science laboratories using animal models of SUDEP and within clinical groups studying human patients with epilepsy.

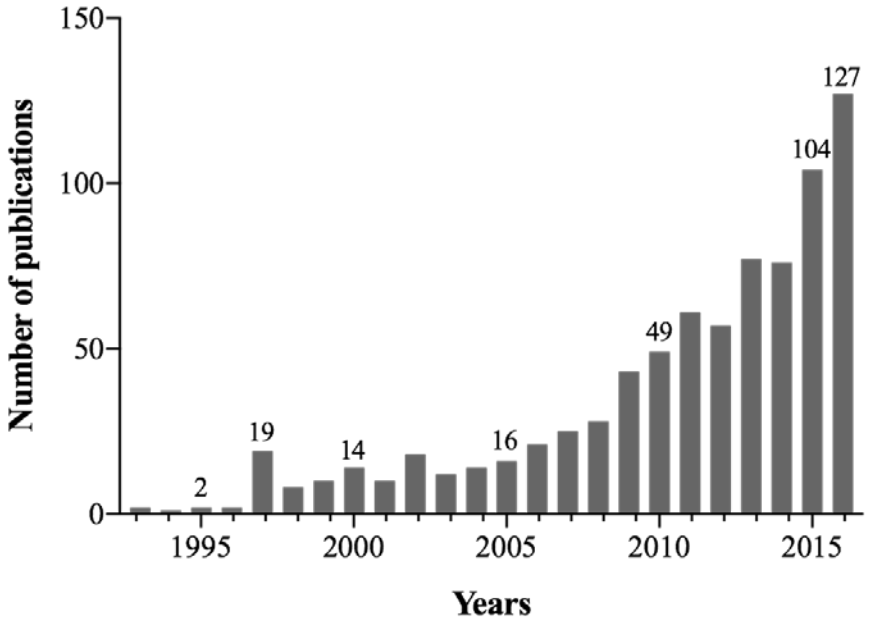

Figure 1. Increase in SUDEP publications.
The number of published studies on SUDEP from 1993 to 2016. Materials were searched in PubMed including 'sudden unexpected death in epilepsy' or 'SUDEP'.

Risk factors for SUDEP

A search for risk factors for SUDEP has been tried by retrospective analysis of witnessed SUDEP cases and SUDEP case-control studies. A high frequency of seizures in epilepsy patients is widely believed to be the principal risk factor for SUDEP. Other risk factors more likely to cause SUDEP have been identified such as a longer history of epilepsy, having difficulty controlling seizures, frequent changes to AED treatment, AED polytherapy, young age of onset, and generalized seizures (Hitiris et al., 2007; Hesdorffer et al., 2011; Langan et al., 2000). In contrast, one study implicated that multiple antiepileptic treatments are more likely to induce sedation and no particular drug or drug combination is associated with SUDEP (Walczak et al., 2001).

Identifying consistent risk factors for SUDEP among reports is difficult; different studies have represented disparate information. That may be because SUDEP has

heterogeneous criteria to be considered as definite or probable SUDEP. The incidence of SUDEP among reports is different depending on the definition used, study design and population, and level of documentation. In addition, lack of awareness of SUDEP or limited information surrounding sudden deaths may lead to underdiagnosis of SUDEP (Téllez-Zenteno et al., 2005).

Proposed mechanism(s) of SUDEP

In most SUDEP cases, death is believed to occur after a seizure, which is often attributed to the fact that seizures can induce cardiovascular and respiratory changes, such as arrhythmias, tachycardia, bradycardia, asystole, and apnea (Bateman et al., 2010; Nashef et al., 1996; Rainer Surges & Sander, 2012). Different mechanisms of SUDEP have been proposed including cardiac arrhythmias (Anderson et al., 2014; Auerbach et al., 2013; Johnson et al., 2009; Rainer Surges et al., 2010), dysfunction of cardiovascular autonomic control (Degiorgio et al., 2010; Delogu et al., 2011; Ergul et al., 2013; Glasscock et al., 2010; Kerling et al., 2009; R Surges et al., 2009), apnea/hypoventilation (Bateman et al., 2008; Buchanan et al., 2014; Dlouhy et al., 2015; Feng & Faingold, 2015; Nashef et al., 1996; Zhan et al., 2016), airway obstruction (Nakase et al., 2016), pulmonary edema (Seyal et al., 2010), brainstem spreading depolarization (Aiba & Noebels, 2015) and post-ictal generalized EEG suppression (PGES) (Lhatoo et al., 2010).

Many investigators have focused on cardiac tachyarrhythmias, in part because of an association between SUDEP and mutations of genes expressed in the heart such as those that underlie long QT syndrome (Aurlien et al., 2009; Faingold et al., 2010; Hata et al., 2016; Partemi et al., 2015). In some cases these mutations may cause both arrhythmias and seizures (Johnson et al., 2009; Parisi et al., 2013; Tiron et al., 2015),

whereas in other cases the mutations may predispose patients with any type of seizure to arrhythmias.

Analysis of epilepsy monitoring unit (EMU) data that incorporate recordings of respiratory parameters, electrocardiogram (EKG), electromyography (EMG), and electroencephalogram (EEG) of epilepsy patients provides highly informative data for their pathophysiology status during and after seizures. EMU recordings from human SUDEP cases provide a unique opportunity to improve our understanding of SUDEP mechanisms. In EMU patients, non-fatal seizures can sometimes induce bradycardia, asystole, O_2 desaturation or apnea (Bateman et al., 2008; Massey et al., 2014; Nashef et al., 1996; R Surges et al., 2009; Van Der Lende et al., 2016). A small number of patients (n=11) were recently reported to die of SUDEP while being monitored in EMUs (Ryvlin et al., 2013). In those patients, the typical sequence of events was a generalized tonic-clonic seizure followed by bradycardia and asystole (Ryvlin et al., 2013), along with a decreased respiratory rate leading to terminal apnea. For those patients, measurements of blood pressure, ventilation, CO_2 levels or O_2 saturation were not made, so there are still important unanswered questions about the mechanisms, such as if hypotension, airway obstruction or paradoxical breathing were present. It was also not clear what happened during the seizures, as respiratory movements and the EKG were obscured by movement artifact. Finally, most of the monitored SUDEP patients had temporal lobe epilepsy, so it is not clear whether those data are relevant to SUDEP in patients with other types of epilepsy.

Respiratory dysfunction is proposed as a cause of SUDEP with data from animal studies and evidence from most witnessed and recorded cases of SUDEP (Bateman et al.,

2010; Espinosa & Tedrow, 2009; Hewertson et al., 1994; Hitiris et al., 2007; Kloster, R.; Engelskjon, 1999; Langan et al., 2000; Lhatoo et al., 2010; So et al., 2000; Tao et al., 2010; Tomson et al., 2008). SUDEP occurs commonly after generalized tonic-clonic seizures with impaired consciousness and arousal responses. Generalized tonic-clonic seizures often severely impair arousal, brainstem, and sympathetic activity. A proposed mechanism of SUDEP is shown in Figure 2. Seizures spread to both midbrain and medulla and activate brainstem neurons that possibly impair brainstem respiratory and autonomic regulation. A seizure projects to the midbrain and medulla that lead to arousal failure and dysfunction of the ascending and descending arousal systems. Arousal failure combined with an obstruction of air intake due to the patient's face being in the bedding leads to hypoventilation. Ictal and post-ictal sympathetic hyperactivity causes tachycardia, hypertension, elevated blood pressure, and pulmonary edema. Inhibition of cardiovascular activity because of excess parasympathetic output would lead to bradycardia and hypotension. Inhibition of respiratory output would lead to hypoventilation and severe hypercapnia and hypoxia (Figure 2). Hypoventilation, apnea, and arrhythmias develop and lead to severe hypercapnia, hypoxia, and death (Devinsky et al., 2016; Massey et al., 2014; Ryvlin et al., 2013).

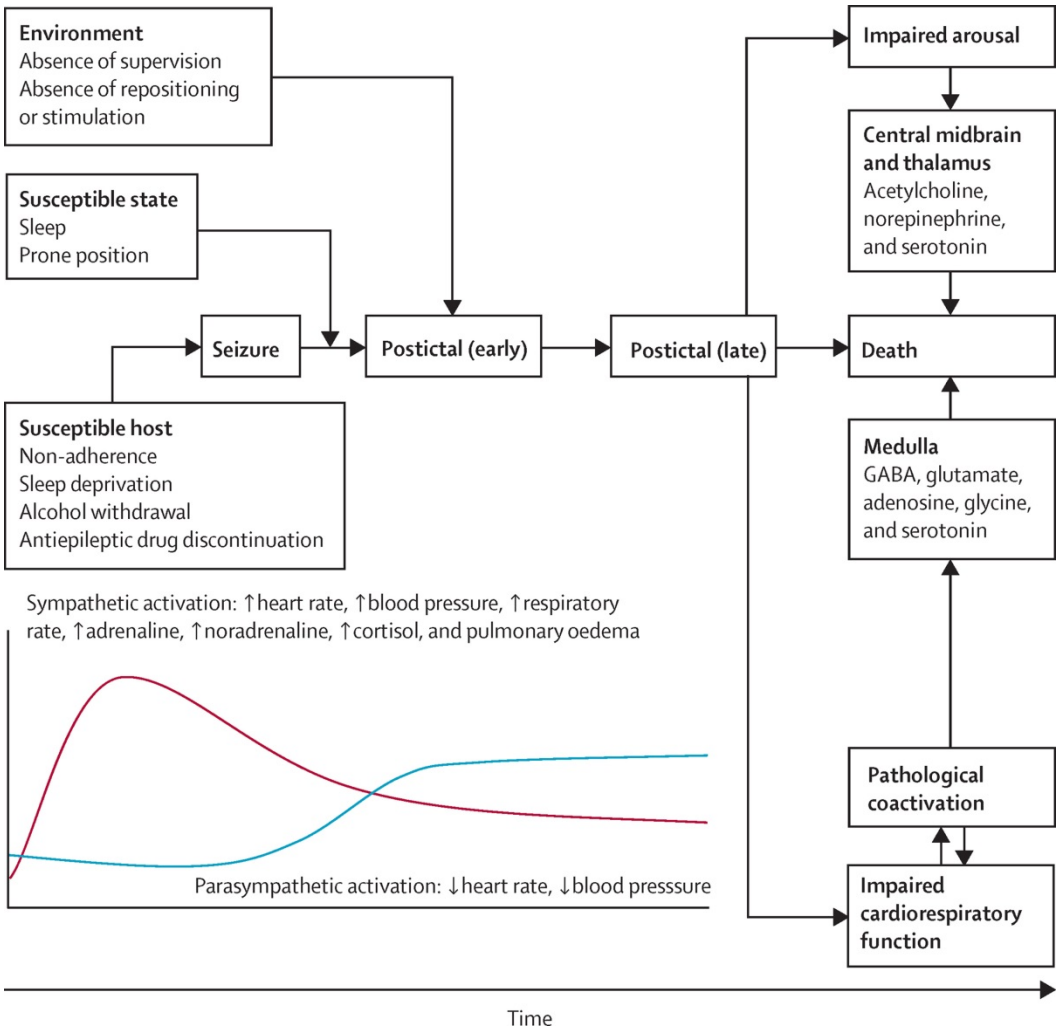

Figure 2. Hypothesized mechanisms of SUDEP.
Epilepsy patients have a seizure that spreads to both the midbrain and medulla. Simultaneous post-ictal activation of both sympathetic and parasympathetic system, along with respiratory depression, might contribute to SUDEP (Devinsky et al., 2016).

Dravet Syndrome

DS is a severe infantile-onset epilepsy with febrile seizures typically appearing in the first 6-12 months of life, followed by other types of severe, refractory seizures and cognitive impairment (Dravet, 2011). In 70-95% of cases, DS is due to mutations of SCN1A (Claes et al., 2001; Hani et al., 2015; Parihar & Ganesh, 2013), which encodes the sodium channel Nav1.1. SUDEP is particularly common in patients with DS, causing

death in more than 5% of cases, most commonly during the first few years of life (Dravet, 2011; Sakauchi et al., 2011).

Dietary therapy for epilepsy

The high-fat, low-carbohydrate Ketogenic Diet (KD) is known as a useful dietary therapy for epilepsy with refractory seizures, mostly given to children. The first KD was proposed in 1921 to mimic starvation (calorie restriction). The rapid development of new anticonvulsant drugs in the mid-20th century led to a drop in KD usage, but it regained its popularity when the American Epilepsy Society (1996) announced its effectiveness for refractory epilepsy patients (Freeman et al., 2007; Kossoff, 2004).

When blood glucose levels become diminished, the liver metabolism of body fat produces ketone bodies that are used as an efficient source of fuel for the body and the brain. Ketone bodies (acetoacetate, beta-hydroxybutyrate, and acetone) are always present in the blood, and the ketone levels elevate during prolonged fasting and starvation (Kossoff, 2004; Laffel, 1999). The KD produces a state of chronic ketosis (high levels of ketone bodies) and appears to reduce the number of seizures.

When effective, the KD leads to a significant seizure reduction, but only in children (Martin et al., 2016). Starting the KD after a fasting period results in a more rapid improvement, but there is no significant seizure reduction in the long-term (Kossoff et al., 2008). The KD efficacy in seven clinical studies reported up to 55% of freedom from seizure rates and as high as 85% of reduction of seizure rates in 427 children and adolescents including DS patients after three months (Laux & Blackford, 2013; Martin et al., 2016). Animal studies have shown that starvation and intermittent fasting raises the seizure threshold (Castel-Branco et al., 2009; Hartman et al., 2010). With these

dramatically successful cases, the KD is widely recommended to patients who have failed to respond to multiple AEDs and even surgery.

Despite the effectiveness of the KD, the true mechanism of anticonvulsant effects of the KD is unknown and theories regarding it abound. Some researchers have shown that ketones act similarly to GABA (e.g., the primary central nervous system inhibitory neurotransmitter) and may play a key role in seizure control (Freeman et al., 2007; McNally & Hartman, 2012). Some other studies suggest other possible factors of anti-epileptic effects of KD, such as calorie restriction, weight loss, and acidosis (Kossoff, 2004; Nordli D.R. & De Vivo, 1997).

Further limitations of KD include requiring a specially trained dietitian to select meals carefully and measure amounts of food restrictively. The smallest changes of carbohydrate intake can lead to more seizures for some children. Moreover, many children are often reluctant to follow this diet due to effects on weight, dislike of the diet, and short-term gastrointestinal-related disturbances. The documented side effects of KD include significant reduction in bone mass, lack of weight gain, growth inhibition, acidosis, constipation, and kidney stones. Also, long-term consumption of KD can increase the risk of cardiovascular complications such as hyperlipidemia (Hahn et al., 1979; Kossoff, 2004).

There are no published data regarding the clinical use of KD in adults with epilepsy. A study of the modified Atkins diet, a form of less restrictive KD, found similar effects of seizure control as the KD in children. More research is required to extend these diets into adult practice (Kossoff et al., 2008). Investigators assume that ketone bodies do not necessarily affect one's health (Freeman et al., 2007), but as of yet there is no

scientific evidence to support this. Therefore, there is a great need for large scale metabolic research on KD.

Animal models of Epilepsy

Death occurs in some mice after seizures. These mouse seizure-related deaths could be models of human SUDEP and may help to explain SUDEP mechanism(s) in humans. Therefore, mouse models are a valuable way to define the primary mechanisms of SUDEP, because, unlike humans, death is an acceptable outcome, and multiple physiological variables can be monitored prior to death. Different mouse models represent different forms of human epilepsies (Figure 3) (Löscher, 2011). Here, we introduce several mouse models that have been used in previous research for epilepsy and SUDEP: 1) chemical and mechanical seizure induction in normal animals, and 2) genetic animal models.

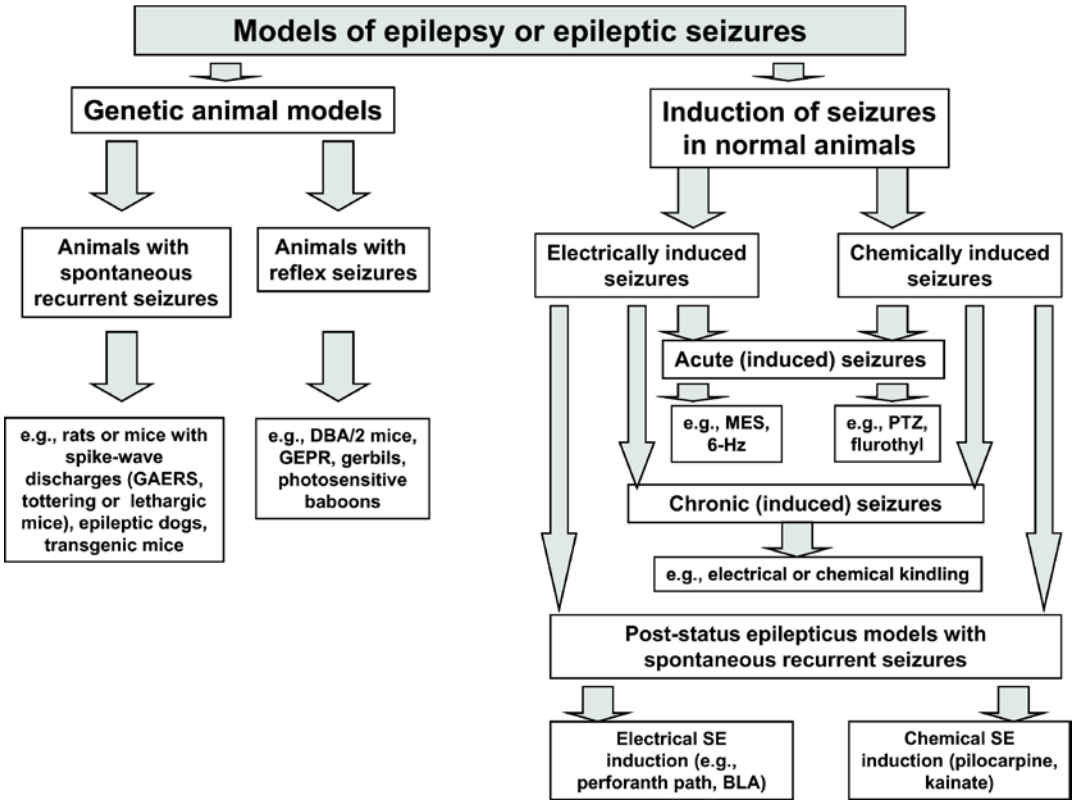

Figure 3. An overview of animal model of epilepsy in research.
A scheme of a classification of experimental animal models of epilepsy or seizures. Note that there are more chronic epilepsy models not included in this figure, in which spontaneous recurrent seizures develop after traumatic brain injury, ischemic brain damage, or febrile seizures (Löscher, 2011).

Seizure induction in normal mice

The most common animal seizure models in normal animals are developed by chemical administration of convulsant drugs and electrical stimulation of particular brain regions. Convulsant substances (e.g., pilocarpine, pentylenetetrazol, kainic acid) are commonly used to develop epileptic seizures in mouse models. As a model of temporal lobe epilepsy (TLE), the pilocarpine injection model in rodents is a widely used method in seizure studies. Pilocarpine induces status epilepticus (SE), hippocampal damage, and spontaneous recurrent seizures. The pilocarpine model is a reliable method of investigating the mechanisms involved in TLE, such as seizure behaviors, EEG, and

histologic features. The TLE syndrome generally exhibits spontaneous epileptic focal seizures and secondarily generalized seizures (Curia et al., 2008). Pentylenetetrazol (PTZ) induces a clonic seizure in 97% of the animals, and is commonly used for anticonvulsant drug test against non-convulsive (absence or myoclonic) seizures (Löscher, 2011). Kainic acid induction is a model of generalized seizure that induces seizures by affecting the limbic system in the hippocampus (Lothman & Collins, 1981). Additionally, the application of penicillin also induces seizures by locally increasing neuronal firing rate and is a model of focal seizure (Avoli et al., 1982; Jones et al., 2012).

The methods of electrically induced seizures were developed over 60 years ago and are still the most widely used in animal seizure models to test the efficacy of AEDs (Toman et al., 1946). Maximal Electroshock (MES) induces convulsive seizures including tonic hind-limb extension, and is a model of generalized tonic-clonic (grand mal) seizures (Castel-Branco et al., 2009; Tedeschi et al., 1956; Toman et al., 1946).

Genetic and Transgenic animal models

Sound-induced (audiogenic) seizures in DBA mice exhibit sudden death due to respiratory arrest, and have been used to show that sudden death can be prevented by oxygenation (Hall, 1946). Mice lacking the Otx1 gene display focal seizures and brain abnormalities (Avanzini et al., 2000). A potassium channel mutation in weaver mice is a genetic model of generalized seizures (Sarkisian, 2001). Various other genetic mouse models of seizures or epilepsy have previously been reported such as maternally-inherited heterozygous UBE3A deletion (hybrid C57BL/6/129SvEv), 1.6-Mb chromosomal deletion from Ube3a to Gabrb3, succinate semialdehyde dehydrogenase deletion, Efhc1 deletion, $GABA_AR$ γ2(R43Q) subunit knock-in, 5-HT neurone deletion (

Lmx1b$^{f/f/p}$), and 5-HT$_{2c}$ knockout (Buchanan et al., 2014; Löscher, 2011; Patil et al., 1995; Sarkisian, 2001; Tecott et al., 1995; van Luijtelaar et al., 2014).

Some transgenic mice are created to mimic the specific genetic characteristics of human epilepsy cases. The mechanisms of post-ictal death after spontaneous seizures in epileptic transgenic mice may be similar as in humans since SUDEP in humans is due to spontaneous, i.e. not induced, seizures.

Seizure episodes are common in long QT syndrome. Mutations in KCNQ1-encoded α subunit of the Kv7.1 potassium channel, KCNH2-encoded α subunit of the Kv11.1, and SCN5A-encoded α subunit of the Nav1.5 sodium channel have been implicated as dominant member of the long QT syndrome gene family (Anderson et al., 2014). *Kcnq1* knock-in mice recapitulates the association of epilepsy and a spectrum of cardiac arrhythmias similar to the human long QT syndrome (Goldman et al., 2009). Mice lacking Kv1.1-potassium channels encoded by the *Kcna1* gene develop spontaneous seizures and exhibit cardiac abnormalities. *Kcna1* is not considered an long QT gene (Glasscock et al., 2010).

The sodium channel α subunit genes SCN1A, SCN2A, and SCN8A play an important role in regulating neuronal excitability. Mutations in these genes can lead to early-onset seizures that are often highly refractory to treatment. SCN1A mutations have been identified in DS (see Dravet Syndrome). Mutations of SCN2A and SCN8A are responsible for Ohtahara syndrome and OMIN #614558, respectively (Wagnon & Meisler, 2015). These mutant mice have convulsive seizures that resemble the human conditions.

Gaps in existing knowledge and plan of study

Despite the sharp increase in research on SUDEP mechanisms in the past decade (Figure 1), we are still in the dark as to whether cardiac and/or respiratory dysfunction is the primary cause of SUDEP. Analysis of data from patients who died of SUDEP in an EMU would be the best method to define the primary cause of death, except that it is unusual for EMUs to record any measure of respiratory activity. The recent MORTality in Epilepsy Monitoring Unit Study (MORTEMUS) (Ryvlin et al., 2013), none of the SUDEP cases had direct measurements of breathing; the breathing rate was assessed by visual observations on videos only. Visual analysis of video recordings suggested that apnea occurred early in the sequence of events preceding death.

Sudden death occurs in some mice after seizures. Investigation of sudden death after seizures in mouse models may help to define the primary mechanisms of SUDEP in humans. In a DS mouse model with an $Scn1a^{R1407X/+}$ mutation, death occurs after spontaneous and MES/heat-induced seizures. This post-ictal death is likely to be relevant to the mechanisms of SUDEP in DS patients. Previous work in DS mouse models has focused only on the effect of cardiac dysfunction in SUDEP using EKG recordings but not respiratory analysis. Since breathing has never been recorded during human SUDEP, and only rarely in models of SUDEP in mice, it is possible that in some cases, respiratory dysfunction, such as central apnea, could be the primary cause of death and cardiac dysfunction is secondarily to the resulting hypoxemia.

The purpose of the work described in this dissertation is to provide a better understanding of SUDEP mechanism(s). The specific aims of this study are to:

1) **Design and develop a mouse EMU.** A mouse EMU can measure mouse physiological changes, such as breathing, cardiac activity, and seizure activity until the occurrence of post-ictal death. Using a mouse EMU we sought to define the primary cause of death in several mouse strains. It is important to know whether these models share a common final pathway for death, or alternatively whether death occurs for different reasons in each model. Development of a mouse EMU and its use in multiple mouse strains with seizure-induced death is described in Chapter 2.

2) **Study post-ictal respiratory dysfunction in DS.** DS patients have a high risk of SUDEP, and death is believed to be due to post-ictal bradycardia. We found that DS patients had frequent post-ictal respiratory dysfunction, while cardiac activity was normal. Also, we studied mice with an *Scn1a*$^{R1407X/+}$ mutation to determine the role of respiratory dysfunction in post-ictal death after spontaneous and induced seizures. This DS respiratory dysfunction study is discussed in Chapter 3.

3) **Evaluate a new dietary approach for prevention of SUDEP in a DS mouse model.** The final goal of this study is to evaluate a new alternative dietary therapy for DS patients. A collaborator has found that a diet containing milk whey was able to prevent seizures in Drosophila with an orthologous sodium channel mutation. We proposed that supplementing milk whey in the normal diet of DS mice will also decrease the number of seizures and prevent SUDEP. We characterized the effectiveness of milk whey supplementation in different doses; we also compared the effect of milk whey supplementation to that of a KD. Dietary therapy experiments in DS mice are described in Chapter 4.

The completion of this study will lead to potential new avenues of SUDEP prevention and treatment for DS: 1) the mouse EMU data of sudden death after spontaneous seizures will confirm the cause of death in a DS mouse model and this will bring a better understanding of SUDEP mechanisms in humans; 2) the therapeutic diet study will provide a possible novel therapeutic approach to prevent seizures and SUDEP in DS patients.

CHAPTER 2: DEVELOPMENT OF A MOUSE EPILEPSY MONITORING UNIT (EMU) AND CAUSE OF DEATH AFTER SEIZURES IN MULTIPLE MOUSE STRAINS

Introduction

The objective of this chapter is to define the mechanisms of seizure-related sudden death in multiple mouse models of SUDEP. More specifically, this study identifies how cardiorespiratory dysfunction contributes to post-ictal death in mice and potentially to SUDEP in humans.

With this goal, I designed and built a mouse epilepsy monitoring unit (EMU) that allows recording of peri-ictal physiological changes after induced seizures. It had been hypothesized that analysis of mouse EMU data that incorporated recordings of respiratory parameters, EEG, EKG and EMG could objectively confirm the mechanism of a seizure-related sudden death. These recordings allow us to study whether different mouse models of sudden death induced by seizures have a common final pathway of death or if the cause of death differs among the different mouse models or seizure types. In this chapter, I induced seizures in multiple non-epileptic mouse strains that are prone to sudden death in response to seizures. These strains included: 1) audiogenic seizures in DBA/1 mice, 2) MES-induced seizures in *Lmx1b*$^{f/f/p}$ mice, 3) MES-induced seizures in C57Bl/6 mice.

Methods

Mouse EMU system setup

To evaluate the cause(s) of death after a seizure in mice, I developed an experimental approach to monitor their physiological changes. The EMU unit recorded two EEG channels, nuchal EMG, EKG, animal movement, video, body temperature, chamber temperature and humidity, and whole-body plethysmography pressure

(breathing) traces of individual mice. Individual mice underwent surgery to implant recording electrodes and temperature/activity telemetry probes. After 7 days of recovery, mice were placed in a sealed recording chamber in which they could move freely. When a mouse died after seizures, the monitoring system had been terminated and analyzed the data to identify the primary cause of death: cardiac, respiratory, or other. (Figure 4).

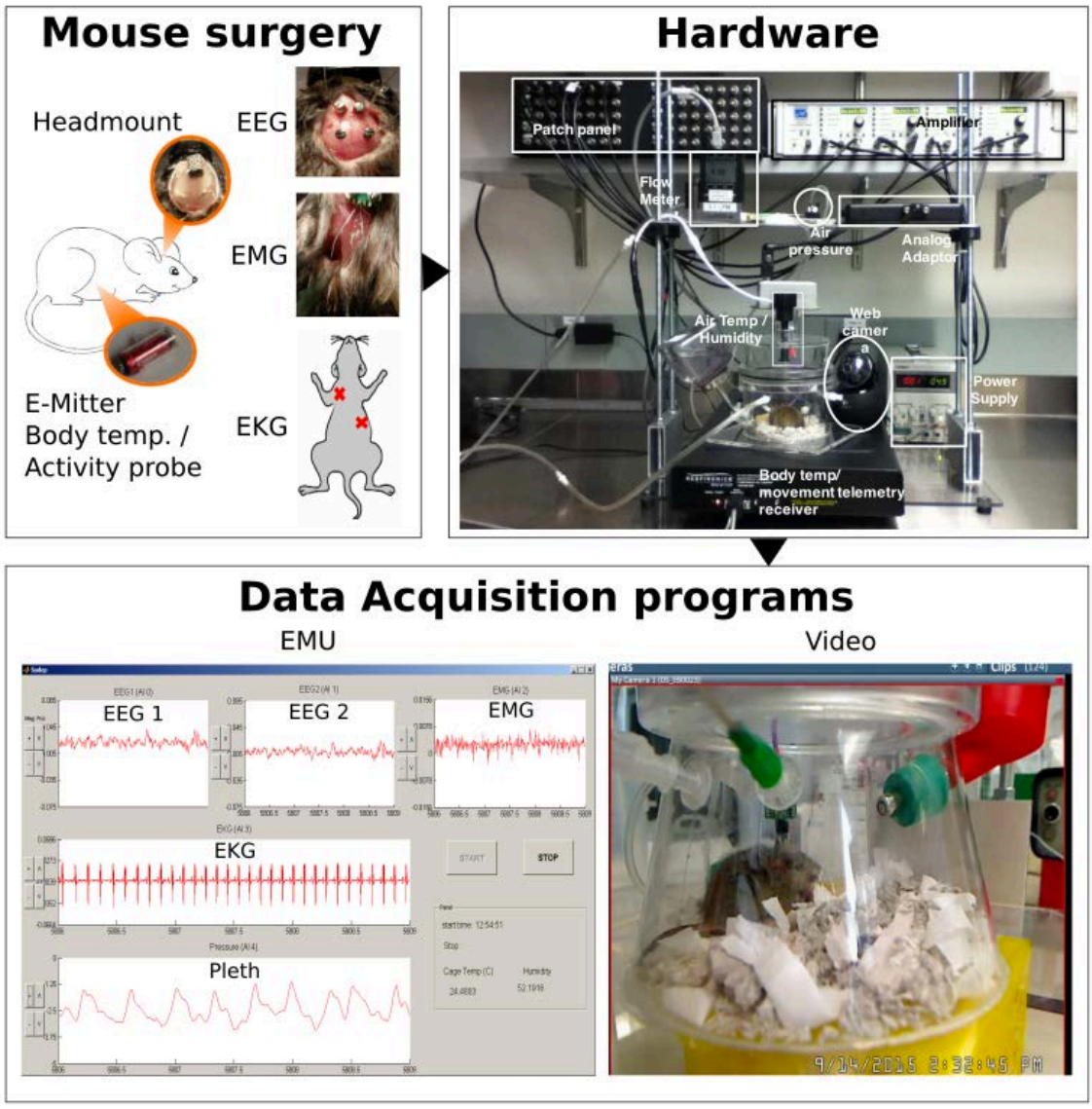

Figure 4. Recordings from the mouse physiology and video.
Individual mice were implanted with recording electrodes for EEG, EMG, and EKG, and with temperature/activity telemetry probes. Mice were placed in a sealed recording chamber. All analog / digital / telemetry signals from the hardware devices were recorded and displayed in real-time on the computer screen via a customized data acquisition software developed using MATLAB. Video was monitored through a network IP web camera and commercially-available video webcam software (Blue Iris 4).

EEG/EKG/EMG headmount and body temperature telemeter implants

Mice received preoperative analgesia (meloxicam, 0.5 mg/kg, I.P.; or buprenorphine, 0.1 mg/kg, I.P.), and then anesthesia was induced, and it was maintained with 0.5 - 3% inhaled isoflurane.

A four-channel tethered mouse EEG/EMG headmount (8400-K1; Pinnacle Technology Inc., Lawrence, KS, USA) was connected with customized EKG electrodes. These custom headmounts (EMG/EKG/2-channel EEG) were constructed with a micro-connector (8 position 2 row IC & Component socket; Mill-Max Mfg. Corp., Oyster Bay, NY). The two EKG electrodes were constructed from 70 mm lengths of insulated silver wire (0.01" coated, A-M Systems). One end of both wires was stripped and soldered to the headmount micro-connector. Two EMG wires were each constructed from 20 mm double twisted bare silver wire (0.01" bare, A-M System) and soldered to the headmount. Four bare stainless steel leads (0.01" bare, A-M System) were soldered to the headmount for EEG. To implant the headmount, a midline skin incision was made over the skull. Four small holes were drilled into the skull, and four micro-screws (0.8*4.2; stainless steel nose pad screw; QTE North America Inc.) with stainless steel leads (0.01" bare, A-M System) were attached to the skull. The four EEG leads from the headmount were connected to the four leads on the screws. The EMG wires from the headmount were inserted into the nuchal muscles in the back of the neck. Two EKG wires from the headmount were tunneled under the skin to the anterior chest and sutured in the thoracic muscles subcutaneously, one in the upper right and one in the lower left quadrants of the chest, in a Lead II configuration. The incisions on the chest were closed with vet-bond (3M Animal Care Product, St. Paul, MN). The base of the headmount and screw heads

were secured with dental acrylic (Jet Acrylic; Lang Dental, Wheeling, IL) and the skin closed with vet-bond leaving only the headmount socket exposed.

Some mice were instrumented with telemetric temperature probes (Emitter G2; Mini-Mitter, Bend, OR) to measure their body temperature. The abdomen was shaved and sterilized, and a midline incision was made. The temperature probes were inserted into the peritoneum through the incision, and the incision was closed with vet-bond (Figure 4).

Mice were given postoperative analgesia (meloxicam, 0.5 mg/kg, I.P.; or buprenorphine, 0.1 mg/kg, I.P.) and recovered for a minimum of 7 days before being recorded. After headmount surgery, mice were housed individually in order to protect the implants from cagemates.

Signal measurements

EEG, EMG, EKG, temperature, humidity, whole body plethysmography, and video were recorded until the occurrence of sudden death after seizures. Note that, during mouse EMU recordings unanesthetized individual mice were placed in a sealed plethysmography chamber in which they could move without disturbances. For acute seizure experiments, seizures were induced after approximately 30 minutes of an acclimation period to get a steady baseline of breathing. Figure 5 shows the schematic design of the mouse EMU system with network connections leading from transducers to display of data by the computer.

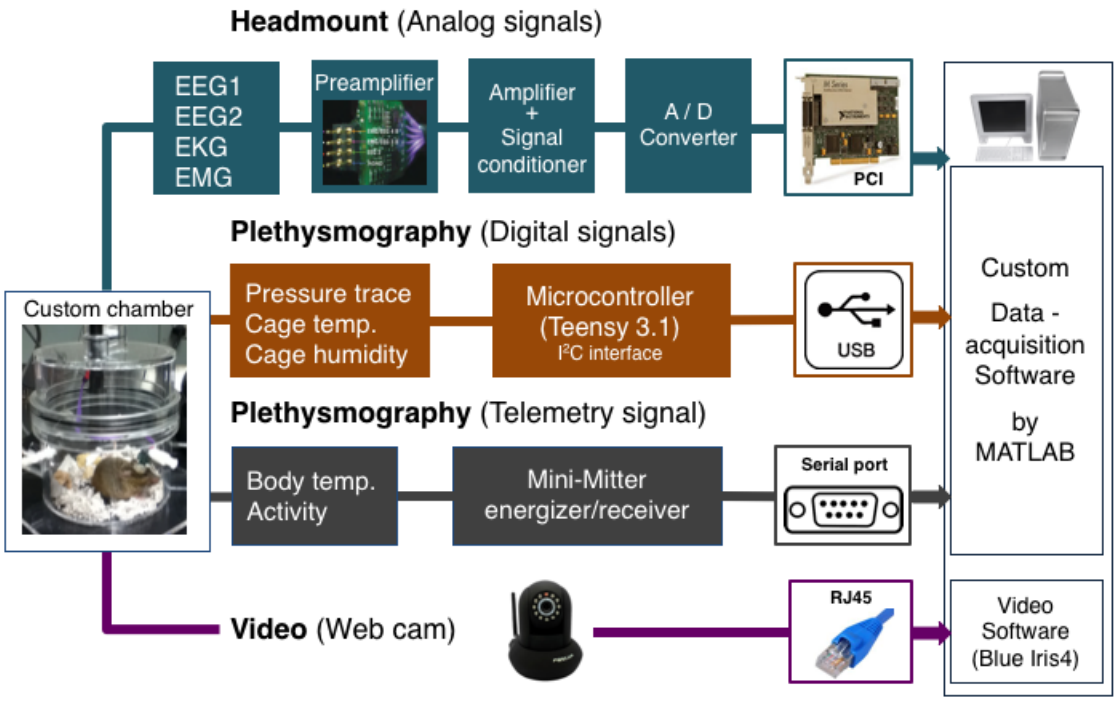

Figure 5. Schematic design of a mouse EMU system.
EEG, EMG and EKG signals were connected through a preamplifier (10X) to an analog amplifier where signals were further amplified by 10X and band-pass filtered. These signals were digitized with an analog-to-digital converter installed in a PCI slot of desktop computer and acquired with data acquisition software custom-written in MATLAB. The plethysmography chamber pressure was measured using a digital differential pressure transducer. Chamber temperature and relative humidity were also continuously monitored. Signal outputs from the pressure transducer and temperature/humidity sensor were acquired continuously at 100 Hz through a USB port with the same custom-written MATLAB data acquisition software. Body temperature and activity were captured by a telemetry receiver placed beneath the recording chamber, transmitted to the computer via a serial port, and sampled every 10 seconds with the same custom-written MATLAB data acquisition software. Video was captured separately by commercially available software.

Headmount

The EKG, EMG, and 2 EEG signals from the headmount passed through a preamplifier (8406-SE31M-C; Pinnacle Technology), then through a commutator (8408; Pinnacle Technology), and finally into an analog adapter (8442; Pinnacle Technology). This preamplifier amplified all four channels (Gain 10X) and applied a 0.5 Hz high pass filter on the EKG, 1.0 Hz high pass filters on the EEGs, and 10 Hz high pass filter on the

EMG. Right after the analog adapter, a secondary amplifier (Model 440 Instrumentation Amplifier; Brownlee Precision Co., San Jose, CA) performed additional amplification on all four channels (Gain 10X), and applied a 1 to 500 Hz band pass filter on the EKG, 10 to 500 Hz band pass filter on the EMG channel, and 0.3 to 400 Hz band pass filters on the EEGs. EKG/EMG/2 EEG signals were digitized using an analog-to-digital converter (PCI-6225; National Instruments, Austin, TX), and acquired continuously at 1,000 Hz with data acquisition software custom-written in MATLAB.

Plethysmography

The whole-body plethysmography technique had been used to measure breathing in mice. With this approach, the tidal volume of each breath can be calculated from changes in chamber pressure, along with body the temperature of the animal and the temperature and humidity of ambient air. Whole body plethysmography is a non-invasive method for measuring breathing of unanesthetized mice while the animal is unrestrained. Every time the mouse inhales, there is an increase in pressure in the chamber due to heating and humidification of air in the lungs, both of which cause gas expansion. There is also a decrease in pressure when the mouse exhales (Drorbaugh & Fenn, 1955). The chamber was custom-designed and built to comply with requirements for continuous housing described in the Guide for the Care and Use of Laboratory Animals, 8th edition. The floor was circular and 5 inches in diameter. The walls were semiconical with a roof that was 5.5 inches high and 3 inches in diameter. The chamber volume was 815 ml. This custom-made mouse EMU chamber was attached to air pumps with continuous room-air in-and-out at a flow rate of ~400 ml/min; the air-out pump was made by modifying an air-in pump (MK-1504 Aquarium Air Pump; AQUA Culture, Bentonville,

AR). Thus, the air volume in the chamber with the mouse was constant, and changes in pressure due to inspiratory and expiratory volumes were measured by using a digital differential pressure transducer (SDP610-25Pa; Sensirion AG, Switzerland) (Figure 5; Table 1). The chamber temperature and relative humidity sensor (HIH-6130; Honeywell International Inc., Golden Valley, MN) and the digital differential pressure transducer were attached to the mouse EMU chamber, and these signal outputs were directly connected to a microcontroller (Teensy 3.1; PJRC.COM, LLC., Sherwood, OR) using a custom-designed PCB (Printed Circuit Board). These digital transducers and the microcontroller communicated through an I^2C interface. Arduino software was used (ARDUINO 1.6.9; Arduino LLC, and Teensyduino 1.28; PJRC.COM) to write and upload the configuration code of these digital sensors to the microcontroller board. Chamber temperature, relative humidity and pressure signals were acquired continuously at 100 Hz through a USB port with the same custom-written MATLAB data acquisition software. The chamber with the mouse was set on top of a telemetry temperature energizer/receiver (model ER-4000; Mini-Mitter, Bend, OR). The radiowaves of animal body temperature and activity emitted by the abdominal sensor were captured by a receiving plate (ER-4000 energizer/receiver). The receiving plate communicated with the computer via an RS-232 serial communications port, and sampled every 10 seconds with the same custom-written MATLAB data acquisition software.

Video recording

Video recording of the mouse EMU was collected at 30 fps using a night-vision web camera (FL8910W; Foscam Digital Technologies LLC). This camera was connected to a computer with a network cable (RJ45 Cat6) and the video was stored on an external

hard drive using commercial video webcam software (Blue Iris 4; Foscam Digital Technologies LLC) (Figures 4 and 5).

Data acquisition software

All headmount / plethysmography / video signals from the hardware devices in the mouse EMU were acquired and displayed in real-time on a computer monitor by a custom data acquisition software developed using MATLAB (MathWorks, Natick, MA). Data acquired from the headmount / plethysmography inputs were saved in a binary file at 1,000 Hz on EKG, 100 Hz on EMG/EEGs/pressure, and 1/10 Hz on cage temperature/humidity/body temperature. All digitized data were saved on external hard drives. To assess the accuracy of the analog data reading from our data acquisition software, a function generator was used as an input signal connecting to analog input channels. Data measurements from our data acquisition software were compared to a measurement tool (Measurement & Automatic Explorer (MAX)) provided by National Instrument. To assess the data accuracy of the digital output sensors (differential pressure sensor, humidity/temperature sensor), a rodent mechanical ventilator (MiniVent type 845) and a digital thermometer with humidity (model: 00477DIACURITE, Lake Geneva, WI) were used as inputs. The data readings from the MATLAB software were compared to the volume of air in the ventilator and readings on the thermometer. Lastly, the reading of telemetry probes for measuring animal body temperature were validated by measuring the temperature of telemetry devices in warm water with a mercury thermometer before animal surgery was performed.

Animal and seizure induction

Three non-epileptic mouse strains were used in this study to determine the post-ictal cause of death, and whether the causes of death after seizures were affected by different types of seizure induction. In the following section, we introduce two different ways of acute seizure induction in three mouse strains.

Ethical approval

All mice used in this dissertation were housed and maintained on a 12-hour light/dark cycle, at constant (70°F) room temperature, with *ad libitum* access to food and water in an animal room within the University of Iowa animal facility. All procedures and protocols performed on all mouse strains in this study were approved by The University of Iowa Institutional Animal Care and Use Committee, and were in strict accordance with the recommendations of the Guide for the Care and Use of Laboratory Animals, 8th edition (ACP. *Guide for the Care and Use of Laboratory Animals*, National Academies Press, Washington, DC, 2011). The minimum possible number of animals was used, and care was taken to reduce any discomfort.

DBA/1 with audiogenic seizures

The DBA mouse strain was developed in 1909 by CC Little from mice used in segregating coat color experiments. The DBA is the oldest of all inbred strains of mice. After crosses between the substrains of DBA in 1929-30, new substrains DBA/1 and DBA/2 were established due to substantial residual heterozygosity. The susceptibility of DBA mice to audiogenic seizures was reported by Hall (Hall, 1946). DBA/1 mice are genetically susceptible to generalized convulsive seizures evoked by acoustic stimulation, which lead to seizure-induced respiratory arrest and sudden death unless they are rapidly

resuscitated (Faingold & Randall, 2013). However, DBA/1 mice are not epileptic as they do not have spontaneous seizures. DBA/1 mice of both genders from Envigo (Indianapolis, IN) between the ages of 21 days postnatal (P21) and P24 were given 3-4 days of seizure induction stimuli (see method: Ventilatory support after seizures) to increase the susceptibility to acoustically-induced audiogenic seizure and respiratory arrest, as previously described (Faingold et al., 2010; Hall, 1946). Only those DBA/1 mice that were resuscitated after tonic hind-limb extension and respiratory arrest were used for mouse EMU recording at P60-P90.

Acute seizures were induced by sound in a group of DBA/1 mice. Mice were individually placed into a 4L glass cylinder. A broad-band acoustic stimulus was generated by an electric bell alarm clock at an intensity of approximately 110 dB. The stimulus was given for a maximum duration of 60 seconds or until the mouse exhibited a tonic seizure, which ended in tonic hind-limb extension convulsions and respiratory arrest. The responses to sound of individual mice were scored as the following: no response, wild running only, wild running plus tonic-clonic seizure, or wild running plus tonic-clonic seizure plus respiratory arrest. During the seizure initial test (Faingold et al., 2010), audiogenic seizure induction and resuscitation were carried out daily for 3-4 consecutive days at P21-P28 in all individual mice.

For running a mouse EMU, individual mice were placed into a mouse EMU chamber and the electrical bell sound stimulation was given for a maximum duration of 60 seconds or until the mouse exhibited a tonic seizure.

Lmx1b$^{f/f/p}$ mice with MES seizures

Serotonin neurons are involved in many brain functions, including cognition, circadian rhythms, and mode (Jacobs & Azmitia, 1992). The *Lmx1b*$^{f/f/p}$ mouse strain was generated in the Zhou-Feng Chen laboratory and has been described previously (Zhao et al., 2006). Briefly, homozygous loxP-flanked(floxed) *Lmx1b* female mice (*Lmx1b*$^{f/f}$) were mated with hemizygous ePet-Cre *Lmx1b*$^{f/f}$ male mice to generate *Lmx1b*$^{flox/flox;ePet\text{-}Cre/+}$ (*Lmx1b*$^{f/f/p}$) mice, in which both Lmx1b alleles were deleted selectively in all ePet-Cre-expressing cells. This deletion leads to the selective absence of virtually all central 5-HT neurons.

A study of acute seizures in *Lmx1b*$^{f/f/p}$ mice induced by MES has been previously described (Buchanan et al., 2014). I repeated this experiment in our *Lmx1b*$^{f/f/p}$ mouse colony to test our MES device (Rodent shocker Type 221; Hugo SACHS Electronic-Harvard Apparatus GmbH, Germany) and mice mortality. Mice were placed in the mouse EMU chamber and subjected to MES stimulus from a rodent shocker delivered with either an electrode implanted under the scalp or via ear-clip electrodes: 50 - 200 mA fixed current; 60 Hz pulse frequency; 0.2 - 5s stimulus duration. After seizure induction, surviving mice were euthanized within 6 hours of the initial seizure.

C57BL/6 mice with MES seizure

C57Bl/6 is a common inbred strain of laboratory mouse used around the world. Breeding pairs of these mice from Jackson Laboratories (Bar Harbor, Maine) were used to begin our colony. This mouse colony was maintained in our lab, and these mice do not have any transgenic mutations. Male and female C57Bl/6 (n=8) were used for mouse EMU recording with acute seizures induced by MES.

Data analysis of EMU recording

Analyses of respiratory rate and heart rate from the EMU recording were performed on binary files of acquired data using software custom-written in MATLAB (Mathworks Co.; Natick, MA). The raw plethysmography data was conditioned with a bandpass filter of 1 - 10 Hz, then inspiratory peak locations and values were automatically detected using a peak analysis method in MATLAB (Figure 6A). The time interval between peaks (interbreath interval; IBI) was computed as the mean for 10s epochs and shown as cardiorespiratory pattern (example in Figure 9B).

R-wave detection of EKG data was performed by applying a similar method. Instead of applying the bandpass filter, a continuous wavelet transform (CWT) was applied as a filter method. The locations and value of R-wave peaks were found as a result of peak detection in MATLAB (Figure 6B). The R-R interval from these detected R-waves was computed as the mean for 10s epochs and displayed as cardiorespiratory patterns (in the example shown in Figure 9B).

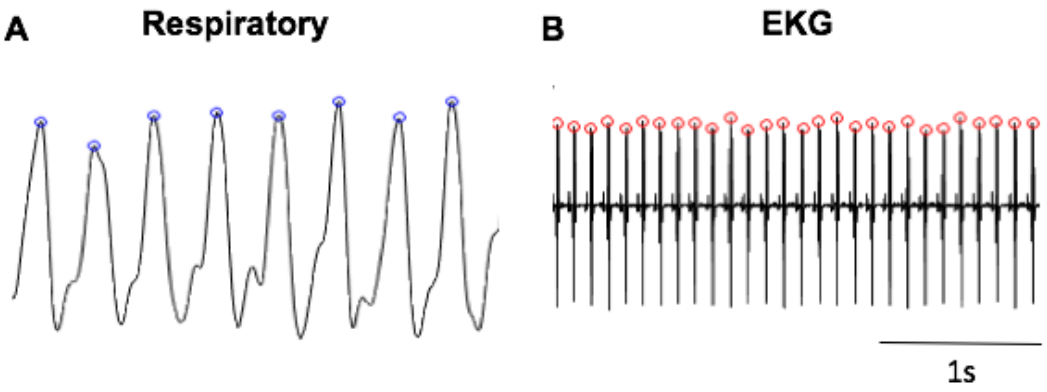

Figure 6. Examples of respiratory and EKG analyses.
(A) Plot of breathing data in time domain. Respiratory recording from a mouse shows a trace of breathing movements. Blue circles were automatically detected inspiratory peaks. (B) EKG recording of same mouse shown in A. A continuous wavelet transform (CWT) was applied to raw EKG data. R-waves (red circles) of filtered EKG data were detected by the same MATLAB peak detection algorithm as respiratory analysis with a small change of parameter inputs.

Ventilatory support after seizures

In the experiment on DBA/1 mice, resuscitation occurred during the initial test with a rodent mechanical ventilator (MiniVent type 845; Hugo SACHS Electronic-Harvard Apparatus GmbH, Germany) (Figure 7). The ventilator was already in operation pumping room air (180 strokes/min), and when the outflow polyethylene tube of the ventilator was placed over the nostrils, the 200 µl volume induced visible displacement of the chest. Resuscitation was instituted within 2 - 5 seconds after respiratory arrest to effectively revive the mice.

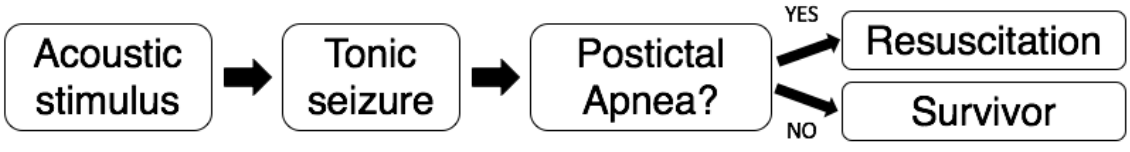

Figure 7. A sequence of animal resuscitation.
A single seizure was induced by acoustic stimulation outside the mouse EMU. A rodent ventilator was used to resuscitate animals if there was a prolonged post-ictal period without chest movement (>5 seconds).

Results

Development of mouse EMU system

The first version of mouse EMU was designed in early 2012, and the system has been improved in two important aspects: the system (a) achieved high-accuracy signals and precision timing for sensors in data acquisition and (b) had substantially better noise filtering in data analysis. Table 1 shows the improvement of the mouse EMU over time. Pressure, temperature, and humidity transducers attached to the chamber were used to analyze animal breathing traces. These transducers were replaced from analog output transducers (SSCSNBN001NDAA5; Honeywell International Inc., Golden Valley, MN) to digital output transducers in 2014. This change made the system able to measure small breathing changes with high sensitivity and reliability. The calibration range was improved to be 10 times more sensitive (from ± 1″ H_2O to ± 0.1″ H_2O). The specifications of current version were described in method section of current chapter. During experiments using the first version, chamber pressure was maintained near atmospheric with continuous room-air in-and-out at a flow rate of ~400 ml/min via supply (Cole-Parmer Gas Mass Flow Controller, model#: 32907-67; Cole-Parmer, Vernon Hills, IL) and exhaust air pumps (Buxco 4 channel Bias Flow Regulator; Buxco, Wilmington, NC). These air pumps were replaced by modifying an air-in pump (MK-1504 Aquarium Air Pump; AQUA Culture, Bentonville, AR) and (2510 Machined Acrylic Flow Meter; Brooks Instrument, Hatfield, PA) (Table 1). These changes maintained equivalent performance with previous version, but reduced cost considerably. This cost reduction was essential when we duplicated the mouse EMU. A time delay on the video recording was detected due to the communication between the MATLAB data

acquisition program and the USB port of the web camera. We separated the video recording from the MATLAB data acquisition software, and the video was recorded through a network cable (RJ 45) with a commercial video webcam software (Blue Iris 4) (Figure 5; Table 1). The quality of signals acquired in the data acquisition software was improved by preventing environmental noise through the use of grounding and shielded cables. An anti-aliasing filter was implemented in the data acquisition software using oversampling; sampling rates were at least twice that of the frequency of interest (Nyquist sampling theorem). An example of the graphical display of information by the data acquisition software after the final update is shown Figure 8.

Table 1: Progression of mouse EMU version as time passes.

Feature	Before 2016	Current version	Improvement
Pressure / temp. / humidity transducers	Analog outputs 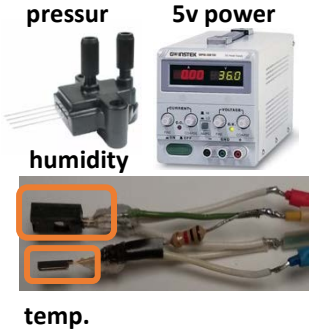	SDP610-25Pa Digital I^2C outputs 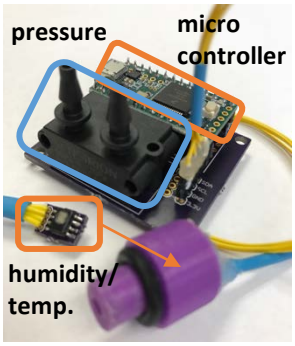	↑ calibration range 10X
Air flow (Air-in)			Cost reduction From $2,014 to $160
(Air-out)			
Video camera	Video recorded through the EMU data acquisition USB cable 	Video recording Network cable (RJ 45) 	Night vision Eliminated video time delay (5 - 40s)
Data acquisition	100 Hz sample rate on EEGs/EMG/EKG/ Plethysmography	Grounding Shielded cables Anti-aliasing filter (oversampling)	Noise reduction

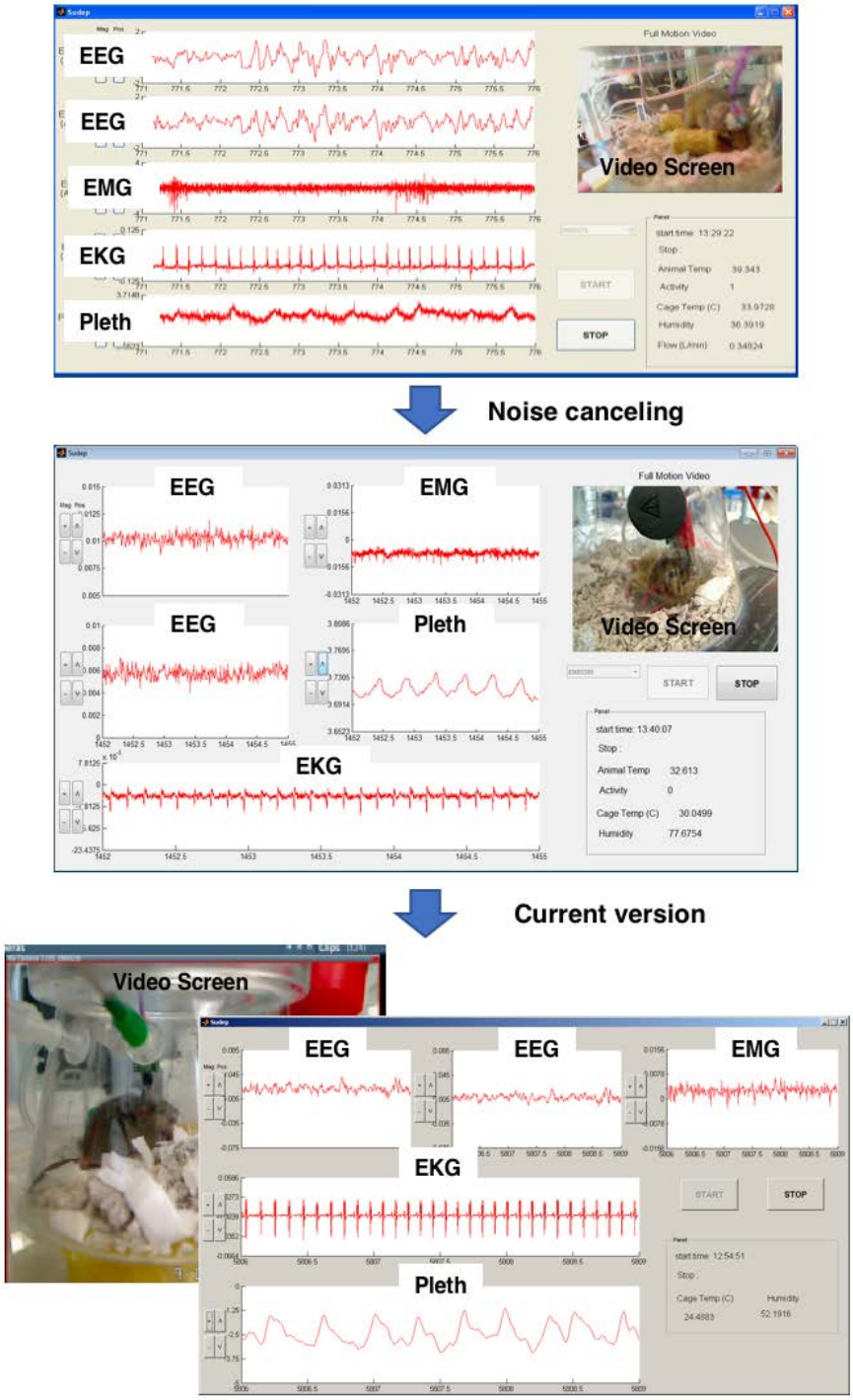

Figure 8. Graphical display of data by acquisition software written in MATLAB. Changes in the data acquisition software over time. (Top) Raw signals received from A/D converter were plotted with minimum filtering from pre-amplifier in the headmount and amplifier. (Middle) The quality of signals had been improved by dealing with environmental noises (described in Table 1). All data shown in Chapter 2 were acquired with this version. (Bottom) Video recording was separated from the data acquisition program to avoid time delay on the video. All data shown in Chapter 3 were acquired with this final updated version.

DBA/1 mice with audiogenic seizures

DBA/1 mice are susceptible to audiogenic seizure-induced respiratory arrest, leading to death. Generalized convulsive seizures were induced by acoustic stimulation generated by an electric bell at an intensity of approximately 110 dB while animals were monitored in a mouse EMU (n=8). 100% of DBA/1 mice died at the end of acoustic stimulus. An example of EMU traces from an individual mouse is shown in Figure 9A. EEG, EKG, and breathing traces were normal prior to seizure induction. After an acoustic stimulus (black bar), an induced seizure altered all physiological traces. When death occurred, complete respiratory arrest always occurred during or immediately after the seizure. This was slowly followed by bradycardia, and then asystole after 3-7 minutes (Figure 9B).

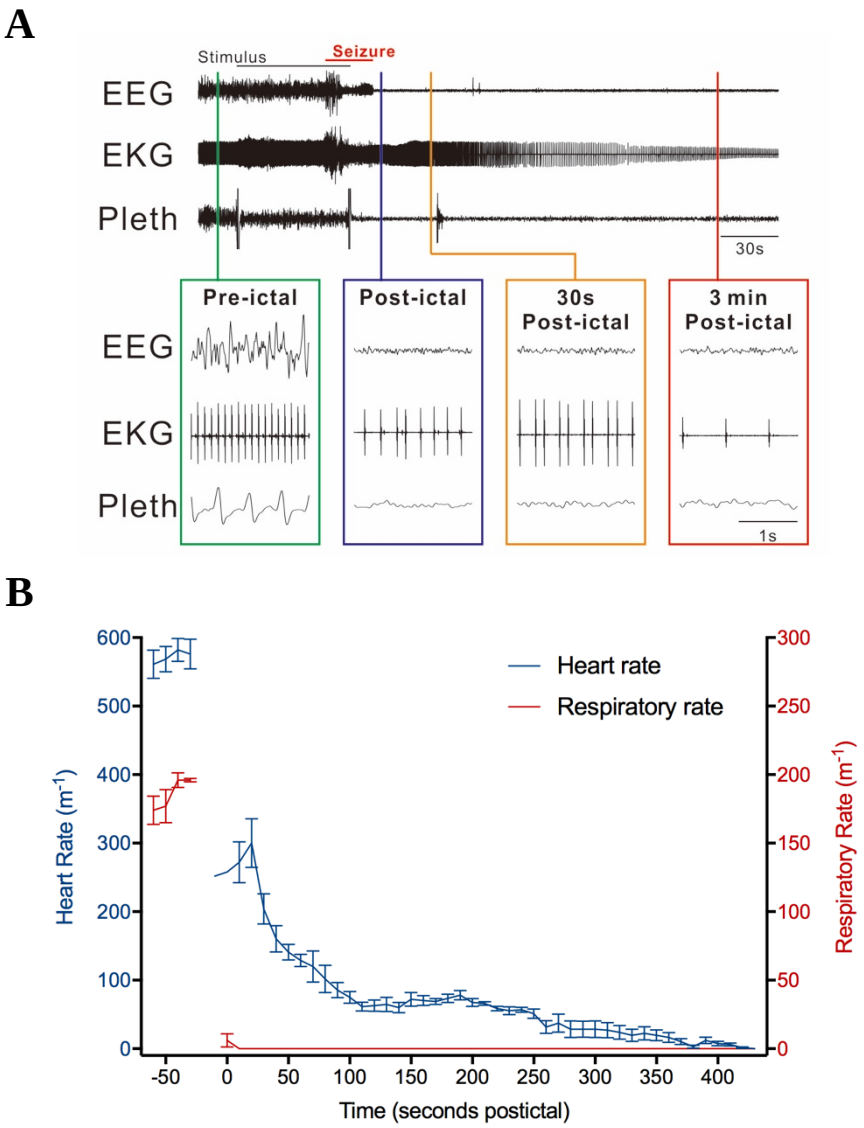

Figure 9. DBA/1 mice with audiogenic seizure induction.
Generalized convulsive seizure (tonic hind limb extension convulsions) induced by an acoustic stimulus generated by an electric bell. (A) 5-minute traces of EEG, EKG and plethysmography pressure of an individual DBA/1 mouse. The seizure induced respiratory arrest immediately, but EKG activity continued for more than 3 minutes after terminal apnea. (B) Post-ictal cardiorespiratory patterns of DBA/1 mice (n=8). Time of zero was defined as the end of seizure.

Lmx1b$^{f/f/p}$ mice with MES seizures

MES stimuli were performed through ear-clip electrodes: 1 or more pulses of 50 - 200 mA peak-to-peak AC current for 0.2 - 5 second stimulus duration. A single MES induction usually did not produce mortality in the *Lmx1b*$^{f/f/p}$ mouse strain. MES induced tonic seizures in all *Lmx1b*$^{f/f/p}$ mice (n=19). However, only eight of these *Lmx1b*$^{f/f/p}$ mice died after multiple MES stimuli. The other eleven *Lmx1b*$^{f/f/p}$ mice did not die despite induction of multiple seizures with a maximum of 10 MES stimuli. The sequence of events leading to post-ictal death in *Lmx1b*$^{f/f/p}$ mice was similar to the sequence of events in DBA/1 mice. An example of a fatal MES-induced seizure in an *Lmx1b*$^{f/f/p}$ mouse is shown in Figure 10A. Electrical noise existed on all EEG, EKG, and plethysmography traces, but it was still possible to measure respiratory frequency and heart rate (see expanded 2-second recordings in Figure 10A). Average traces of heart rate and breathing frequency in post-ictal death *Lmx1b*$^{f/f/p}$ mice (n=8) demonstrated that MES-induced fatal seizures accompanied by tonic extension were followed by immediate and permanent respiratory arrest (terminal apnea) and a decrease in heart rate that slowly worsened over 6 minutes (Figure 10B). Figure 10C shows an example of a surviving *Lmx1b*$^{f/f/p}$ mouse after a MES seizure induction. The stimulus induced a convulsive seizure but the animal resuscitated itself. A brief apnea (< 15s) occurred after the seizure ended, but normal respiratory activity returned 45-second from the end of the stimulus. Note that bradycardia recovered to normal when breathing activity had returned. In other *Lmx1b*$^{f/f/p}$ mice that survived after MES induction, there was either no apnea or a short period of apnea followed by autoresuscitation.

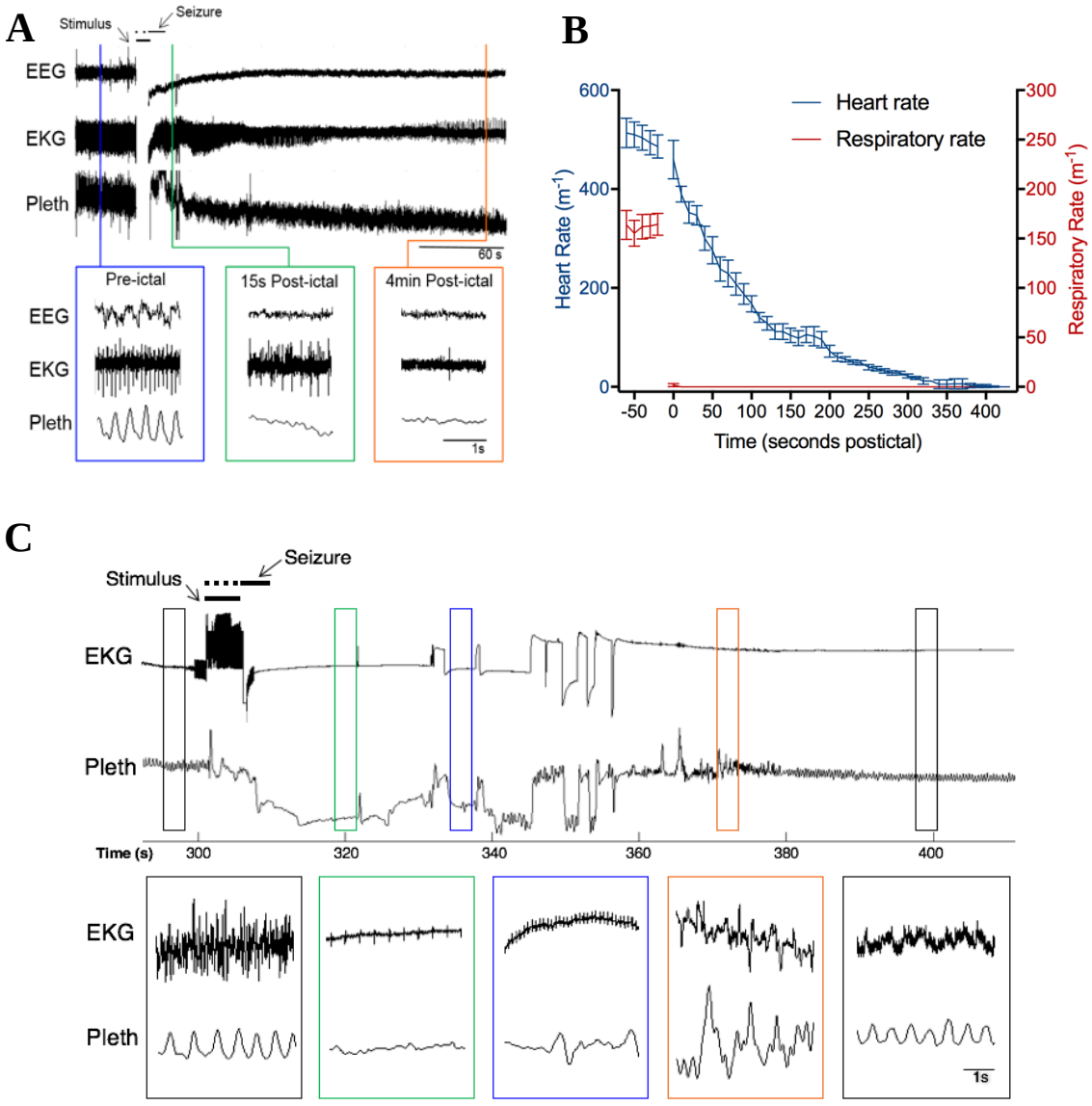

Figure 10. *Lmx1b*$^{f/f/p}$ mice given MES.
(A) 5-minute traces of EEG, EKG and plethysmography pressure of an individual mouse. The seizure induced respiratory arrest immediately, but EKG activity slowed down continuously for more than 4 minutes after terminal apnea. (B) Average traces of heart rate and respiratory frequency in *Lmx1b*$^{f/f/p}$ mice (n=8). Time of zero was defined as the end of seizure. (C) Auto-resuscitation in a surviving *Lmx1b*$^{f/f/p}$ mouse after a seizure. Upper traces show 120-second recordings of EKG and breathing using plethysmography. A seizure was induced by MES. Lower traces show 3-second recordings of EKG and breathing immediately before and four time points after the seizure. Note that the seizure induced abnormal breathing, but the respiratory pattern activity returned to normal 45-second from the end of the stimulus.

C57Bl/6 mice with MES seizures

Seizures were induced by MES through ear-clip electrodes in C57Bl/6 mice (n=8) while animals were monitored in a mouse EMU. 100% of C57Bl/6 mice died after the first trial of MES, in all cases after a tonic seizure. The sequence of events leading to post-ictal death in C57Bl/6 mice was similar to that seen in DBA/1 and *Lmx1b*$^{f/f/p}$ mice. EKG and plethysmography traces from a mouse are shown in Figure 11A. Breathing and heart rate were both normal prior to the seizure. After a MES stimulus (red), the mouse suddenly developed complete apnea that never recovered. There was also a rapid decrease in heart rate shortly after the onset of apnea, but the heartbeat remained above 32-70% of control for 60 seconds after the onset of apnea, and continued for almost six minutes after the end of the seizure with slowly worsening bradycardia eventually leading to terminal asystole. A similar sequence of events was seen in all 8 mice. Complete respiratory arrest always occurred after the seizure. This was slowly followed by bradycardia, and then asystole after 3-6 minutes (Figure 11B).

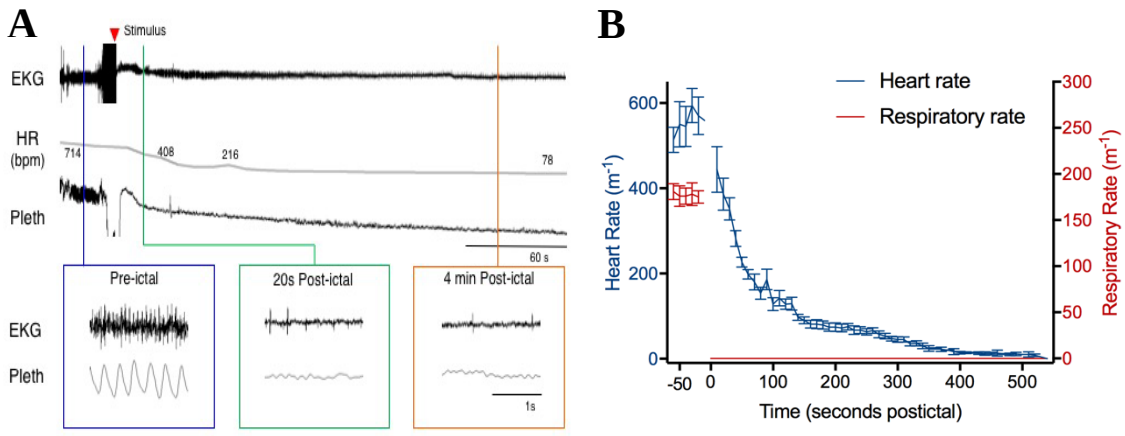

Figure 11. C57Bl/6 mice with MES induction.
(A) Traces of EKG and breathing before and after a seizure. Note that the seizure induced central apnea and bradycardia. (B) Average traces of heart rate and breathing frequency in C57Bl/6 mice (n=8). Time of zero was defined as the end of seizure.

Discussion

I conducted experiments using a specially developed mouse EMU in three mouse strains to detect mouse post-ictal deaths with acutely-induced seizures. The mouse EMU described in this chapter is a powerful method to trace peri-ictal physiological changes of sudden death in mice. I found that fatal seizures always involved terminal apnea in all 3 strains of mice. This apnea occurred during or at the end of the seizure. In contrast, mild to moderate bradycardia often occurred shortly after the onset of apnea, but there continued to be a heartbeat that slowly decreased over time for 3-7 minutes until terminal asystole. I interpret these data as indicating that the primary cause of sudden death was central apnea that began during the seizures and induced secondarily bradycardia due to hypoxia, ultimately leading to terminal asystole.

To provide a better understanding of SUDEP mechanisms, now I plan to expand these methods to epileptic mouse models in which SUDEP occurs spontaneously, since SUDEP in humans is due to spontaneous, not induced seizures. This post-ictal death in mice is likely to be relevant to the mechanisms of SUDEP in epilepsy patients. In Chapter 3, a DS mouse model with a $Scn1a^{R1407X/+}$ mutation had been studied to determine the role of respiratory dysfunction in post-ictal deaths.

CHAPTER 3: POST-ICTAL RESPIRATORY DYSFUNCTION IN DRAVET SYNDROME

Introduction

Dravet Syndrome (DS) is an infantile-onset epilepsy with severe seizures commonly due to SCN1A mutation. The effective treatments are unknown for DS patients with refractory seizures, and DS patients have a high risk of SUDEP. The mechanisms of death are not well defined, but are widely believed to be due to post-ictal bradycardia progressing to asystole (Massey et al., 2014). From the results of post-ictal deaths in multiple non-epileptic mouse strains of Chapter 2, it had been hypothesized that the respiratory arrest is also the primary cause of post-ictal death in DS mice. In this chapter, DS patients and mice with an *Scn1a*$^{R1407X/+}$ mutation (Ogiwara et al., 2007) had been studied to evaluate a potential role of post-ictal breathing dysfunction in SUDEP.

Background

DS was briefly introduced in Chapter 1. Febrile seizure is the most common seizure for children and DS patients are highly susceptible to febrile seizure (Hessel et al., 2009). Clinical data have pointed to cardiac mechanisms being important for SUDEP in DS. For example, mutations of *SCN1A* in patients with DS cause increased QT and P wave dispersion and a decrease in heart rate variability (Delogu et al., 2011; Ergul et al., 2013). However, there are no published reports of EKG changes after fatal or non-fatal generalized seizures in patients with DS, other than a single case report after status epilepticus (Daverio et al., 2016). Post-ictal breathing has not been measured in DS patients.

Since SUDEP is always identified after death and is impossible to predict its incidence, it is practically impossible to run clinical trials in patients. Therefore, developing animal models of SUDEP is beneficial. Mice with mutations of SCN1A have seizures that occur spontaneously and in response to hyperthermia, similar to patients with DS. Seizures in DS mice can be followed by death (Auerbach et al., 2013; Kalume et al., 2013; Oakley et al., 2009), and this post-ictal death is likely to be relevant to the mechanisms of SUDEP in DS patients. Nav1.1 is expressed in the sinoatrial node (Maier et al., 2003), and cardiac myocyte dysfunction has been reported in mice with an *Scn1a*$^{R1407X/+}$ mutation (Auerbach et al., 2013). EKG recordings from Scn1a heterozygous KO mice have shown that post-ictal death after heat-induced seizures is due to progressive bradycardia and asystole (Kalume et al., 2013). Bradycardia and death can be prevented by pretreatment with atropine (1 mg/kg), which has led to the conclusion that death in DS mice is due to either increased vagal parasympathetic output to the heart (Kalume et al., 2013) or to a cardiac arrhythmia (Auerbach et al., 2013; Cao et al., 2012). However, measurements of breathing have not been performed during spontaneous or heat-induced seizures in DS mice, so it is not known whether changes in respiratory output contribute to post-ictal death.

The effective treatments are unknown for DS patients with refractory seizures, and DS patients have a high risk of SUDEP. The mechanisms of SUDEP are not well defined. Since SUDEP is always identified after death and is impossible to predict its incidence, it is practically impossible to run clinical trials in patients. Therefore, developing animal models of SUDEP is beneficial. In a DS mouse model with a

Scn1a$^{R1407X/+}$ mutation, death occurs after spontaneous and induced seizures. This post-ictal death is likely to be relevant to the mechanisms of SUDEP in DS patients.

The principal risk factor for SUDEP is a high frequency of seizures. Despite the sharp increase in research on SUDEP mechanisms in the past decade, it is still not clear whether cardiac and/or respiratory dysfunction is the primary cause of SUDEP. The recent MORTEMUS reported 11 cases of SUDEP while in EMUs (Ryvlin et al., 2013). None of the SUDEP cases had direct measurements of breathing, but visual analysis of video recording suggested that apnea occurred early in the sequence of events preceding death.

Previous work in DS mouse model has focused only on the effect of cardiac dysfunction in post-ictal death with evidence of EKG recordings without respiratory analysis (Kalume et al, 2013). Since breathing was not recorded during many of the case reports and other studies, it is possible that in some cases, respiratory dysfunction, such as central apnea, could be the primary cause of death and cardiac dysfunction would be then secondarily to the resulting hypoxemia.

Methods

Monitoring of DS patients with video EEG telemetry

All experimental protocols were approved by the Northwestern University Institutional Review Board and performed under the direct supervision of a faculty neurologist. Patients were admitted to the Pediatric EMU at Lurie Children's Hospital in Chicago, IL for routine video-EEG monitoring of refractory seizures. Seven patients with DS were selected for video analysis along with seven patients with localization-related epilepsy. Respiratory movements were difficult to visualize in some of these

video recordings. Therefore, visualization of these movements was enhanced using phase-based Eulerian video magnification motion processing with MATLAB open-source software developed by a group at MIT (Wadhwa et al., 2013). Video motion magnification processing was performed on video recordings with amplification of 4X or 10X, applying a bandpass filter of 0.05-3Hz.

To better visualize breathing in video images, a vertical line was drawn through a part of the body that appeared to show the largest movements. Using a custom-written MATLAB script, the color value was determined at each point along the vertical line for each frame of a video. These values were used to create a still image with time (consecutive video frames) represented on the x-axis, vertical location on the y-axis and color in relative units on the z-axis (Figure 12). The breathing trace in this spatiotemporal YT slice was rendered more apparent by converting the image to grayscale and enhancing the contrast. The most visible single breathing trace was selected by cropping the spatiotemporal YT image (Figure 12C) or drawing a line along the center of the trace (Figure 12E) using image editing software (Corel PhotoPaint).

In a single patient (Figure 16) video monitoring was supplemented with measurements of breathing using respiratory impedance plethysmography (RIP; Piezo Crystal Respiration Effort Sensors, SleepSense, Elgin, IL), $tcCO_2$ and SaO_2 (Sentec Digital Monitoring System, provided by SenTec AG, Therwil, Switzerland), EKG and EEG.

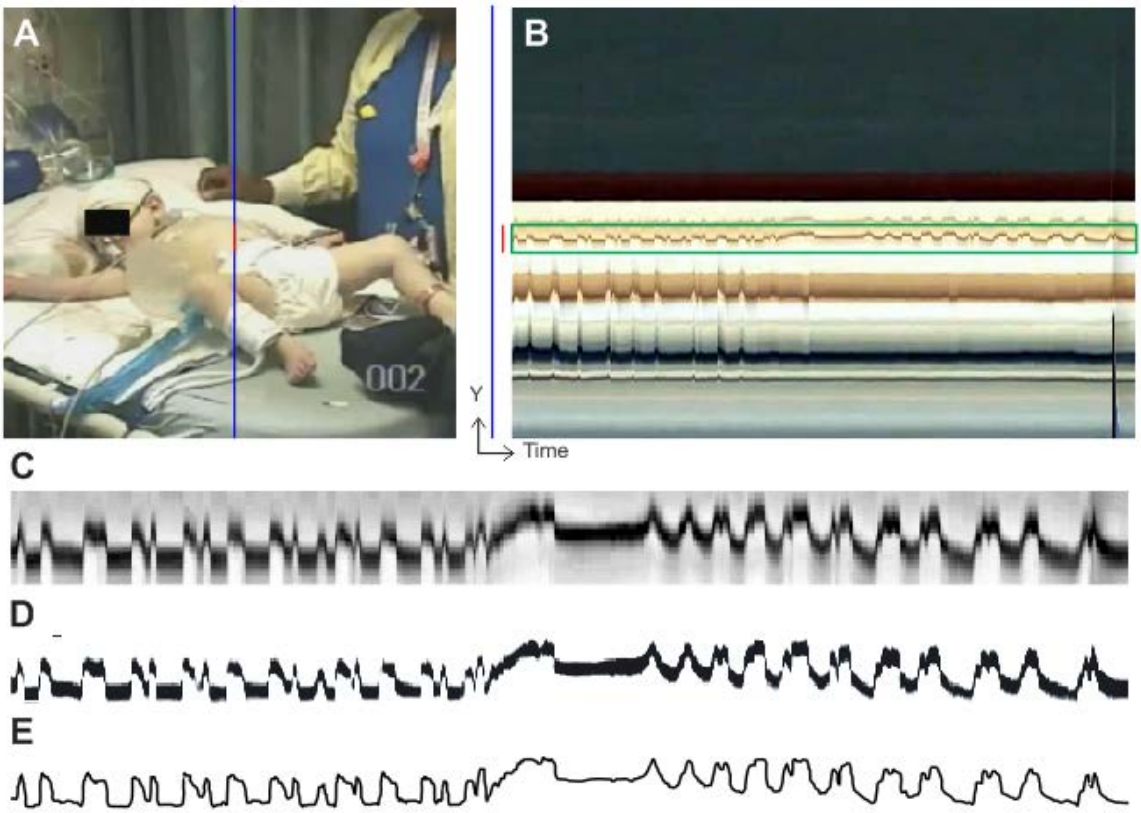

Figure 12. Schematic of respiratory trace extraction.
Method used to analyze respiratory movements in videos of DS patients. (A) A region of interest was chosen from a frame of a video image (in this case a vertical blue line). (B) A plot was generated with y-axis representing the color values extracted for each pixel along the region of interest, and the x-axis representing successive video frames of the video (or time with video frame rate of 24 Hz). A band was then chosen where respiratory movements were maximized (in this case the box drawn around the umbilicus, which moved up and down with each breath). (C) Enlargement of the chosen band after conversion to grayscale image and contrast adjustment. (D) Movement of umbilicus clarified by cropping of surrounding image and conversion to black and white. (E) A line was drawn down the middle of the black region in D to obtain a line drawing of breathing movements.

DS mouse model (Scn1a$^{R1407X/+}$ mice)

The *Scn1a*$^{R1407X/+}$ mutant mouse strain was made to resemble human Dravet syndrome in its progressive severe seizures and high rate of death. Generation and genotyping of heterozygous SCN1A-R1407X knock-in mice have been previously described (Ogiwara et al.,2007; Auerbach et al., 2013). Briefly, genetically engineered

mice, R1407X, in the Scn1a gene, are identical to the human Dravet syndrome mutation. $Na_v1.1$ haploinsufficiency from the absence of truncated mutant $Na_v1.1$ in their brain causes epileptic recurrent seizures in these mice.

To increase litter size in our lab, a pair of *Scn1a*^{R1407X} heterozygous mutant male mice (maintained on the C57Bl/6J background), were obtained from the University of Michigan (PI: Miriam H. Meisler), were backcrossed with C3HFeB/HeJ (Jackson Laboratory, Bar Harbor, ME). Breeding and genotyping of these mice have been previously described (Auerbach et al., 2013). DS mice were genotyped by PCR amplification with the primers DS-F (5' CAATGATTCCTAGGGGGATGTC 3') and DS-R (5'GTTCTGTGCACTTATCTGGATTCAC 3'). Digestion of the PCR product with HpaII generated 2 fragments, 295 and 223 bp, from the wildtype allele and an uncut 518 bp fragment from the mutant allele. Genomic DNA was PCR amplified, digested with HpaII, and separated on 2% agarose gels containing 0.15 μg/ml ethidium bromide. Male and female heterozygous mutant mice were used in this dissertation to identify the primary cause of death after MES and heat-induced and spontaneous seizures in this chapter, were also used in the dietary therapy study (Chapter 4). Heterozygous *Scn1a*^{R1407X} mice are designated as DS mice throughout this manuscript.

Long-term EMU recording

Implantation of EEG/EMG/EKG headmount and activity/body temperature telemetry were described in Chapter 2. Using the same setting of the mouse EMU in Chapter 2, prolonged mouse EMU recordings were required to detect mouse deaths with spontaneous seizures. Mouse EMU data were continuously stored in an external hard drive (DRDR5A21-20TB, DroboWorks.com, Irvine, CA). When a mouse died, the

monitoring system was terminated and was used to assess the cause of death. In one set of experiments, DS mice (n=19) were monitored for 195 mouse-days inside of a mouse EMU, two mice died spontaneously.

Heat-induced seizure deaths in a DS mouse model

In a second set of experiments, DS mice (n=7) were used to study acute seizures by thermal seizure induction. Mice were instrumented with headmounts and telemetry probes. Mice were then placed in the mouse EMU chamber and allowed to recover for 30 minutes. Animal body temperature was gradually increased with a heat lamp placed next to the mouse EMU chamber, controlled by a feedback controller (TCAT-2AC; Physitemp Instrument, Clifton, NJ). The heat-lamp challenge was given to increase the body temperature of 43°C or until a generalized seizure with tonic hind-limb extension was exhibited. Animal body temperature was monitored by telemetry probes (IPTT-300; BMDS, Seaford, DE), implanted into the abdominal cavity at the time of headmount surgery (at least 5 days before recordings).

MES-induced seizures and ventilatory support

In a third set of experiments, DS mice (n=13) instrumented with headmounts and telemetry probes seizures were also induced by MES (described in Chapter 2) while animals were being monitoring under an mouse EMU. In a fourth set of experiments, outside of the mouse EMU, DS mice were resuscitated after a MES-induced seizure by placing Tygon tubing over the snout and inflating the lungs with air using a mechanical ventilator as described in Chapter 2. This rodent mechanical ventilator was used if there was a prolonged post-ictal period without chest movement (>5 seconds).

Spectrogram data analysis using short-time Fourier transform

Time-frequency power spectrum analysis was performed with MATLAB based on a short-time Fast Fourier Transform (FFT). An overview of the short-time FFT method with an example of EKG is showed in Figure 13. The time-dependent power spectrum density of the signal was computed and displayed with discrete-time sections calculated for each 0.5 second interval. Sections overlapped by 20% to smooth the signal. The EKG sampling rate was 1 kHz, while EEG, EMG, and plethysmography were sampled at 100 Hz.

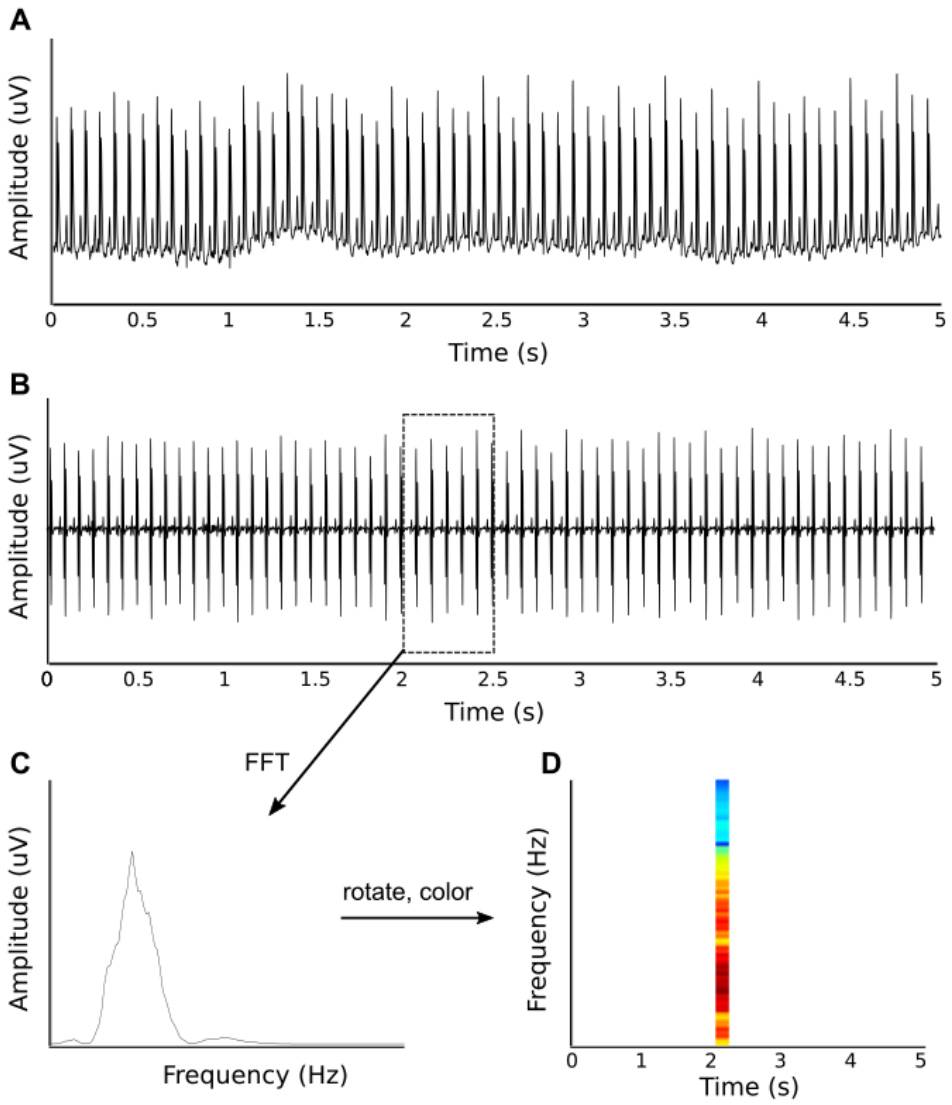

Figure 13. Overview of the short-time FFT method.
(A) An example of time series EKG raw data was plotted. (B) A continuous wavelet transform (CWT) was applied into the data shown in A. Edge artifacts and a linear trend from the raw data were removed. A small section of the data (0.5 s) is taken (dotted box) to apply short-time Fast Fourier Transform (FFT). (C) The Fourier transform of the time series section taken in B. (D) The power spectrum of that section was placed into a time-frequency space with the frequencies corresponding to that of the FFT and the time point corresponding to the time section from B. The power intensity is displayed in color.

Statistical analysis

Abnormal breathing in DS patients was compared to localization-related epilepsy patients (Table 1) using a Chi square test. Statistical comparisons of seizure severity and duration were made using a Mann-Whitney U Test with an overall significance level set to $p<0.05$ (GraphPad Prism V6.01). When data is presented as X ± Y, X is the group mean and Y is the standard deviation. All error bars represent the standard error of the mean.

Results

Post-ictal respiratory dysfunction in DS patients

In the previous observation, post-ictal abnormal breathing patterns were evaluated by a neurologist (George B. Richerson) from video recording of generalized seizures from seven DS patients and seven patients with localization-related epilepsy blind to the cause of epilepsy. These recordings did not include direct measurements of airflow or other breathing parameters, but visualization of chest and abdomen movements, aided by Eulerian video magnification, was possible to evaluate breathing patterns and frequency.

DS patients were significantly more likely to have post-ictal abnormal breathing consistent with disturbances of respiratory rhythm generation or patterned output (Table 2; $p=0.018$, Chi-square test), including paradoxical breathing, inspiratory efforts with two or three peaks (respiratory bigeminy or trigemini), ataxic breathing or apnea of 5 s or longer (Figure14-16). Many patients produced loud sounds on expiration consistent with airway obstruction, but this was not significantly more common in either group (Table 2). In all of these cases, breathing abnormalities were transient and all patients survived the post-ictal events.

Table 2: Patients with Dravet Syndrome have abnormal breathing patterns after seizures.

	Dravet Syndrome	Localization-related epilepsy
Respiratory rhythm disturbance		
Yes	4	0
No	3	7
Loud post-ictal upper airway sounds*		
Yes	1	3
No	6	4

* noisy expiration, stertor, and grunting

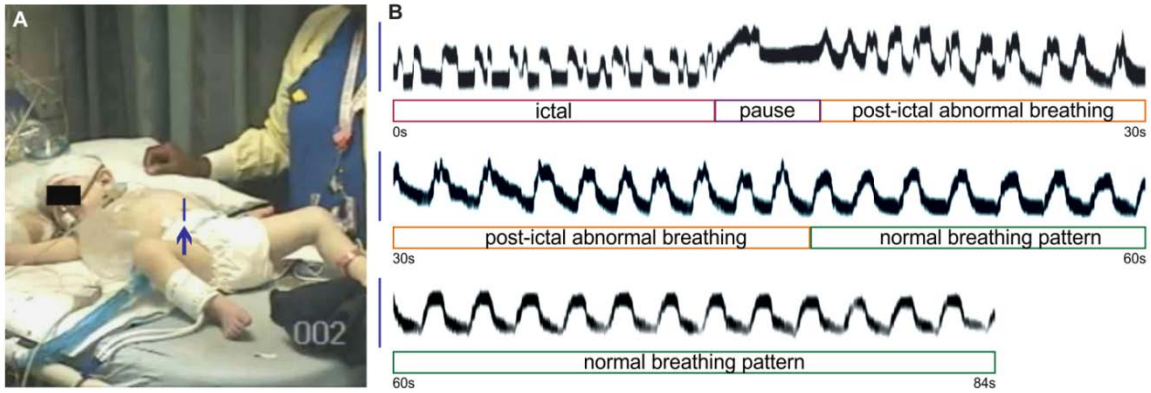

Figure 14. Seizures induce ataxic breathing in a DS patient.
Irregular breathing during and after a seizure. Video frame (A) from Supplementary Video 1 showing region of interest (vertical line pointed to by arrow) used to visualize respiratory movements. Using the methods illustrated in Figure 12, respiratory movements were plotted during and after a generalized seizure (B; traces are contiguous). During the seizure (1st 13 seconds) most inspirations had more than one peak. Immediately after the seizure there was a respiratory pause followed by continued abnormal inspirations lasting until 32 seconds post-ictal. A normal breathing pattern then resumed with regular, monophasic inspiratory efforts. The video of this patient can be played from Supplementary Video 1.

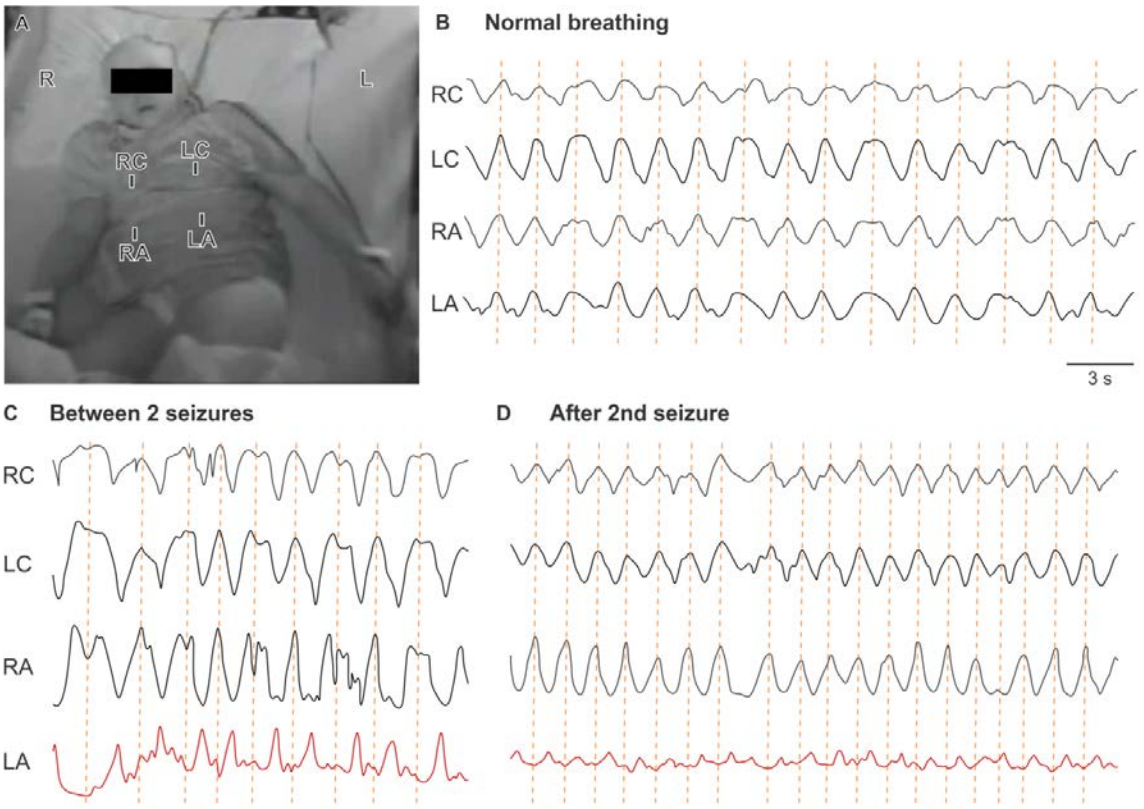

Figure 15. Severe paradoxical post-ictal breathing in a DS patient.
(A) Video frame illustrating four separate regions of interest for analysis of respiratory movements. (B) Normal breathing movements from the four regions of interest. Analysis was performed as illustrated in Figure 12, except that a single line was used to illustrate breathing movement for each region of interest. Note that breathing occurs in phase for each quadrant of the torso (vertical dashed lines). (C) Breathing between two convulsive seizures. Note that breathing is irregular and erratic, and that movements at LA are 180 degrees out of phase with the other three quadrants. (D) Breathing after second convulsive seizure. Note that the LA movements are now much smaller and remain out of phase. RC & LC – Right and left chest. RA & LA – Right and left abdomen. The video of this patient can be played from Supplementary Video 2.

A nine year old girl with DS and an associated de novo missense mutation of *SCN1A* was admitted for recording of video-EEG, along with EKG, respiratory impedance plethysmography (RIP), and transcutaneous CO_2 ($tcCO_2$). Interictal plethysmography revealed normal, regular breathing (Figure 16), with $tcCO_2$ of 44 mmHg. The patient had an asynchronous convulsive event off camera. Subsequently, while on camera, the patient had three asynchronous convulsive seizures, each lasting one

minute and separated by 2-3 minutes. Between seizures the patient's eyes were open, but she had a limited response to verbal and tactile stimuli. After each seizure, the patient took a deep breath, closed her eyes, and then developed noisy, labored and paradoxical breathing along with periods of apnea lasting up to 13 seconds (Figure 16 C-E). Oxygen desaturation occurred and was treated with O_2 delivered by a non-rebreather mask at an initial rate of 15 LPM and subsequently adjusted to keep O_2 saturation > 92%. $tcCO_2$ showed a steady increase to 70 mmHg over 60 minutes. After a painful stimulus, the patient aroused and $tcCO_2$ slowly declined but remained greater than 50 mmHg for an additional 3 hours before returning to baseline. During most of the four hours in which $tcCO_2$ was elevated, the patient continued breathing at a rate of 18-22 without apnea (Figure 16E). However, the elevated $tcCO_2$ indicated there was marked hypoventilation. This case was remarkable for such prolonged post-ictal impairment of respiratory CO_2 chemoreception. Three years after this recording was made the patient died of SUDEP, being found face down in bed, blue and pulseless.

Taken together, these data indicate that some patients with DS have post-ictal respiratory dysfunction, including defects in respiratory rhythm generation, impaired central CO_2 chemoreception, and loss of airway patency. In the nonfatal episodes documented here, these changes were transient, but the severe defects in breathing in the patient who died of SUDEP suggest these changes may be biomarkers of patients at high risk.

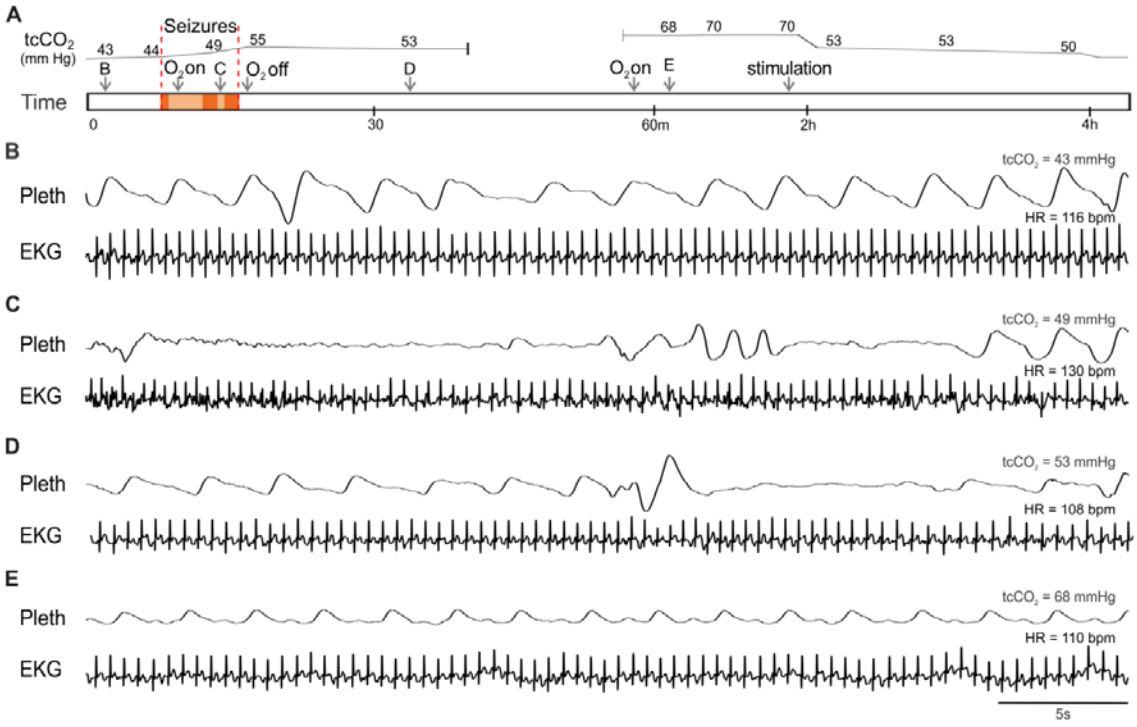

Figure 16. Prolonged post-ictal hypoventilation in a DS patient.
(A) Schematic of events while recording cardiorespiratory activity during and after a seizure in a 9 year old girl with DS. The numbers above the upper line in A are measured values of $tcCO_2$. The upper line shows the approximate time course of the changes in $tcCO_2$. Arrows labeled "B-E" denote the time of recordings shown in B-E. Arrows also denote when supplemental O_2 was administered or discontinued, and when the patient was stimulated to cause arousal. Orange shading denotes nonconvulsive seizures and red shading denotes convulsive seizures. (B-E) Respiratory impedance plethysmography (Pleth) and EKG during normal breathing when $tcCO_2$ was 43 mmHg (B), between convulsive seizures (C), after the seizure when $tcCO_2$ had risen to 53 mmHg (D), and 44 minutes after the seizure when $tcCO_2$ had risen to 68 mmHg (E). At 2 hours, $tcCO_2$ decreased when the patient was stimulated to arouse, but did not return to baseline until 4 hours.

Spontaneous seizures caused death in *Scn1a*$^{R1407X/+}$ mice

Heterozygous *Scn1a*$^{R1407X/+}$ knock-in (DS) mice, which express a mutation described in three unrelated DS patients, were used to define the cause of death after seizures. While continuously monitoring *Scn1a*$^{R1407X/+}$ mice in a custom-designed mouse EMU, two mice died from spontaneous fatal seizures. In an example shown in Figure 17, tonic extension was accompanied by seizure activity on the EEG. Breathing and heart rate were both normal prior to the seizure. There were movement artifacts shown during the seizure, but it was still possible to measure respiratory frequency and heart rate. During the seizure, the mouse suddenly developed complete apnea that never recovered. There was also a rapid decrease in heart rate shortly after the onset of apnea, but the heartbeat remained above 25-51% of control for 60 seconds after the onset of apnea, and continued for almost four minutes after the end of the seizure with slowly worsening bradycardia eventually leading to terminal asystole. A similar sequence of events was seen in a second mouse (Figure 18). These observations suggest that post-ictal respiratory arrest played a key role in the death of these animals. Notably, the EEG rapidly became flat after the seizure, consistent with PGES (Lhatoo et al., 2010).

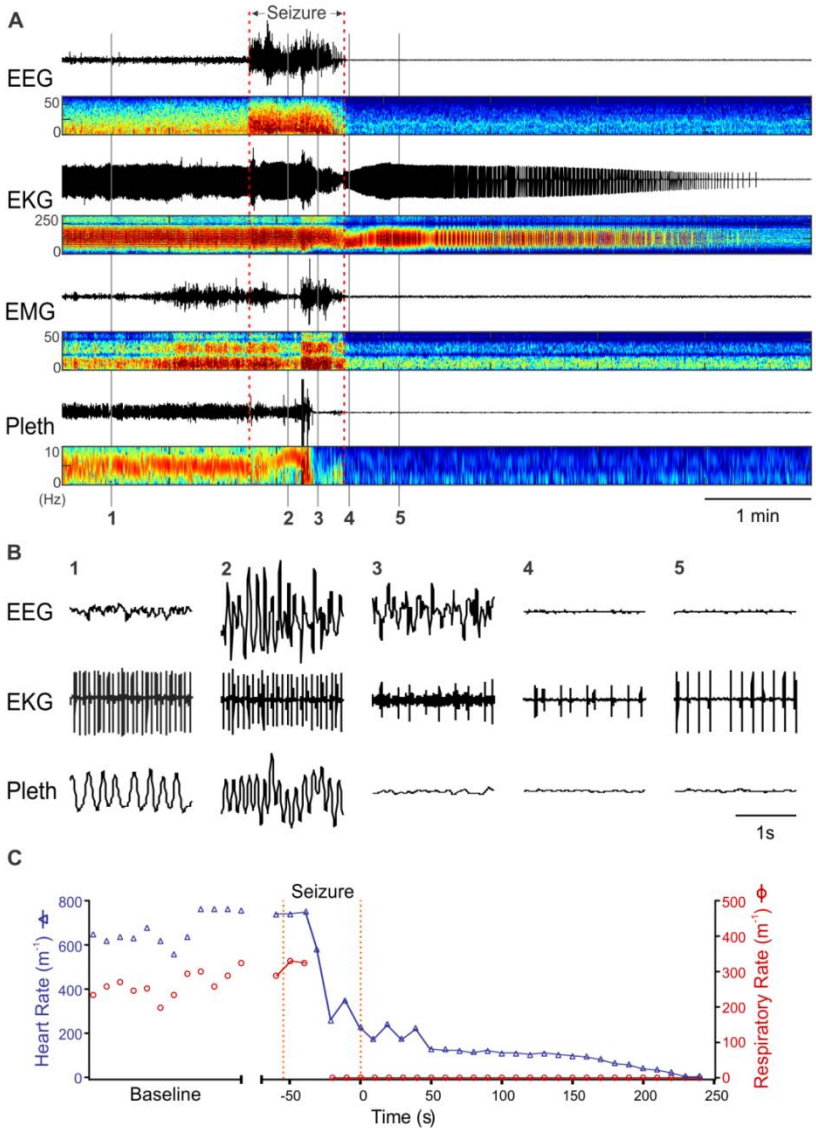

Figure 17. Death of a DS mouse (P40) after a spontaneous seizure.
Post-ictal death was due to respiratory arrest followed by secondarily bradycardia. (A) Events leading to death. Traces from top down are EEG, EKG, EMG and whole animal plethysmography, in each case with paired power spectrum heat maps. A spontaneous seizure occurred at the time indicated, and this was followed by PGES in the EEG. Shortly after the onset of the seizure breathing became disrupted, seen best on the plethysmography heat map. Respiratory activity ceased halfway through the seizure. In contrast, the EKG did not change until near the end of the seizure, after which the frequency and amplitude slowly decreased over the next four minutes. (B) Expanded traces of EEG, EKG and plethysmography at the times labelled 1-5. (C) Respiratory rate and heart rate for the data shown in (A & B). Data is discontinuous during the baseline period, because accurate measurements could be made only when the mouse was resting quietly. Data points are continuous from the onset of the seizure, except for one data point during which breathing was obscured by movement artifact.

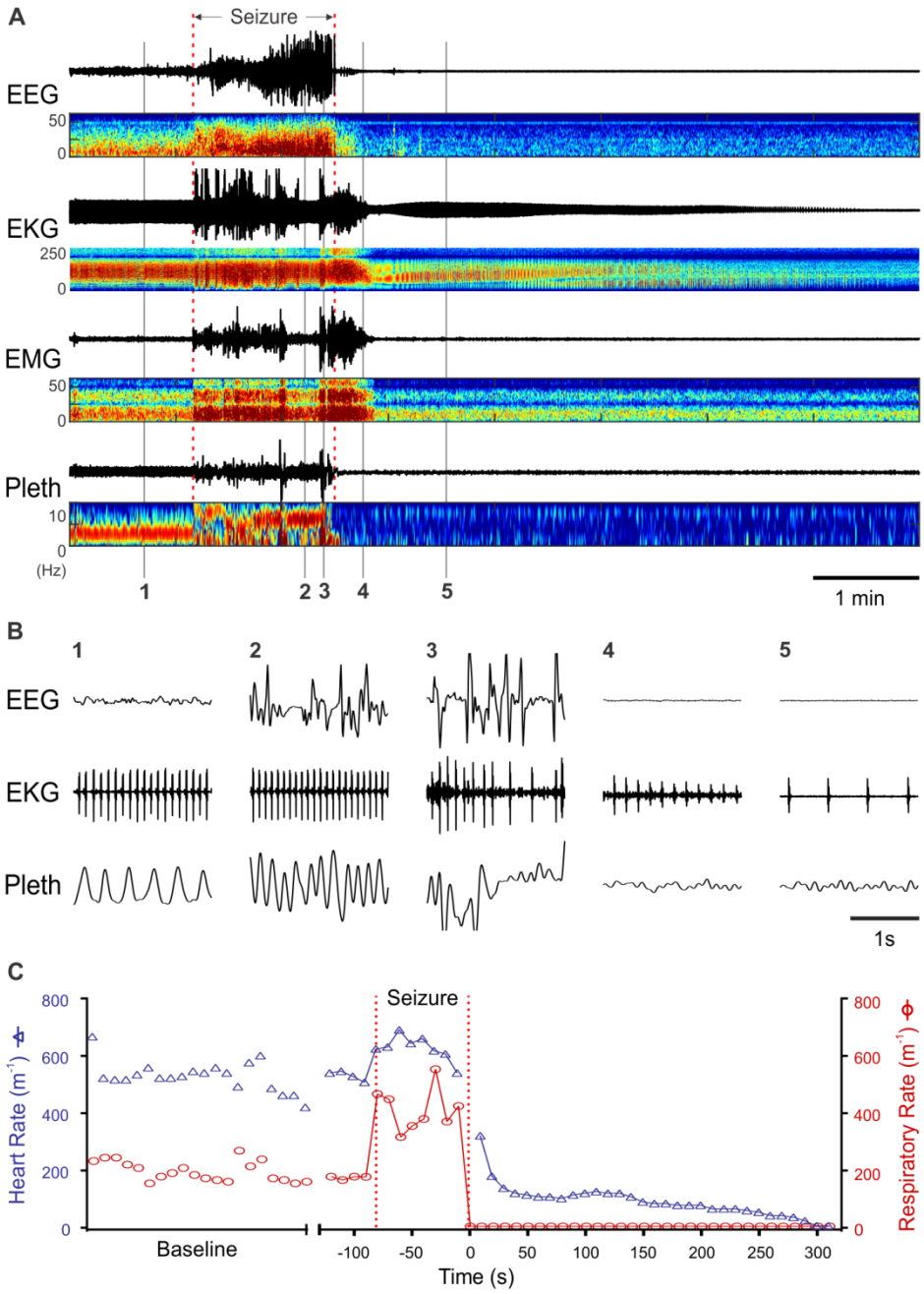

Figure 18. Post-ictal death after a spontaneous seizure in a 2nd DS mouse (P24). (A) Physiological recordings with corresponding power spectrum heat maps (using same format as Figure 17) showing events leading to death. Breathing became disrupted shortly after the onset of the seizure. In contrast, bradycardia began later and terminal asystole did not occur until nearly 5 minutes after the end of the seizure. (B) Expanded traces of EEG, EKG and plethysmography from times marked by vertical lines labelled in A as 1-5. (C) Plot of breathing and heart rate for the data in A.

Heat-induced seizures also caused respiratory arrest in *Scn1a*$^{R1407X/+}$ mice

As in DS patients (Dravet, 2011), an increase in body temperature can induce seizures in *Scn1a*$^{R1407X/+}$ mice (Cao et al., 2012) and *Scn1a* knockout mice (Kalume et al., 2013). It has been reported that heat-induced seizures in DS mice lead to bradycardia followed by death (Kalume et al., 2013). However, breathing has not been measured under those conditions. Here we verified that a rise in body temperature above 43 °C induced seizures in *Scn1a*$^{R1407X/+}$ mice, eventually leading to death in all 7 mice after 4±2 seizures. As reported previously with fatal heat-induced seizures in *Scn1a* knockout mice (Kalume et al. 2013), tonic extension was followed by a gradual decrease in heart rate, eventually resulting in terminal asystole (Figure 19). However, plethysmography revealed that fatal heat-induced seizures also always involved terminal apnea, when bradycardia developed more slowly. This apnea usually occurred precipitously during the seizure or within seconds of the end of the seizure. In contrast, mild to moderate bradycardia often occurred shortly after the onset of apnea, but there continued to be a heartbeat that slowly decreased over time with terminal asystole not occurring until 3.89 ± 0.92 minutes after the end of seizures.

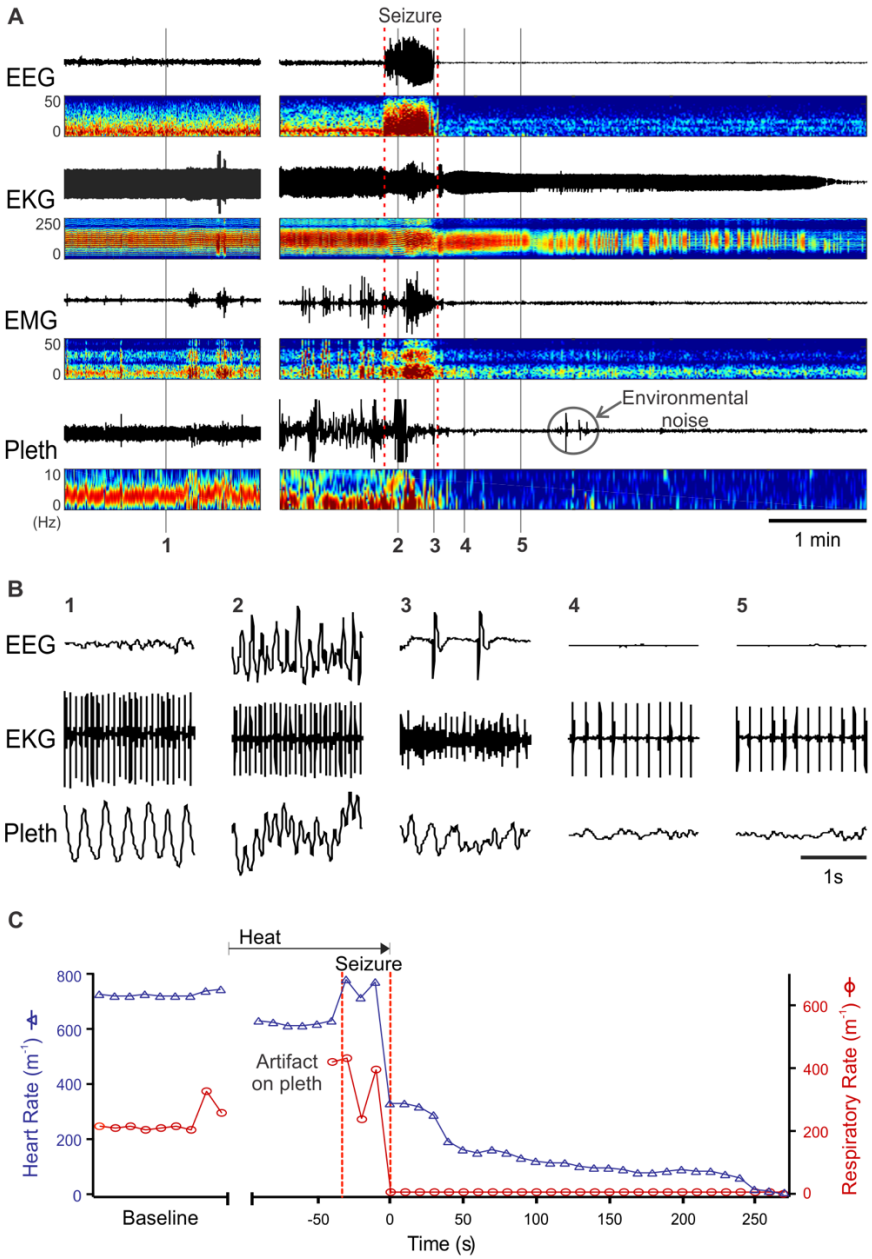

Figure 19. Death of a DS mouse after heat-induced seizure.
Post-ictal death was also due to respiratory arrest followed by bradycardia. (A) Events leading to death. Data are shown in same format as in Figure 17. Traces are discontinuous to show baseline recordings prior to hyperthermia. At the time indicated, a seizure occurred after the animal's temperature had increased to 38.9 ^{0}C. After the seizure, PGES was seen on the EEG. Towards the end of the seizure, breathing became erratic, and then respiratory activity suddenly ceased. The EKG showed a rapid decrease in heart rate at the end of the seizure, after which the frequency and amplitude slowly decreased over the next four minutes. (B) Expanded traces of EEG, EKG and plethysmography at the times labelled 1-5. (C) Respiratory rate and heart rate for the data shown in (A & B). Data points are discontinuous prior to the seizure due to movement artifact.

The duration and severity of fatal seizures in both heat-induced seizures and spontaneous seizures have been compared (Figure 20). The duration of spontaneous fatal seizures (n=2) was 67.0 ± 18.4 seconds and the mean EEG power between 0.5 and 20 Hz (as a measure of seizure severity) was 0.040 ± 0.020 power/s. In contrast, the duration of fatal heat-induced seizures (n=7) was 25.7 ± 9.2 seconds and the mean EEG power was 0.083±0.026 power/s. These differences were not statistically significant (Mann-Whitney U Test).

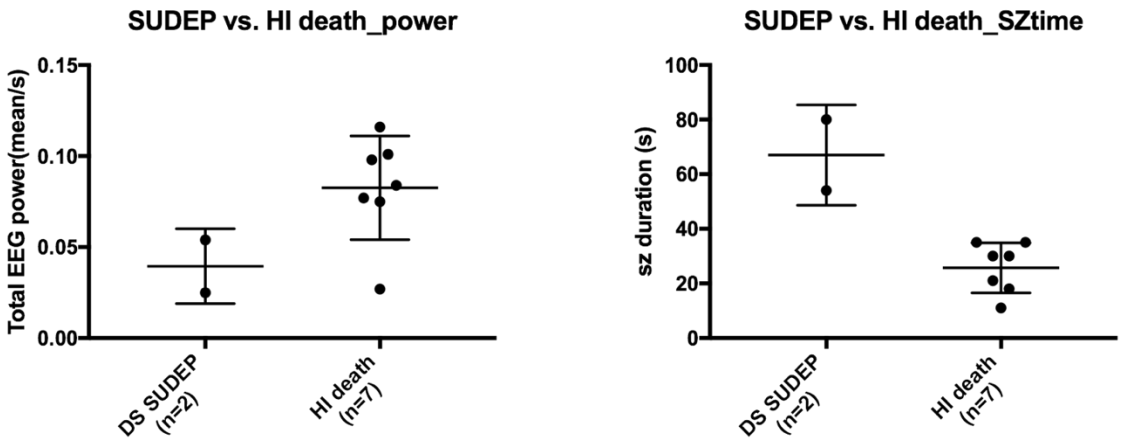

Figure 20. Comparison of seizure severity and duration.
The severity and duration of fatal seizures (a measure of mean EEG power) in each individual mouse were compared between spontaneous seizure vs. heat-induced seizure. There is no statistical difference in the fatal seizure severity and duration between spontaneous and heat-induced deaths in DS mice.

Post-ictal death and survival after a MES seizure induction

A group of DS mice (n=13) were instrumented with headmounts and telemetry probes. MES applied while animals were monitored under a mouse EMU induced generalized seizure in all DS mice. However, only 3 of these mice died, and in each case this occurred after the first seizure (Figure 21A). The other 10 DS mice did not die despite induction of between 1 and 12 tonic seizures. In DS mice that survived, there was

either no apnea (n=8) or a short period of apnea followed by auto-resuscitation (n=2) (Figure 21B).

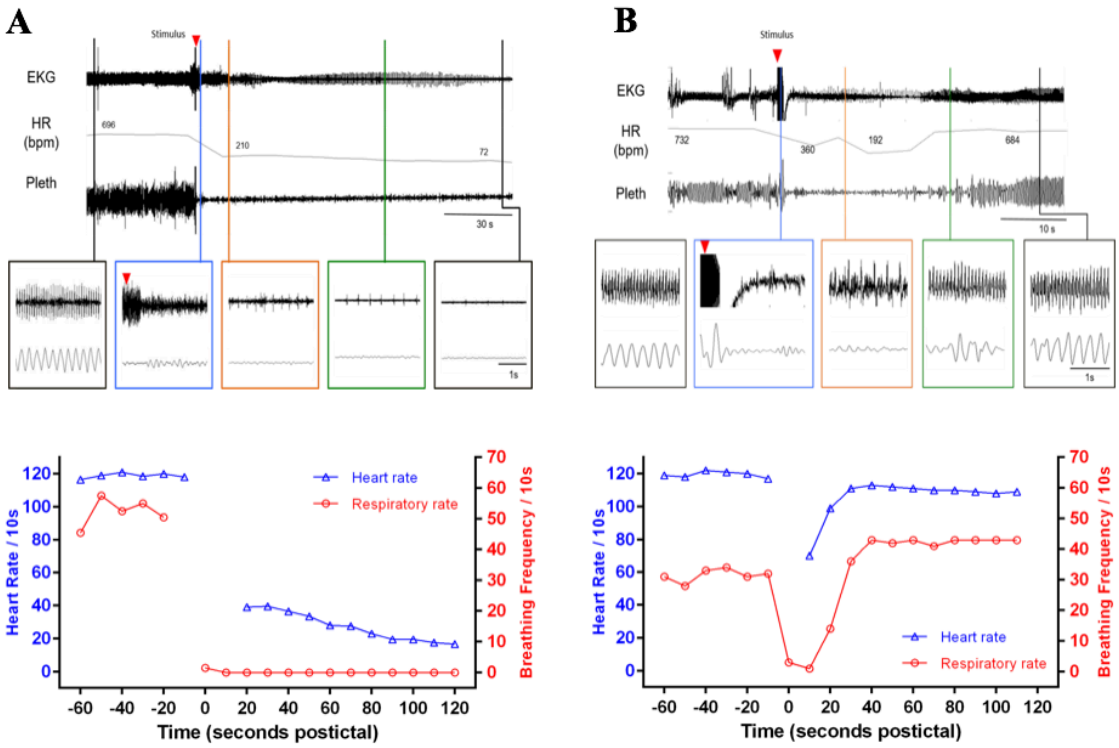

Figure 21. MES seizure induction in DS mice.
(A) A post-ictal death after MEA induction in a DS mouse. (A-Top) Traces of EKG and breathing before and after a seizure. Note that the seizure induced central apnea and bradycardia. (A-Bottom) A trace of heart rate and breathing frequency in the same animal (Top). Time of zero was defined as the end of seizure. (B) Auto-resuscitation in animal surviving from a seizure. B-Top: Traces of EKG and breathing before and after a seizure. B-Bottom: A trace of heart rate and breathing frequency in the same animal (Top). The seizure induced bradycardia and a short period of apnea, but the cardiac and respiratory activities fully recovered 20 and 35-second from the end of the stimulus, respectively. Time of zero was defined as the end of seizure.

Respiratory support from mechanical ventilator prevented deaths

In one set of experiments, heat-induced seizures were applied in DS mice outside of the EMU. In some mice, death could be prevented if mechanical ventilation was initiated within 5-10 seconds of the onset of apnea using a rodent ventilator (MiniVent

type 845; previously described in Chapter 2) connected to plastic tubing placed over the mouse's nostrils (n=5 mice).

In a different set of experiments, a single seizure was induced by MES (60 mA / 0.2 s) outside of the EMU in a separate cohort of DS mice (n=34) and litter mates, but these seizures were less likely to cause apnea (four episodes of apnea after seizures in 34 mice- Table 3). When apnea occurred, death was prevented by mechanical ventilation in three out of four mice. No deaths occurred due to cardiac arrest in any of the above experiments without apnea.

Table 3: MES-induced seizures in DS mice and litter mates WT.

	Seizure	Post-ictal apnea	Resuscitation
DS (n = 34)	34	4 (11.7 %)	3
WT (n = 9)	9	1 (11.1 %)	1

Discussion

Here I show that patients with DS have post-ictal breathing dysfunction, including ataxic respiratory output, paradoxical breathing, stridor and prolonged depression of CO_2 chemoreception that lasted as long as 4 hours. The respiratory abnormalities I recorded were reversible, but one child with particularly severe and prolonged post-ictal hypoventilation later died of SUDEP. These results suggest that post-ictal ventilatory abnormalities contribute to SUDEP in patients with DS, and may be a biomarker for those at highest risk. DS mice were chosen because they closely recapitulate SUDEP in DS patients. Death in a mouse with spontaneous seizures meets the criteria for SUDEP and may be directly related to the mechanism of SUDEP in humans. I detected a number of DS mice in which death occurred after a spontaneous and MES / hypoxia-induced

seizures. I found that our DS mice died due to post-ictal central apnea followed by progressive bradycardia, and death could be prevented with mechanical ventilation. Time course of EKG and breathing patterns in MES / hypoxia-induced mice were similar to that seen in post-ictal spontaneous death of DS mice (Figure 17).

It has previously been reported that post-ictal death in mouse models of DS is due to severe bradycardia caused by an increase in vagal parasympathetic tone. This conclusion was supported by data showing that death was prevented by blocking muscarinic receptors with atropine (Kalume et al. 2013). The experiment of muscarinic receptor antagonists was replicated by another person in the lab, Eduardo Bravo, who found that bradycardia was not due to increased parasympathetic output. Instead, it was due to an effect in the brainstem. Atropine used in Kalume's paper (1 mg/kg; i.p.) prevented post-ictal apnea and death, but that dose is 20-50 times higher than is recommended for specific blockade of peripheral muscarinic receptors in mice (0.02-0.05 mg/kg i.p.). Atropine can readily penetrate into the CNS involved respiratory control. N-methylscopolamine used as a selective blockade of peripheral muscarinic receptor, which is less likely to cross the blood brain barrier. Recommended dose of atropine (0.03 mg/kg; i.p.) and N-methylscopolamine (1 mg/kg; i.p.) did not prevent post-ictal apnea, bradycardia or death.

It is important to obtain data on both cardiac and respiratory function to make conclusions about the cause of SUDEP and potential treatments in both humans and animals. I demonstrate that severe post-ictal respiratory dysfunction contributes to SUDEP in DS. For those cases due to apnea, ventilatory support to re-initiate breathing may be effective intervention to SUDEP prevention. These data may lead to better

understanding of SUDEP in other types of epilepsy, as well as shed light on possible therapeutic approaches to prevent SUDEP.

CHAPTER 4: AN ALTERNATIVE DIETARY SUPPLEMENT FOR SUDEP PREVENTION IN A DS MOUSE MODEL

Introduction

The final goal of this dissertation is to evaluate a new alternative dietary therapy for DS patients. Dietary therapies for neurological disorders have great potential in that they are cost-effective and free from serious side effects compared to AED therapies. Some epilepsy children with refractory seizures, especially DS patients, have been able to reduce their seizures by following a strict KD. Use and effects of KDs in previous studies for both patients and animals were introduced in Chapter 1. Despite the apparent effectiveness of KDs, there is not good scientific evidence for their anti-epileptic mechanism. Ketone bodies and ketosis have been widely believed to contribute to the anti-epileptic effects. Children on the KD often become hesitant to follow, mostly because the restricted food choices and some side-effects as described in Chapter 1 (Kossoff, 2004).

A collaborator (PI: Toshihiro Kitamoto, Anesthesia, Univ. of Iowa) has found that a diet containing milk whey prevents seizures in Drosophila with an orthologous sodium channel mutation. It had been hypothesized that supplementing milk whey in the normal diet of DS mice will also decrease their number of seizures, reduce respiratory arrest, and ultimately prevent SUDEP. One important question was how milk whey supplementation is related to ketogenic diets. To address this question, the effect of milk whey on seizures and SUDEP in DS mice was compared to that of commercially available KDs with and without milk additives. I also tested if milk whey supplementation leads to an increase in

ketone bodies by measuring β-hydroxybutyrate (β-HB) level, a hallmark feature of KDs that is proposed to play an important role in reducing severity of seizures.

Methods

Animal

DS mice were randomly divided in different groups to evaluate the efficacy of diet on their seizure frequencies and survival rates (Table 4). Mice were monitored by video from P16 to P60 for seizures and death. Seizure frequency and mortality were compared among groups. To evaluate dietary effects on mouse growth, body weight was measured weekly from when the mice weaned from their mother (P21) until P60.

Table 4: Animal groups of various experimental diets.

	Group
Control	Standard mouse chow
Whey Protein	2.5% in water
	5% in water
	whey pellets (10% equivalent)
	whey pellets (15% equivalent)
KD	KD 1 (dairy product)
	KD 1 + Glucose water
	KD 2 (vegetable oil)

Milk whey (whey protein concentrate; Bob's Red Mill Natural Foods, Milwaukie, Oregon) was dissolved in water at a concentration of 2.5%, or 5% (wt/vol). Mice in their home cage (pups at age P16) were given the milk whey solution as a supplemental source of liquid and allowed to drink from water bottles *ad lib*. From P21 until P60, mice were allowed to eat standard mouse chow (7013; Envigo Teklad Diets, Madison, WI) but the milk whey solution was their only liquid source. The higher concentration of milk whey

in water became thickening and it was not suitable to supply mice as liquid source. Based on the average daily consumption of food and water for mice (Bachmanov et al., 2002), consumptions of 10% and 15% milk whey in liquid were equivalent to 13% and 20% milk whey mixed with standard mouse chow as pellet formula. Mixtures of 13% and 20% milk whey mixed with standard food are designated as 10% and 15% whey pellets throughout this manuscript, respectively. Mice were fed these custom milk whey pellet diet with 10% milk whey pellet (custom order TD.150578; Envigo Teklad Diets, Madison, WI) or 15% milk whey pellet (custom order TD.150575; Envigo Teklad Diets, Madison, WI).

The KD has been used in pediatric epilepsy cases with some success in stopping seizures. Two different types of KDs were used in this study: 1) KD1 containing dairy fats (F3666; Bio-Serv, Frenchtown, NJ) and 2) KD2 containing vegetable oil (soybean) (TD96355; Envigo Teklad Diets, Madison, WI). These KDs were fed to mice in separate experimental groups to compare with whey ingestion. Another set of mice were fed with KD1 plus 5% glucose in water (wt/vol). Based on the average daily food and water intake for mice (Bachmanov et al., 2002), 5% glucose water supplies approximately 20% of the daily carbohydrate intake of standard mouse chow. This diet is still a high-fat diet, but it provides carbohydrate levels that are predicted to eliminate ketone formation. Therefore, addition of glucose water to the KD1 no longer classifies as a KD, and it does not produce ketone bodies.

Long-term video surveillance system to detect SUDEPs in DS mice

In the dietary study of DS mice, cameras were set up to record the animals around the clock. This long-term video surveillance system was used to monitor spontaneous

convulsive seizures and sudden deaths. A total of 32 web cameras were connected to one computer with two Ethernet switches (JGS 524 and GS 16; ProSafe Gigabit Switch, NETGEAR, San Jose, CA). Continuous long-term video recordings were made at 30 fps with high resolution, infrared web cameras (FL8910W) using webcam software (Blue Iris 4), and stored in .avi file format on an external hard drive (DRDR5A21-20TB, DroboWorks.com, Irvine, CA). Uninstrumented mice were housed in their home cages and continuous video monitoring was performed from the age of P16 to P60. Animal seizure activity and deaths were assessed manually by an observer blinded to the animal groups. Videos were reviewed and seizures were detected and scored from 1 to 5 using the modified Racine scale (Racine et al., 1972) of seizure stages: 1-mouth and facial movement; 2-head nodding; 3-forelimb clonus; 4-rearing with forelimb clonus and falling; and 5-falling with loss of postural control and jumping. Once animal death occurred, the number of seizures was counted for the prior 24 hours leading to animal death. In this seizure frequency analysis, stages 4 and 5 were classified as “convulsive” and only these stages were considered as a seizure occurrence.

Ketone body measurement: Beta-hydroxybutyrate (β-HB)

When mice reached the age of P35-40, blood samples of some DS mice in each diet group were collected and tested for β-HB level. Animals were anesthetized by a Ketamine/Xylazine cocktail (87.5 mg/kg Ketamine / 12.5 mg/kg Xylazine) IP injection. Blood samples were collected by cardiac puncture into an EDTA pre-coated syringe to prevent coagulation. To obtain plasma, blood samples centrifuged at 3,500 rpm, 4 °C, for 5 minutes. To plasma samples were stored at - 20 °C before analysis. β-HB level, a

ketone body, was determined in duplicate using a commercially available enzyme colorimetric β-HB Assay kit (BioVision, Mountain View, CA).

Results

Survival curves

Control mice

Video recordings were made continuously from 78 DS mice between P16 and P60. During that time, 38% of the mice spontaneously died (n=30 of 78) (Figure 22). Review of video recordings revealed that all deaths occurred after a generalized seizure characterized by tonic extension (seizure stage 5). Figure 23 shows the frequency of spontaneous seizures in individual animals on control diets that died with SUDEP. Consistent patterns of seizure frequency were not seen for 10 days before SUDEP, but there was an increase in the frequency of seizures during the last 1-2 days prior to death.

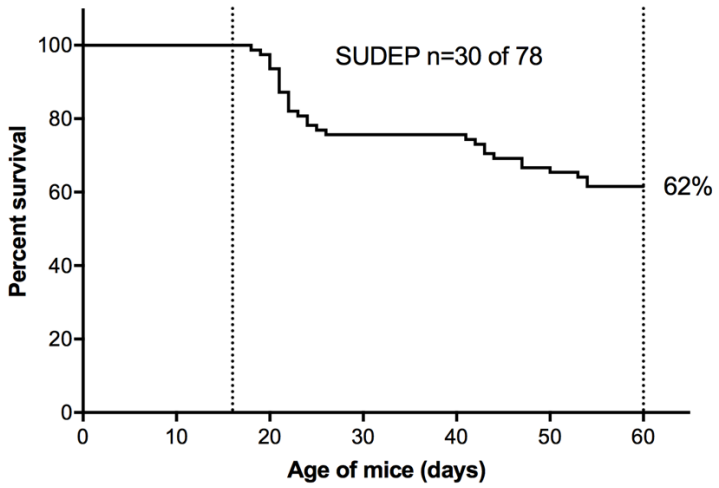

Figure 22. Kaplan-Meier survival curve for DS mice.
Kaplan-Meier survival curve for DS mice. SUDEP occurred after spontaneous seizures in 38% of DS mice (n=30 of 78).

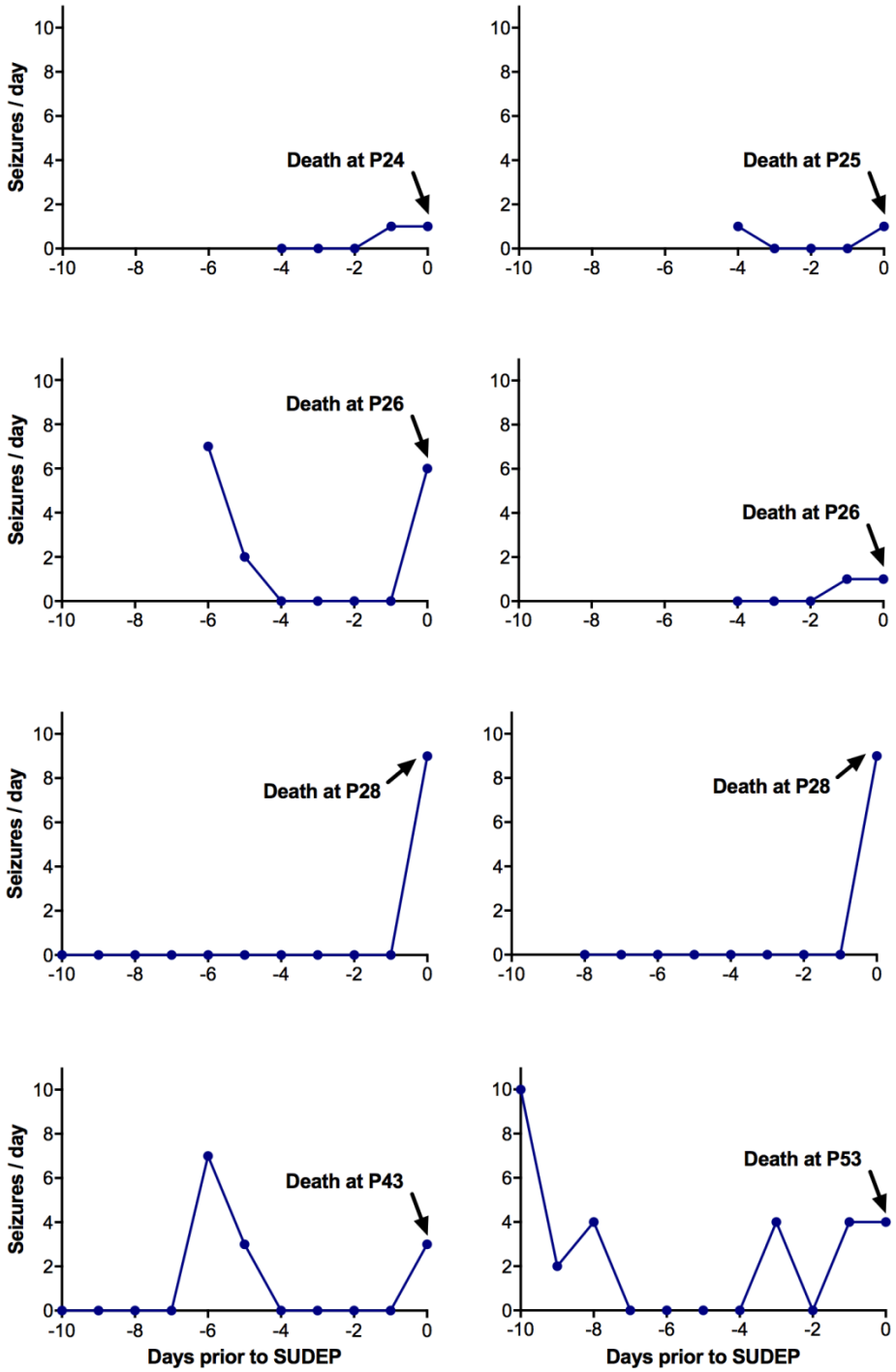

Figure 23. Frequency of seizures in DS mice during 10 days prior to SUDEP. We selected 8 DS mice that died with SUDEP. Video recordings were reviewed and detected the seizure frequencies for the last 5-10 days before the animals died. There was an increase in the frequency of seizures during the last 1-2 days prior to death.

Effects of milk whey diet

Three groups of DS mice were provided 0% (control) (n=44), 2.5% (n=41), or 5% (n=53) milk whey solution, respectively. Kaplan-Meier survival curves for each diet were displayed and compared (Figure 24A). The milk whey supplement reduced the number of SUDEPs, but only the difference between the control group and the 5% whey group was statistically significant ($p<0.0001$, Log-rank test for trend, Survival Test) (Figure 24A). In the second set of experiments, DS mice were fed with custom pellet diets consisting of 0% (control) (n=78), 10% (n=47), or 15% (n=32) milk whey mixed with standard mouse chow. This experiment was performed independently of the milk whey solution, and number of control mice used in here (n=78) was not overlap with control mice shown in Figure 24A. High concentrations of milk whey improved survival rates, but only the 10% milk whey pellets was statistically different from the standard mouse chow group ($p=0.0098$, Log-rank test for trend, Survival Test) (Figure 24B). It is not clear why 15% whey pellets were not more effective, but it was found that mice did not eat this diet as well and lost weight (Figure 28). We used the control group mice of Figure 24B as a reference (used in Figure 22A) to compare the survival rates for different diets in Figure 26.

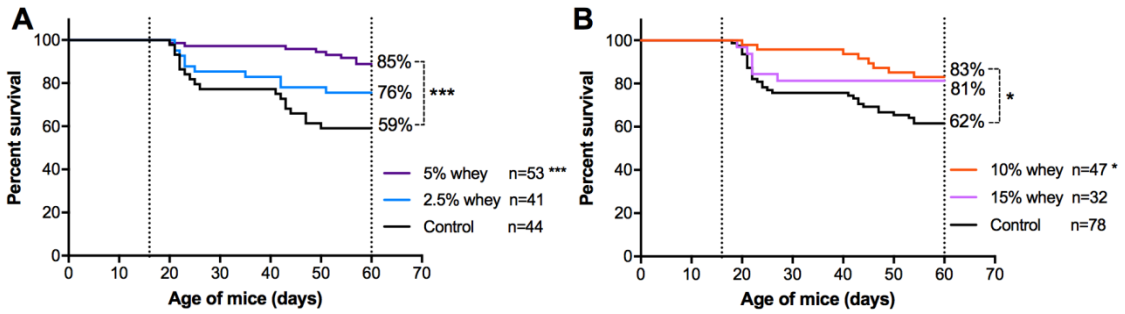

Figure 24. Survival curves for DS mice with milk whey supplements.
(A) Milk whey protein concentrate was dissolved in water at a concentration of 2.5% or 5% (wt/vol). Survival curves of these solutions were compared to the standard diet. 5% whey was significantly more protective for SUDEP: 0% vs 2.5% ($p=0.1203$); 0% vs 5% ($p<0.0001$). (B) DS mice were fed with standard diet, 10%, or 15% of milk whey mixed with standard mouse chow. Survival rates for control diet were compared to 10% and 15% milk whey pellets. 10% whey was significantly more protective for SUDEPs: control vs 10% ($p=0.0098$); control vs 15% ($p=0.0634$). Symbols represent p-values compared to standard mouse chow (control) group. * - $p<0.01$; ** - $p<0.001$; *** - $p<0.0001$.

Effects of high-fat diet

Three groups of DS mice were fed with a dairy KD (KD1) (n=42), a non-dairy KD (KD2) (n=38), or KD1 with 5% glucose water (n=52). All of these diets significantly improved survival rates (Kaplan-Meier survival curve plot). No significant difference was detected among these three diets between each other (Figure 25). Note that, DS mice fed KD1 with glucose water had a similar effect of SUDEP reduction. With this result, we hypothesized that the produced ketone bodies of KDs were not the main reason for an anti-epileptic effect. To confirm this hypothesis, β-HB level was measured in the group with KD added to glucose water.

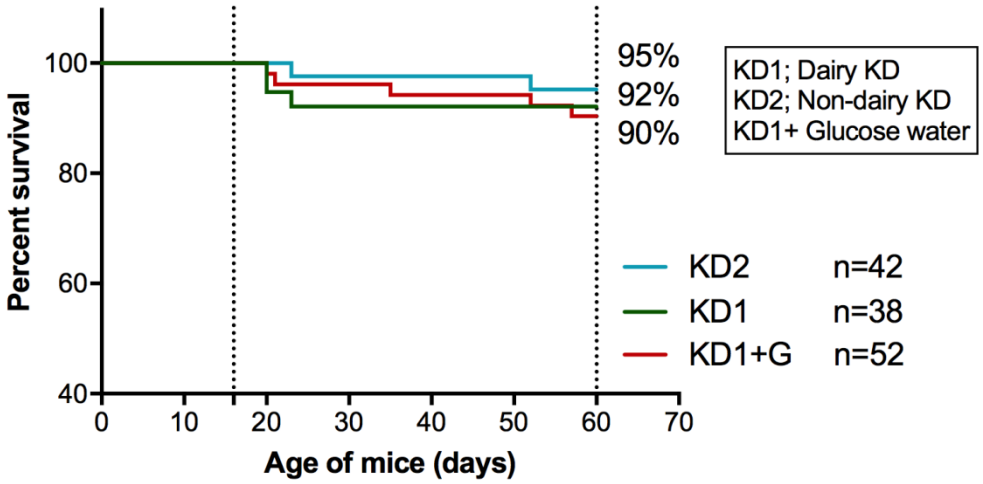

Figure 25. Survival curves for DS mice with high-fat diets.
Three groups of DS mice were fed with a dairy KD, a non-dairy KD, or dairy KD with 5% glucose water. Only a small number of mice died with SUDEP. All these diets showed significant SUDEP reduction.

Summary of survival curves

Here we show the summary survival curves of DS mice with different diets. Compared to control diet, survival rates were significantly improved in the 10% milk whey diet group, KD1, KD2, and KD1 with glucose water (Kaplan-Meier survival curve plot) (Figure 26). More SUDEP occurred in the control group during the ages of P21-P26 and P42-P53. The milk whey supplement and KDs were greatly protective of SUDEP during P21-P26. The number of mice fed 10% milk whey that died after P40 showed a similar pattern with P42-P53, but the SUDEP occurrence between the control and 10% whey group in this time period was still significantly different ($p=0.0098$). Each diet experiment shown in Figure 26 was performed at the same time, and maintained consistent environmental conditions, such as room temperature and humidity, varying only the diets. The milk whey solution experiments in Figure 24A were not included in

this summary figure (Figure 26) due to an inconsistent room temperature was detected during the experiment.

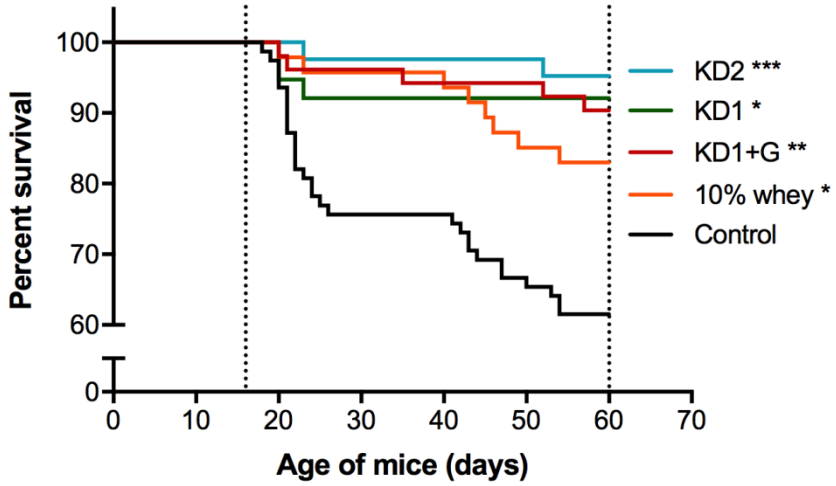

Figure 26. Summary of dietary therapy in DS mice.
Control diet (standard mouse chow) was compared to different diets. SUDEP occurrences with milk whey supplement and KDs were significantly decreased during the monitoring period (P16-P60). A significant number of DS mice died through ages P21-P26. Symbols represent p-values compared to standard mouse chow (control) group. * - $p<0.01$; ** - $p<0.001$; *** - $p<0.0001$.

Video analysis revealed that all deaths from all diet groups occurred after a generalized seizure characterized by tonic extension (seizure stage 5). The time of fatal and non-fatal seizure occurrences were quantified (Figure 27). A total of 101 video recordings captured DS mouse deaths, including control group and other diet groups, and indicated that DS mice were more likely to die during the dark phase (Figure 27A). 13 DS mouse deaths were randomly selected in the control group, and reviewed seizure occurrences during the last 1 - 10 days prior to death. 111 non-fatal seizures were captured in these mice and were also more likely to occur during the dark phase (Figure 27B).

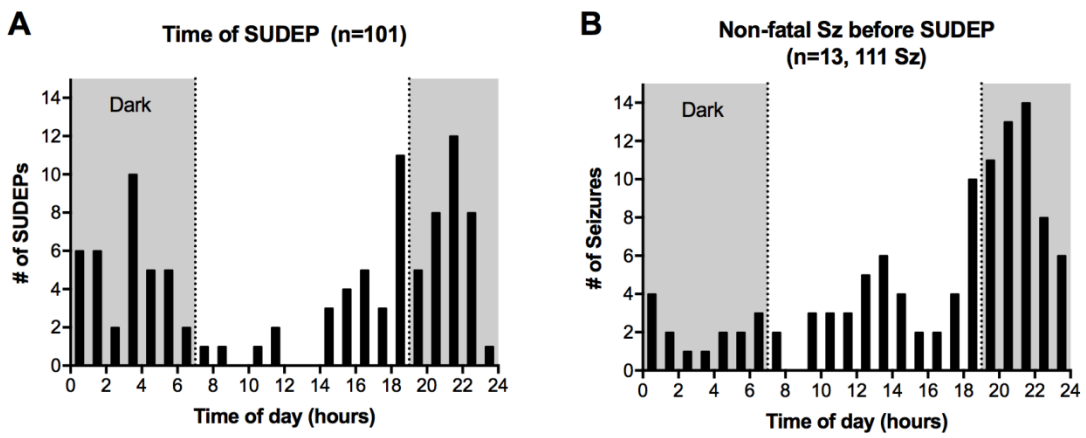

Figure 27. DS mouse video monitoring.
(A) DS mice were more likely to die during the dark phase. Video captured 101 DS mouse SUDEPs from a combination of 30 mice in Figure 22 and other diet groups. (B) 111 non-fatal seizures in 13 DS mouse SUDEPs were reviewed. Non-fatal seizures were also more likely to occur during the dark phase.

Animal growth effects among different diets

While animals were monitored by video from P16 to P60, body weight of individual mice was measured weekly to evaluate dietary effects on mouse growth. Body weight was analyzed for only those animals that survived until P60 on: 1) standard diet (n=18), 2) 10% whey (n=21), 3) KD1 with glucose (n=32), 4) KD1 (n=15), and 5) KD2 (n=29). There was no statistically significant difference of body weights between standard diet and milk whey supplement (Figure 28). Statistical comparison of animal body weights was made using a paired t-test with an overall significance level set of $p<0.05$ (GraphPad Prism V6.01). Compared to control mice, a significantly lower body weight was detected in mice fed with KD1 ($p<0.0001$) and KD1 with glucose water ($p=0.003$) throughout their measurement period (P21-P60). Mice fed with KD2 showed significantly more weight loss than control mice at age from P21-P35, but animals gained weight from P35 and maintained it with the same level of standard diet until P60. Figure 28 also included lost weight of mice fed with 15% whey pellets. Mice fed with 15% milk

whey pellets did not eat sufficient amount this diet. The body weight of 15% whey pellets was analyzed until P45, this weight loss was not statistically different to control mice (p=0.0781).

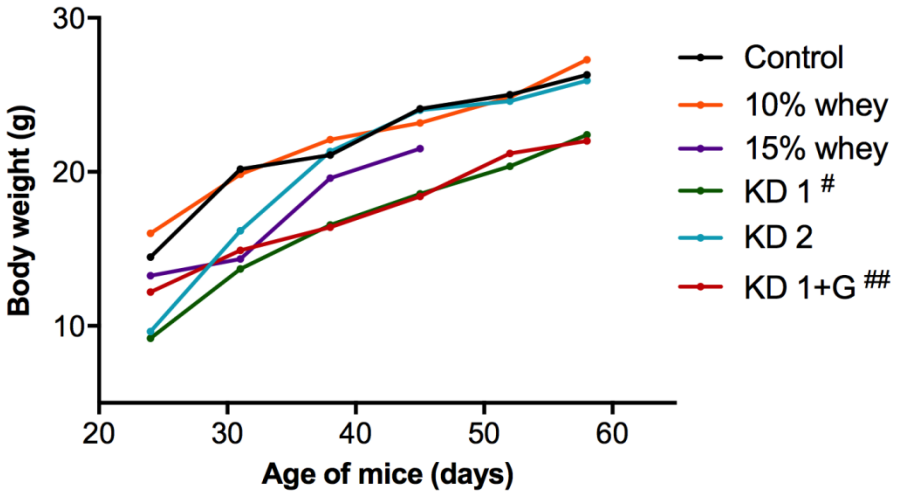

Figure 28. Weights of animals in different diet groups.
Body weights on mice fed the KD1 and KD1 with glucose water were significantly less than standard diet through P21-P60. No significant difference of body weight was detected between 10% milk whey and control mice or between KD2 and control mice. There was significant weight loss at an early age for KD2 mice, but mice recovered their body weight to the same level as control mice until P60. It was found that mice fed 15% milk whey lost weights, but it was not statistically different to control mice. Symbols represent p-values compared to standard mouse chow (control) group. # - $p<0.001$; ## - $p<0.0001$.

Ketoacidosis is not the mechanism of seizure reduction

DS mice in different diet groups were used to measure ketone β-HB levels (Figure 29). Statistical comparison of animal β-HB levels was made using a Mann-Whitney U Test with an overall significance level set to $p<0.05$ (GraphPad Prism V6.01). Levels of the ketone β-HB were significantly higher in mice fed both KDs with and without milk additives (KD1 & KD2) compared to control diet (KD1 vs control, p=0.0012; KD2 vs control, p=0.0043). Although all high-fat diets (KD1, KD2, and KD1 with glucose water) had shown similar effect of SUDEP reduction, the β-HB levels among these groups were

significantly different (KD1 vs KD2, p=0.0152). Note that mice fed KD1 with glucose water did not produce ketosis (KD1 vs KD1+G, p=0.0061) but had a similar effect of SUDEP reduction with KDs. These data indicates that the produced ketone bodies of KDs are not the main reason for an anti-epileptic effect.

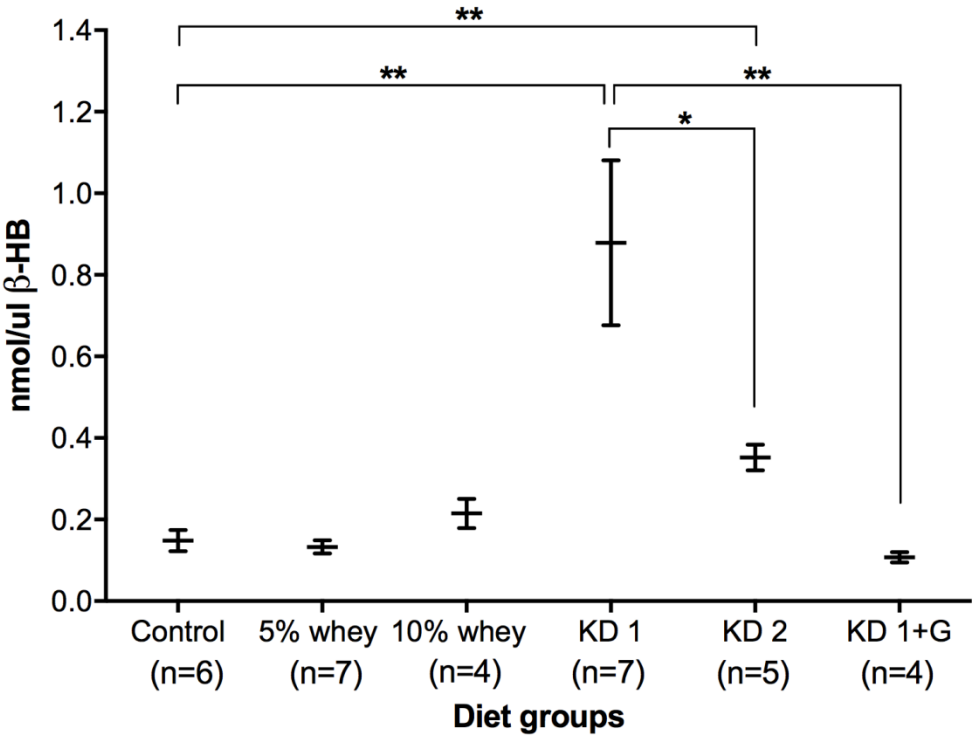

Figure 29. Beta-hydroxybutyrate (β-HB) measurement.
Beta-hydroxybutyrate (β-HB) levels in DS mice among different diet groups. β-HB concentrations were significantly elevated in DS mice in both KD groups unless glucose was added to their water, all comparisons versus control. Symbols represent p-values compared to standard mouse chow (control) group. * -$p<0.05$, ** - $p<0.01$.

Discussion

KD therapy is known to reduce their seizures in DS patients, and this is thought to be due to ketosis. In this chapter, a new alternative dietary therapy composed of milk whey was proposed for DS. Previously, a collaborator (PI: Toshi Kitamoto, Univ. of Iowa) found that a diet containing milk whey was able to prevent seizures in Drosophila

with an orthologous sodium channel mutation. It was expected that a diet containing milk whey might also reduce seizures and spontaneous deaths. The efficacy of milk whey supplementation and different KDs on DS mice was evaluated. DS mice were monitored by video while they were given standard mouse chow, milk whey supplementation, dairy KD, non-dairy KD, and addition of glucose water to dairy KD to eliminate ketone formation from the age of P16 to P60. As a result, mice survival rates, growth effects, and β-HB levels (ketone bodies) were compared among the different diet groups. All KDs, addition of glucose water to the KD, and milk whey supplementation significantly prevented SUDEPs in DS mice. Compared to mice on a standard diet, mice fed a dairy KD and addition of glucose water to a dairy KD showed significantly lower body weight throughout their measurement period (P21-P60). Another significant weight loss different from the standard diet mice was detected in non-dairy KD mice between ages P21-P35. Milk whey supplementation also showed an anti-epileptic effect, but there was no significant body weight change compared to control mice. Milk whey supplementation may be beneficial for DS patients wanting to avoid disadvantages of KD such as effects on weight and restrictive food choices. Previous KD studies suggest that the anti-epileptic property of KD is due to the production of ketone bodies. KDs produced high β-HB levels, but milk whey supplementation and the addition of glucose water to the KD did not produce ketosis but still showed significant anti-epileptic effects. These results suggest that the elevated ketone bodies are not the main reason for the anti-epileptic effect of KDs. Instead, some component of KDs that is also found in milk whey may be the active agent.

The results presented in this chapter may be relevant to SUDEP in DS patients. Milk whey supplementation is cost-effective, less restrictive, and free from side effects when compared to KDs. Milk whey supplementation could be considered a new alternative dietary therapy for DS patients. Identification of the active compound(s) in milk whey may allow a more targeted treatment to reduce seizures and SUDEP that may be effective in DS, as well as possibly other types of epilepsy.

CHAPTER 5: SUMMARY AND FUTURE DIRECTIONS

Summary

SUDEP has recently drawn considerable attention from scientists, clinicians, and the public. Researchers have focused on identifying the mechanisms as well as preventative approaches. A major unknown issue is whether the primary cause of death is cardiac arrest or respiratory arrest. SUDEP is historically believed to simply be sudden cardiac death triggered by the stress of a seizure, whereas respiratory dysfunction has only drawn researchers' attention recently. The main goal of this dissertation is to understand the mechanisms of SUDEP in DS mice and evaluate a prevention strategy for SUDEP through an alternative diet composed of a milk whey compound.

To define the causes of death after a seizure in mice, a mouse EMU had been developed that can monitor physiological changes including breathing, cardiac activity, and seizure activity from mice until the occurrence of sudden death. The initial question of these experiments was whether or not mouse sudden death after a seizure shares a common final pathway for death. I induced seizures acutely in three non-epileptic mouse strains that are prone to sudden death in response to seizures: audiogenic seizures in DBA/1 mice and MES-induced seizures in *Lmx1b*$^{f/f/p}$ and C57Bl/6 mice. When a death occurred after an induced seizure, the seizure caused immediate and permanent respiratory arrest in all 3 seizure models. In each strain, EKG activity continued for 3 to 5 minutes after terminal apnea. I interpreted these data as indicating that the primary cause of sudden death was central apnea in each case, and the resulting hypoxia then caused bradycardia and asystole (Chapter 2).

Dravet Syndrome patients have a high risk of SUDEP, and mouse models exist that share many features including spontaneous post-ictal death. Recent studies have concluded that cardiac dysfunction causes SUDEP in DS. Based on the data in Chapter 2, it has been hypothesized that the primary cause of post-ictal death in DS mice may also be central apnea and probably induce secondarily bradycardia due to the hypoxia. In Chapter 3, it demonstrates that primary respiratory arrest can play an important role in post-ictal death in DS mice. DS mouse deaths detected after spontaneous seizures and MES / heat-induced seizures were due to central apnea, and the resulting hypoxia probably caused later progressive bradycardia and asystole. The time course of EKG and breathing changes in DS mice were similar to that seen in post-ictal death of non-epileptic mice in Chapter 2. Figure 30 shows the summary of cardiorespiratory patterns in all 4 mouse strains' post-ictal deaths. I also show that DS patients commonly have post-ictal respiratory dysfunction, and in fact one of the patients shown in this dissertation who had severe post-ictal hypoventilation later died of SUDEP. In conclusion, SUDEP in DS can result from primary central apnea, causing bradycardia due to an effect of hypoxemia on cardiac muscle. The findings of severe respiratory dysfunction in DS may bring a better understanding of SUDEP mechanisms in humans.

The KD is known as a useful dietary therapy for DS patients, and its anti-epileptic effect is widely assumed to be ketosis. Here a new alternative dietary therapy composed of milk whey for DS had been proposed and compared its effect to KDs (Chapter 4). Through the DS mouse diet study, I found the anti-epileptic effects of milk whey supplement, two KDs, and a KD to which glucose was added. In addition, I demonstrated

the anti-epileptic effects of the KDs were not from ketosis and KDs cause growth defect in some cases. With this result, milk whey supplementation should be considered as a new therapeutic approach to treat seizures and prevent SUDEP in DS patients.

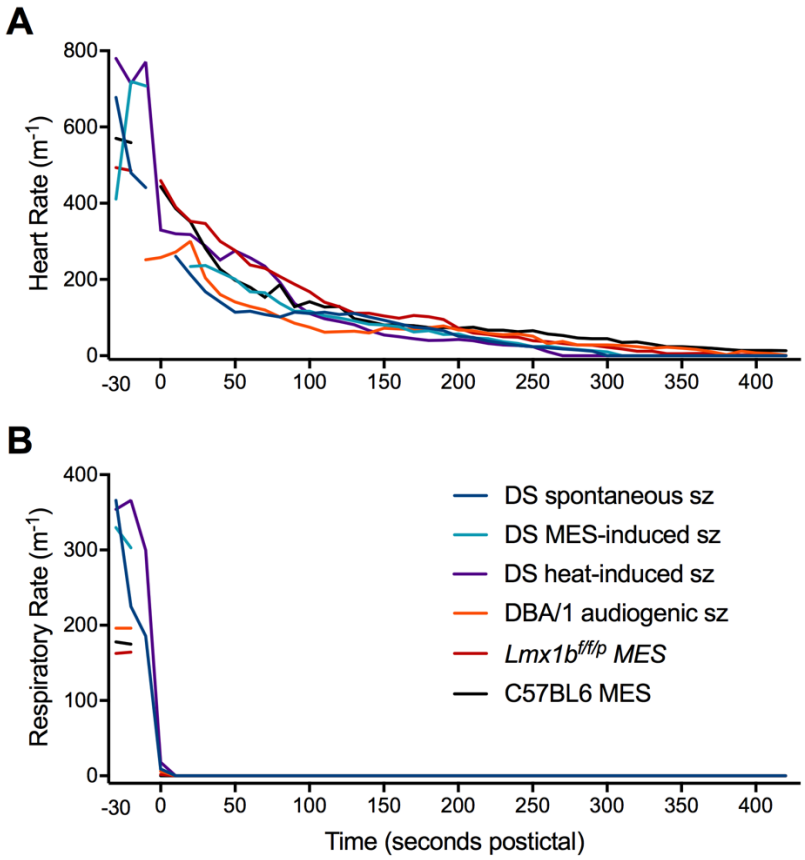

Figure 30. Summary of cardiorespiratory patterns in multiple post-ictal death mouse models.
Average traces of heart rate (A) and breathing frequency were plotted in post-ictal mouse deaths: 1) DS mice with spontaneous and MES / heat-induced seizures, 2) DBA/1 mice with audiogenic seizures, 3) *Lmx1b*$^{f/f/p}$ with MES-induced seizures, and 4) C57Bl/6 mice with MES-induced seizures. All data in this figure were described in Chapter 2 and 3. Time zero was defined as the end of seizures.

Future directions

A seizure in mice disturbs respiratory and cardiac functions. Simultaneous monitoring of both cardiac and respiratory function is important for making conclusions

about mechanisms of post-ictal death. Mouse EMU data is particularly important because there are some mice whose cause of death has been assumed without direct evidence. For example, some mice with mutations in Long QT syndrome genes might die from respiratory arrest, not cardiac arrest, since all LQTS genes are expressed in both the heart and brain. With results of DS mouse death with spontaneous seizures as described in Chapter 3, the same methods should be utilized to identify the cause of sudden death after spontaneous seizures in a variety of mutant mouse models of epilepsy. Several gene mutant mice have convulsive seizures that resemble the orthologous human condition; KCNQ1 (long QT syndrome), SCN2A (Ohtahara syndrome), SCN8 (EIEE; early-infantile epileptic encephalopathies), Dup15q syndrome, and DEPDC5 (focal epilepsy) (Devinsky et al., 2016; Wagnon & Meisler, 2015). These will bring a better understanding of SUDEP mechanisms in humans, as well as shed light on possible therapeutic practices to prevent SUDEP.

To perform an efficient analysis of long-term EMU recording over days to weeks, developing data analysis software that automatically identifies seizures status would be beneficial. Based on the methods used manually in this dissertation, the data analysis program could be designed to automatically detect abnormalities in EEG, EKG, and breathing such as post-ictal generalized EEG suppression (PGES), and perform analysis of heart-rate variability, breathing frequency, and tidal volume.

This dissertation demonstrates that post-ictal death in multiple mouse seizure models always occurred after central apnea. Not every seizure causes apnea, and some recover on there own, but some seizures lead to apnea and death. Future studies need to identify the mechanisms of post-ictal apnea.

For elucidation of the mechanisms underlying milk whey-dependent suppression of seizures, it is essential to identify dietary components responsible for the observed anti-epileptic property. Identification of the active components in milk whey is also of practical significance because it may lead to novel interventions for refractory epilepsy and other related neurological disorders.

APPENDICES

Video processing MATLAB code of DS patients

The following algorithms are written in MATLAB R2016a version, to display the breathing trace. This spatiotemporal YT slice was created with time on the x-axis (consecutive video frames), vertical location on the y-axis (e.g. Figures 9, 11, and 12, see methods in Ch3).

```
%%Loading Image function test file
clc;
clear all;

[handles.file_name,handles.path_name] = uigetfile('*.avi','Select File To Load.');

if(handles.file_name == 0),
   %set(handles.Display,'string', 'No .avi files selected');
   return;
end % user pressed the cancel button

nFrames = 0;
vidHeight = 0;
vidWidth = 0;

vid = VideoReader([handles.path_name, handles.file_name]);

nFrames = vid.NumberOfFrames;
vidHeight = vid.Height;
vidWidth = vid.Width;

% Preallocate movie structure.
mov(1:nFrames) = ...
   struct('cdata', zeros(vidHeight, vidWidth, 3, 'uint8'),...
         'colormap', []);

% Read entire images, one frame at a time.
for k = 1 : nFrames
   mov(k).cdata = read(vid, k);
   %Gray_mov = rgb2gray(mov(k).cdata);
end

imshow(mov(1).cdata)

impixelinfo;

 [x,y] = getpts(gca);

 x=floor(x);
```

```
 y=floor(y);

line([x x],[0 vidHeight],'LineWidth',1,'Color','b');

%% vid slice: one dimension (X or Y axis on the image)

% YT slice   X: time axis Y: Y-slice

y_firstFrame = mov(1).cdata(:,x,:);  %entire Y-slice

for ii = 1:nFrames

    B = mov(ii).cdata(:,x,:); %entire y-slice

    C = squeeze(B);
    array(:,:,ii) = C;
end
    slice = permute(array,[1, 3, 2]);
   figure;
    imshow(slice)
    xlabel('X'); ylabel('Time');
    title('Up-down movement by time')
    impixelinfo;

%% Enhance truecolor composite with a Contrast Stretch
    stretched_slice = imadjust(slice, stretchlim(slice)); % Contrast Stretch
    figure;
    imshow(stretched_slice)
    xlabel('Time'); ylabel('Y');
    title('Truecolor Composite after Contrast Stretch')
    impixelinfo;

%% Extract a band for breathing trace
part1 = stretched_slice(370:407,:,:);
slice_part1 = imresize(part1,2);
figure; imshow(slice_part1)
title('Original')

slice_gray = rgb2gray(part1); % convert to grayscale
slice_gray = imadjust(slice_gray);
figure; imshow(slice_gray)
title ('grayscale and adjustment')

slice_gray=imresize(slice_gray,2);
figure; imshow(slice_gray)   % figure 3
title('grayscale and adjustment')

AA = imadjust (part1,[.2 .3 0; .6 .7 1],[]);
AA = rgb2gray(AA);
figure; imshow(AA)
title ('adjustment and grayscale')
```

```
AA=imresize(AA,2);
figure; imshow(AA)
title ('adjustment and grayscale')
```

Mouse EMU data acquisition program code

The following algorithms are written in MATLAB R2014b version, in order to acquire all signals of mouse EMU simultaneously in one file and display in screen real-time.

MATLAB program code: 'MouseEMU_single.m'

```
% Data Acquisition Application for Animal EMU system of one unit
%
% modified 12/21/15 by YuJaung Kim
% removed timer handles - RealTimePlot function will be called from NI
% system
%
% modified 10/29/15 by YuJaung Kim
% changed the digital device to 125Pa: COM13
%
% modified 10/4/15 by YuJaung Kim
% deleted the '5s timer delay'

% modified 3/11/2015 by YuJaung Kim
% change all caracters from 'MouseEMU_single' to 'MouseEMU_single'
% change the way to write time stamp written at 1s, 11s,,,,
% add a global variable 'time_now'
%
% modified 12/8/2014 by YuJaung Kim
% EKG sampling rate: 1 kHz
% EEG1/EEG2/EMG/Plethy channel sampling rate: 100 Hz
% Cage temp. and Humidity save one data point at saving interval(every 10s)
% No E-mitter device (using small body-temp radio-telemetry device
% Signal inputs:
%   Analog inputs from headmount : EEG1/ EEG2 / EMG / EKG
%   Digital inputs from teensy3.1 micro-controller : Plethysmography / cage
%   temp. / humidity
%
% fixed delayed display on the screen - timer object used
% changed the way to store time value on the binary file
%   previous: it saved the time at the moment of writing on the binary
%   file (first time data would be 10s after clicking "start" button.
%   changed: it saved the first time data when click the "start" button,
%   rest of data will be written after all EEG - humidity data stored.

function varargout = MouseEMU_single(varargin)
% MouseEMU_single MATLAB code for MouseEMU_single.fig
%      MouseEMU_single, by itself, creates a new MouseEMU_single or raises the existing
```

```
%      singleton*.
%
%      H = MouseEMU_single returns the handle to a new MouseEMU_single or the handle to
%      the existing singleton*.
%
%      MouseEMU_single('CALLBACK',hObject,eventData,handles,...) calls the local
%      function named CALLBACK in MouseEMU_single.M with the given input arguments.
%
%      MouseEMU_single('Property','Value',...) creates a new MouseEMU_single or raises the

%      existing singleton*.  Starting from the left, property value pairs are
%      applied to the GUI before MouseEMU_single_timer_OpeningFcn gets called.  An
%      unrecognized property name or invalid value makes property application
%      stop.  All inputs are passed to MouseEMU_single_timer_OpeningFcn via varargin.
%
%      *See GUI Options on GUIDE's Tools menu.  Choose "GUI allows only one
%      instance to run (singleton)".
%
% See also: GUIDE, GUIDATA, GUIHANDLES
% Edit the above text to modify the response to help MouseEMU_single
% Last Modified by GUIDE v2.5 04-Oct-2012 11:51:02

% Begin initialization code - DO NOT EDIT
gui_Singleton = 1;
gui_State = struct('gui_Name',       mfilename, ...
                   'gui_Singleton',  gui_Singleton, ...
                   'gui_OpeningFcn', @MouseEMU_single_timer_OpeningFcn, ...
                   'gui_OutputFcn',  @MouseEMU_single_timer_OutputFcn, ...
                   'gui_LayoutFcn',  [] , ...
                   'gui_Callback',   []);
if nargin && ischar(varargin{1})
    gui_State.gui_Callback = str2func(varargin{1});
end

if nargout
    [varargout{1:nargout}] = gui_mainfcn(gui_State, varargin{:});
else
    gui_mainfcn(gui_State, varargin{:});
end
% End initialization code - DO NOT EDIT
% --- Executes just before MouseEMU_single is made visible.
function MouseEMU_single_timer_OpeningFcn(hObject, eventdata, handles, varargin)
% This function has no output args, see OutputFcn.
% hObject    handle to figure
% eventdata  reserved - to be defined in a future version of MATLAB
% handles    structure with handles and user data (see GUIDATA)
% varargin   command line arguments to MouseEMU_single (see VARARGIN)

% Choose default command line output for MouseEMU_single
handles.output = hObject;
```

```
delete(daqfind), clear global   % necesarry if recording multiple times, difference between clear all?
delete(instrfindall)          % delete any serial port objects

handles.all_buttons = findobj('style','pushbutton');
handles.all_axes = findobj('type','axes');

% Update handles structure
guidata(hObject, handles);

% --- Outputs from this function are returned to the command line.
function varargout = MouseEMU_single_timer_OutputFcn(hObject, eventdata, handles)
% varargout  cell array for returning output args (see VARARGOUT);
% hObject    handle to figure
% eventdata  reserved - to be defined in a future version of MATLAB
% handles    structure with handles and user data (see GUIDATA)

% Get default command line output from handles structure
varargout{1} = handles.output;

% --- Executes on button press in start.
function start_Callback(hObject, eventdata, handles)
% hObject    handle to start (see GCBO)
% eventdata  reserved - to be defined in a future version of MATLAB
% handles    structure with handles and user data (see GUIDATA)

% user inputs name of file to save data
[filename, path_name] = uiputfile('*.bin','Save File As');
if filename == 0, return, end   % user pressed the cancel button

% open the selected file for binary writing
[handles.fid,message] = fopen([path_name, filename], 'wb');
if strcmp(message,'')==0, msgbox(message,'Error','error','modal'), return, end
%
=================================================================

global time_now izz save_interval time_buffer_1000Hz time_buffer_100Hz data_buffer_1000Hz
data_buffer_100Hz data_to_save_1000Hz data_to_save_100Hz LastestTime StartTime numbytes
time_now = 0; % time stamp for writing in binary file
izz = 1;    % RealTimePlot function counter
LastestTime = 0;
StartTime = 0;
numbytes = 8;
save_interval = 10; % time interval(s) between fwrite calls

handles.SampleRate = 1000; % HZ per second (al; channels of Analog Input except EKG)
handles.sweep_values = 3; % graph time sweep on the screen
handles.sweep_duration = handles.sweep_values;

% define plotting buffers
```

```
chans_100Hz = 4;    % EEG1/EEG2/EMG/Plethy data
time_buffer_1000Hz = NaN(handles.SampleRate*handles.sweep_values,1);
time_buffer_100Hz = NaN(handles.SampleRate/10*handles.sweep_values,1);

data_buffer_1000Hz =NaN(handles.SampleRate*handles.sweep_values,1);
data_buffer_100Hz = NaN(handles.SampleRate/10*handles.sweep_values,chans_100Hz);

% define buffers for writing file
data_to_save_1000Hz = NaN(save_interval*handles.SampleRate,1);
data_to_save_100Hz = NaN(save_interval*handles.SampleRate/10,chans_100Hz);

handles.all_buttons = findobj('style','pushbutton');
handles.graph_axes = findobj('type','axes','Units','characters');

set(handles.all_buttons,'enable','on')
set(handles.start,'enable','off')
set([handles.rh_label handles.cage_temp_label],'string','')

delete(findobj('type','line'))

% Graph setting
set(handles.graph_axes,'xlim',[0 handles.sweep_duration])

handles.hLine_eeg1 =
line('XData',time_buffer_100Hz,'YData',data_buffer_100Hz(:,1),'color','r','parent',handles.eeg1_a
xes);
handles.hLine_eeg2 =
line('XData',time_buffer_100Hz,'YData',data_buffer_100Hz(:,2),'color','r','parent',handles.eeg2_a
xes);
handles.hLine_emg =
line('XData',time_buffer_100Hz,'YData',data_buffer_100Hz(:,3),'color','r','parent',handles.emg_a
xes);
handles.hLine_ekg =
line('XData',time_buffer_1000Hz,'YData',data_buffer_1000Hz(:,1),'color','r','parent',handles.ekg_
axes);
handles.hLine_pressure =
line('XData',time_buffer_100Hz,'YData',data_buffer_100Hz(:,4),'color','r','parent',handles.pressur
e_axes);

%**************************************************************************
% Registering of Digital Input (Teensy 3.1 microcontroller board)

handles.s = serial('COM13');  %creat a serial port object
set(handles.s,'BaudRate',9600,'Terminator','CR')
set(handles.s,'InputBufferSize',100*numbytes*2)
fopen(handles.s);    % Connect a serial port object to the device

%**************************************************************************

%**************************************************************************
% Registering of AnalogInput (National Instrument board)
```

```
% NI PCIe-6321 board Input range: +- 10V, 5V, 1V, 0.2V
nidaq_info = daqhwinfo('nidaq');
devID = nidaq_info.InstalledBoardIds{1};
handles.AI = analoginput('nidaq',devID);
set(handles.AI,'InputType','SingleEnded')

addchannel(handles.AI,0:3,1:4,{'eeg1','eeg2','emg','ekg'});
set(handles.AI.channel(1),'InputRange',[-0.2 0.2],'SensorRange',[-0.2 0.2],'UnitsRange',[-0.2
0.2],'Units','Volts');
set(handles.AI.channel(2),'InputRange',[-0.2 0.2],'SensorRange',[-0.2 0.2],'UnitsRange',[-0.2
0.2],'Units','Volts');
set(handles.AI.channel(3),'InputRange',[-1 1],'SensorRange',[-1 1],'UnitsRange',[-1
1],'Units','Volts');
set(handles.AI.channel(4),'InputRange',[-1 1],'SensorRange',[-1 1],'UnitsRange',[-1
1],'Units','Volts');

% Configure AI property values.
set(handles.AI,'SampleRate',handles.SampleRate) % 1000 Hz, per channel
set(handles.AI,'SamplesPerTrigger',inf)     % 1 trigger, infinite sampling
set(handles.AI,'BufferingConfig',[handles.SampleRate/5 30])
set(handles.AI,'SamplesAcquiredFcnCount',handles.SampleRate)
set(handles.AI,'SamplesAcquiredFcn',{@RealTimePlot,handles})

start(handles.AI)
waitfor(handles.AI.InitialTriggerTime~=0)
set(handles.start_label,'string',['start time: ',datestr(handles.AI.InitialTriggerTime,31)])
set(handles.stop_label,'string','stop time:')
set(handles.file_name_text,'string',filename)
%**************************************************************************

% % handles.t = timer('TimerFcn',{@RealTimePlot,handles},'Period',1.0);
% handles.t = timer;
% handles.t.ExecutionMode = 'fixedSpacing';
% handles.t.Period = 1;
% handles.t.TimerFcn = {@RealTimePlot,handles};
% % handles.t.StartDelay = 5;
%
% start(handles.t);

% Update handles structure
guidata(hObject, handles);

%image (handles.vid,'Parent',handles.video_axes);
%handles.hImage = image(zeros(vidRes(2), vidRes(1), nBands),'Parent',handles.video_axes );

% --- Executes on button press in stop.
function stop_Callback(hObject, eventdata, handles)
% hObject    handle to stop (see GCBO)
% eventdata  reserved - to be defined in a future version of MATLAB
% handles    structure with handles and user data (see GUIDATA)
```

```
%set(handles.all_buttons,'enable','off')
stop(handles.AI)

% %setappdata(handles.hImage,'UpdatePreviewWindowFcn',[]);
% stop(handles.vid)
% close(handles.vid.DiskLogger)
% delete (handles.vid)
% clear handles.vid

events = handles.AI.EventLog;
set(handles.stop_label,'string',['stop time: ',datestr(events(end).Data.AbsTime,31)])
delete(daqfind)
delete(instrfindall)
delete(handles.AI)

% stop(handles.t)
% delete(handles.t)
%fclose(handles.s);
fclose(handles.fid);
handles = rmfield(handles,{'fid','AI'});
clear global
set(handles.start,'enable','on')

function RealTimePlot(obj,event,handles)    % called once every second

global time_now izz save_interval time_buffer_1000Hz time_buffer_100Hz data_buffer_1000Hz
data_buffer_100Hz data_to_save_1000Hz data_to_save_100Hz LastestTime StartTime numbytes

try
   % extracts 1 second of data from engine, creates vector of relative time
  % [data,time] = getdata(obj,handles.SampleRate);
  time_now = now();
  [data,time] = getdata(handles.AI,handles.SampleRate);

   %Shirink 1000 Hz samples to 100Hz samples on EEG1 &2, EMG, and pressure
   time_100Hz= time(10:10:handles.SampleRate);
   EEG1_data = data(10:10:handles.SampleRate,1);
   EEG2_data = data(10:10:handles.SampleRate,2);
   EMG_data = data(10:10:handles.SampleRate,3);
   EKG_data = data(:,4);

   % extracts 1 second of data from engine, creates vector of relative time
   handles.digitalData = fread(handles.s,100*numbytes,'uint8');

   flow_high = uint16(handles.digitalData(2:numbytes:end));
   flow_low = uint16(handles.digitalData(3:numbytes:end));
   pressure = bitshift(int16(flow_high),8) + int16(flow_low);
   pressure_data = double(pressure) / 240; % scale factor: 125Pa-240 / 25Pa-1200

   if izz == 1
```

```
        rh = double(bitshift(uint16(handles.digitalData(5:numbytes:end)),8) +
uint16(handles.digitalData(6:numbytes:end)))* 6.10e-3;
        cage_temp = double(bitshift(uint16(handles.digitalData(7:numbytes:end)),8) +
uint16(handles.digitalData(8:numbytes:end))) / 4 * 1.007e-2 - 40.0;
        set(handles.rh_label,'String',num2str(rh(end)))
        set(handles.cage_temp_label,'String',num2str(cage_temp(end)))
        %time_now = now();

        % Save the start time data in file
        % fwrite(handles.fid, time_now,'double');
    end

    theTime = handles.digitalData(4:numbytes:end);
    timediff = theTime(2:end)-theTime(1:end-1);
    timediff(timediff<0) = timediff(timediff<0) + 256;
    timediff = [0; timediff];

    time_100Hz_hide = cumsum(timediff)/1000 + LastestTime;
    LastestTime = time_100Hz(end);

    data_100Hz = [EEG1_data EEG2_data EMG_data pressure_data];

    time_buffer_100Hz = [time_buffer_100Hz(length(time_100Hz)+1:end); time_100Hz];
    time_buffer_1000Hz = [time_buffer_1000Hz(length(time)+1:end); time];

    data_buffer_1000Hz = [data_buffer_1000Hz(length(EKG_data)+1:end); EKG_data];
     data_buffer_100Hz = [data_buffer_100Hz((length(pressure_data)+1:end),:); data_100Hz(:,:)]; %
4 chans data store in 10s save data buffer

   data_to_save_1000Hz = [data_to_save_1000Hz(length(EKG_data)+1:end); EKG_data];
   data_to_save_100Hz = [data_to_save_100Hz((length(pressure_data)+1:end),:);
data_100Hz(:,:)]; % 4 chans data store in 10s save data buffer

    %--------------------------------------------------------------------------------
    % Plot graphs and update every second

    % t1 = max(0,izz-handles.sweep_duration);
    t1 = max(0,izz-handles.sweep_duration);
    t2 = t1 + handles.sweep_duration;
    set(handles.graph_axes,'xlim',[t1 t2])

    set(handles.hLine_eeg1,'XData',time_buffer_100Hz,'YData',data_buffer_100Hz(:,1))
    set(handles.hLine_eeg2,'XData',time_buffer_100Hz,'YData',data_buffer_100Hz(:,2))
    set(handles.hLine_emg,'XData',time_buffer_100Hz,'YData',data_buffer_100Hz(:,3))
    set(handles.hLine_ekg,'XData',time_buffer_1000Hz,'YData',data_buffer_1000Hz(:,1))
    set(handles.hLine_pressure,'XData',time_buffer_100Hz,'YData',data_buffer_100Hz(:,4))

    %--------------------------------------------------------------------------------
  %%
  % Write time stamp at 1s, 11s...
  if(rem(izz,save_interval)==1)
```

```
    fwrite(handles.fid, time_now,'double');
end

   % At the writing time
   if(rem(izz,save_interval)==0)

      rh = double(bitshift(uint16(handles.digitalData(5:numbytes:end)),8) +
uint16(handles.digitalData(6:numbytes:end)))* 6.10e-3;
      cage_temp= double(bitshift(uint16(handles.digitalData(7:numbytes:end)),8) +
uint16(handles.digitalData(8:numbytes:end))) / 4 * 1.007e-2 - 40.0;
      rh_data = rh(end);
      cage_temp_data = cage_temp(end);
      set(handles.rh_label,'String',num2str(rh_data))
      set(handles.cage_temp_label,'String',num2str(cage_temp_data))
      % time_now = now();

      % Save data in file
      fwrite(handles.fid, data_to_save_1000Hz,'float32');
      fwrite(handles.fid, data_to_save_100Hz,'float32');
      other_data = [cage_temp_data, rh_data,zeros(1,3)];
      fwrite(handles.fid,other_data,'float32');
      % fwrite(handles.fid, time_now,'double');
      data_to_save_1000Hz(:,:) = NaN;
      data_to_save_100Hz(:,:) = NaN;

      %=================================================================
================
      % display data to the screen every 10 seconds

      set(handles.rh_label,'String',num2str(rh_data))
      set(handles.cage_temp_label,'String',num2str(cage_temp_data))

      %=================================================================
================
   end

   izz = izz + 1;

catch
   msgbox('Data Acquisition Has Stopped.','Error','error','modal')
   error_catch = lasterror;
   disp(error_catch.message)
   disp(error_catch.stack)
   stop_Callback(obj, event, handles)
end

% --- Executes on button press in pos_up.
function pos_up_Callback(hObject, eventdata, handles)
% hObject    handle to pos_up (see GCBO)
% eventdata  reserved - to be defined in a future version of MATLAB
% handles    structure with handles and user data (see GUIDATA)
```

```
switch get(gco,'Tag')
   case 'pos_up1', h_axes = handles.eeg1_axes;
   case 'pos_up2', h_axes = handles.eeg2_axes;
   case 'pos_up3', h_axes = handles.emg_axes;
   case 'pos_up4', h_axes = handles.ekg_axes;
   case 'pos_up5', h_axes = handles.pressure_axes;
end
axes_range = get(h_axes,'YLim');
midpoint = (axes_range(2) - axes_range(1))/2 + axes_range(1);
amplitude = (axes_range(2) - axes_range(1))/2;
midpoint = midpoint - amplitude/2;
set(h_axes,'YLim',[(midpoint-amplitude) (midpoint+amplitude)],'YTick',(midpoint-
amplitude):(2*amplitude/4):(midpoint+amplitude))

% --- Executes on button press in pos_down.
function pos_down_Callback(hObject, eventdata, handles)
% hObject    handle to pos_down (see GCBO)
% eventdata  reserved - to be defined in a future version of MATLAB
% handles    structure with handles and user data (see GUIDATA)
switch get(gco,'Tag')
   case 'pos_down1', h_axes = handles.eeg1_axes;
   case 'pos_down2', h_axes = handles.eeg2_axes;
   case 'pos_down3', h_axes = handles.emg_axes;
   case 'pos_down4', h_axes = handles.ekg_axes;
   case 'pos_down5', h_axes = handles.pressure_axes;
end
axes_range = get(h_axes,'YLim');
midpoint = (axes_range(2) - axes_range(1))/2 + axes_range(1);
amplitude = (axes_range(2) - axes_range(1))/2;
midpoint = midpoint + amplitude/2;
set(h_axes,'YLim',[(midpoint-amplitude) (midpoint+amplitude)],'YTick',(midpoint-
amplitude):(2*amplitude/4):(midpoint+amplitude))


% --- Executes on button press in mag_up.
function mag_up_Callback(hObject, eventdata, handles)
% hObject    handle to mag_up (see GCBO)
% eventdata  reserved - to be defined in a future version of MATLAB
% handles    structure with handles and user data (see GUIDATA)
switch get(gco,'Tag')
   case 'mag_up1', h_axes = handles.eeg1_axes;
   case 'mag_up2', h_axes = handles.eeg2_axes;
   case 'mag_up3', h_axes = handles.emg_axes;
   case 'mag_up4', h_axes = handles.ekg_axes;
   case 'mag_up5', h_axes = handles.pressure_axes;
end

axes_range = get(h_axes,'YLim');
midpoint = (axes_range(2) - axes_range(1))/2 + axes_range(1);
amplitude = (axes_range(2) - axes_range(1))/2;
amplitude = amplitude/2;
```

```
set(h_axes,'YLim',[(midpoint-amplitude) (midpoint+amplitude)],'YTick',(midpoint-
amplitude):(2*amplitude/4):(midpoint+amplitude))

% --- Executes on button press in mag_down.
function mag_down_Callback(hObject, eventdata, handles)
% hObject    handle to mag_down (see GCBO)
% eventdata  reserved - to be defined in a future version of MATLAB
% handles    structure with handles and user data (see GUIDATA)
switch get(gco,'Tag')
   case 'mag_down1', h_axes = handles.eeg1_axes;
   case 'mag_down2', h_axes = handles.eeg2_axes;
   case 'mag_down3', h_axes = handles.emg_axes;
   case 'mag_down4', h_axes = handles.ekg_axes;
   case 'mag_down5', h_axes = handles.pressure_axes;
end

axes_range = get(h_axes,'YLim');
midpoint = (axes_range(2) - axes_range(1))/2 + axes_range(1);
amplitude = (axes_range(2) - axes_range(1))/2;
amplitude = amplitude*2;
set(h_axes,'YLim',[(midpoint-amplitude) (midpoint+amplitude)],'YTick',(midpoint-
amplitude):(2*amplitude/4):(midpoint+amplitude))
```

Mouse EMU data acquisition GUI: 'MouseEMU_single.fig'

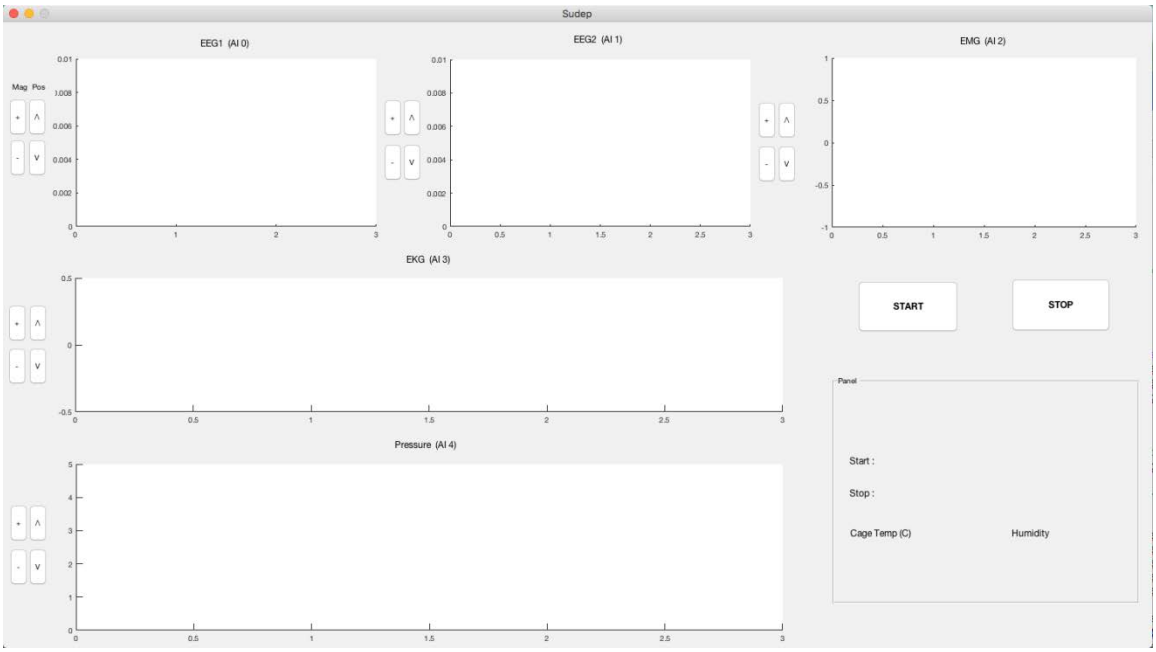

Mouse EMU data viewer program code

The following algorithms are written in MATLAB R2014b version, in order to display the EMU data recorded from the data acquisition program.

MATLAB program code: 'MouseEMU_single_reading.m'

```
 % updated on 11/09/2014
% smoothing all graphs using moving average window 3
% EEG filter: 0.3 - 70 Hz band-pass with a 60 Hz notch
% EMG filter: 10 - 80Hz band-pass with a 60 Hz notch
% EKG filter: Perform CWT with scale 3 and wavelet Coiflet-1 on EKG
% Plethysmography: 1-10 Hz band-pass

function varargout = MouseEMU_single_reading(varargin)
% MouseEMU_single_reading MATLAB code for MouseEMU_single_reading.fig
%      MouseEMU_single_reading, by itself, creates a new MouseEMU_single_reading or raises
the existing
%      singleton*.
%
%      H = MouseEMU_single_reading returns the handle to a new MouseEMU_single_reading or
the handle to
%      the existing singleton*.
%
%      MouseEMU_single_reading('CALLBACK',hObject,eventData,handles,...) calls the local
%      function named CALLBACK in MouseEMU_single_reading.M with the given input
arguments.
%
%      MouseEMU_single_reading('Property','Value',...) creates a new
MouseEMU_single_reading or raises the
%      existing singleton*.  Starting from the left, property value pairs are
%      applied to the GUI before MouseEMU_single_reading_OpeningFcn gets called.  An
%      unrecognized property name or invalid value makes property application
%      stop.  All inputs are passed to MouseEMU_single_reading_OpeningFcn via varargin.
%
%      *See GUI Options on GUIDE's Tools menu.  Choose "GUI allows only one
%      instance to run (singleton)".
%
% See also: GUIDE, GUIDATA, GUIHANDLES

% Edit the above text to modify the response to help MouseEMU_single_reading

% Last Modified by GUIDE v2.5 18-Oct-2013 15:02:26

% Begin initialization code - DO NOT EDIT
gui_Singleton = 1;
gui_State = struct('gui_Name',       mfilename, ...
                   'gui_Singleton',  gui_Singleton, ...
                   'gui_OpeningFcn', @MouseEMU_single_reading_OpeningFcn, ...
```

```
                'gui_OutputFcn',  @MouseEMU_single_reading_OutputFcn, ...
                'gui_LayoutFcn',  [] , ...
                'gui_Callback',   []);
if nargin && ischar(varargin{1})
    gui_State.gui_Callback = str2func(varargin{1});
end

if nargout
    [varargout{1:nargout}] = gui_mainfcn(gui_State, varargin{:});
else
    gui_mainfcn(gui_State, varargin{:});
end
% End initialization code - DO NOT EDIT

% --- Executes just before MouseEMU_single_reading is made visible.
function MouseEMU_single_reading_OpeningFcn(hObject, eventdata, handles, varargin)
% This function has no output args, see OutputFcn.
% hObject    handle to figure
% eventdata  reserved - to be defined in a future version of MATLAB
% handles    structure with handles and user data (see GUIDATA)
% varargin   command line arguments to MouseEMU_single_reading (see VARARGIN)

% Choose default command line output for MouseEMU_single_reading
handles.output = hObject;

handles.graph_axes = findobj('type','axes','Units','characters');
handles.sweep_values = [5 10 30 60 120 300 420 600];
handles.sweep_index = 2;
handles.sweep_duration = handles.sweep_values(handles.sweep_index);
set(handles.sweep_duration_label,'string',num2str(handles.sweep_duration))
set(handles.graph_axes,'XLim', [0 handles.sweep_duration])

% Update handles structure
guidata(hObject, handles);

% UIWAIT makes MouseEMU_single_reading wait for user response (see UIRESUME)
% uiwait(handles.figure1);

% --- Outputs from this function are returned to the command line.
function varargout = MouseEMU_single_reading_OutputFcn(hObject, eventdata, handles)
% varargout  cell array for returning output args (see VARARGOUT);
% hObject    handle to figure
% eventdata  reserved - to be defined in a future version of MATLAB
% handles    structure with handles and user data (see GUIDATA)

% Get default command line output from handles structure
varargout{1} = handles.output;

% --- Executes on button press in loading.
function loading_Callback(hObject, eventdata, handles)
% hObject    handle to loading (see GCBO)
```

```
% eventdata  reserved - to be defined in a future version of MATLAB
% handles    structure with handles and user data (see GUIDATA)

% initialize handles structure variables
handles.first_plot_point = 0;
handles.last_plot_point = handles.sweep_duration;

% user inputs name of file to analyze
[handles.file_name,handles.path_name] = uigetfile('*.bin','Select File To Analyze.');

if(handles.file_name == 0), return, end % user pressed the cancel button

% open the selected file for binary reading
handles.fid = fopen([handles.path_name,handles.file_name],'r');

handles.file_name_length = numel(handles.file_name);

% determine size of file (bytes)
fseek(handles.fid, 0, 'eof');
filesize = ftell(handles.fid);
fseek(handles.fid, 0, 'bof');

% save file to variable
handles.SampleRate = 1000;
other_fs = 100;
handles.time_data = fread(handles.fid,1*floor(filesize/56028),'1*double',56020);

fseek(handles.fid, 8, 'bof');
handles.EKG_data =
fread(handles.fid,handles.SampleRate*10*floor(filesize/56028),'10000*float32',16028);
handles.EKG_data = smooth(handles.EKG_data);

fseek(handles.fid, 40008, 'bof');
[handles.EEG1_data,handles.EEG1_count] =
fread(handles.fid,other_fs*10*floor(filesize/56028),'1000*float32',52028);

fseek(handles.fid, 44008, 'bof');
handles.EEG2_data = fread(handles.fid,other_fs*10*floor(filesize/56028),'1000*float32',52028);
%handles.EEG2_data = smooth(handles.EEG2_data);

fseek(handles.fid, 48008, 'bof');
handles.EMG_data = fread(handles.fid,other_fs*10*floor(filesize/56028),'1000*float32',52028);
%handles.EMG_data = smooth(handles.EMG_data);

fseek(handles.fid, 52008, 'bof');
handles.plethy_data = fread(handles.fid,other_fs*10*floor(filesize/56028),'1000*float32',52028);
handles.plethy_data = smooth(handles.plethy_data);

fseek(handles.fid, 56008, 'bof');
handles.cage_temp_data = fread(handles.fid,1*floor(filesize/56028),'1*float32',56024);
```

```
fseek(handles.fid, 56012, 'bof');
handles.rh_data = fread(handles.fid,1*floor(filesize/56028),'1*float32',56024);

% creat time index
handles.file_length_seconds = handles.EEG1_count / other_fs;
handles.time_index_1000Hz =
(1/handles.SampleRate:1/handles.SampleRate:handles.file_length_seconds)';
handles.time_index_100Hz = (1/other_fs:1/other_fs:handles.file_length_seconds)';
handles.time_index_other = (1/0.1:1/0.1:handles.file_length_seconds)'; %0.6Hz data: time_data,
cage_temp, rh

% display file information on GUI
set(handles.file_name_label,'string', handles.file_name);
set(handles.file_length_label, 'string',[num2str(handles.file_length_seconds),'seconds'])
set(handles.started_time,'string', datestr(handles.time_data(1),31))

% EEG filter: 1 - 20 Hz band-pass with a 60 Hz notch
wn=[1 20]/50;
[b,a]=butter(1,wn,'bandpass');
handles.EEG1_data_filtered = filter(b,a,handles.EEG1_data);
handles.EEG2_data_filtered = filter(b,a,handles.EEG2_data);

% % 60 Hz notch filter EEGs
% wo = 60/(100/2);  BW = wo/35;
% [b,a] = iirnotch(wo,BW);
% handles.EEG1_data_filtered = filter(b,a,handles.EEG1_data_filtered);
% handles.EEG2_data_filtered = filter(b,a,handles.EEG2_data_filtered);

% EMG filter: 10 - 80Hz band-pass with a 60 Hz notch
% band-pass filtering on EMG data (5 - 40 Hz)
wn=[5 40]/50;
[b,a]=butter(1,wn,'bandpass');
handles.EMG_data_filtered = filter(b,a,handles.EMG_data);
% % 60 Hz notch filter EMGs
% wo = 60/(100/2);  BW = wo/35;
% [b,a] = iirnotch(wo,BW);
% handles.EMG_data_filtered = filter(b,a,handles.EMG_data_filtered);

% Perform CWT with scale 4 and wavelet Coiflet-1 on EKG
handles.EKG_data_filtered=cwt(handles.EKG_data,4,'coif1')';

% % % detrend on EKG data
% EKG_data = detrend(handles.EKG_data);
% % EKG filter: 1 - 50Hz band-pass
% wn=[1 50]/500;
% [b,a]=butter(5,wn,'bandpass');
% handles.EKG_data_filtered = filter(b,a,handles.EKG_data_filtered);

% detrend on respiratory data
breathing_data = detrend(handles.plethy_data);
```

```
% band-pass filtering on plethysmography data (1 - 10 Hz)
wn=[1 10]/50;
[b,a]=butter(1,wn,'bandpass');
handles.plethy_data_filtered = filter(b,a,breathing_data);

% plot entire raw file
handles.hLine_eeg1 =
line('XData',handles.time_index_100Hz,'YData',handles.EEG1_data,'color','black','parent',handles
.eeg1_axes);
handles.hLine_eeg2 =
line('XData',handles.time_index_100Hz,'YData',handles.EEG2_data,'color','black','parent',handles
.eeg2_axes);
handles.hLine_emg =
line('XData',handles.time_index_100Hz,'YData',handles.EMG_data,'color','black','parent',handles
.emg_axes);
handles.hLine_ekg =
line('XData',handles.time_index_1000Hz,'YData',handles.EKG_data_filtered,'color','black','paren
t',handles.ekg_axes);
handles.hLine_pressure =
line('XData',handles.time_index_100Hz,'YData',handles.plethy_data_filtered,'color','black','parent
',handles.plethy_axes);

%
set(handles.view_scrollbar, 'enable','on')
% initialize view_scrollbar (slider)
set(handles.view_scrollbar, 'min', handles.first_plot_point)

if(handles.file_length_seconds < handles.sweep_duration)
   set(handles.view_scrollbar,'Max', handles.file_length_seconds)
   set(handles.view_scrollbar,'sliderstep', [0 0])
   set(handles.increase_x,'enable', 'off')
else
   set(handles.view_scrollbar, 'Max', handles.file_length_seconds-handles.sweep_duration)
   handles.view_scrollbar_max_min = get(handles.view_scrollbar, 'Max') -
get(handles.view_scrollbar, 'min');
   set(handles.view_scrollbar, 'sliderstep', [1/handles.view_scrollbar_max_min
handles.sweep_duration/handles.view_scrollbar_max_min])
end

% Update handles structure
guidata(hObject, handles);

% --- Executes on slider movement.
function view_scrollbar_Callback(hObject, eventdata, handles)
% hObject    handle to view_scrollbar (see GCBO)
% eventdata  reserved - to be defined in a future version of MATLAB
% handles    structure with handles and user data (see GUIDATA)

% Hints: get(hObject,'Value') returns position of slider
%        get(hObject,'Min') and get(hObject,'Max') to determine range of slider
```

```
set(hObject,'Value', round(get(hObject, 'Value')))
% set(handles.view_scrollbar,'Value', round(get(handles.view_scrollbar,'Value')))
handles.first_plot_point = get(handles.view_scrollbar,'Value');
handles.last_plot_point = handles.first_plot_point + handles.sweep_duration;
if(handles.last_plot_point > handles.file_length_seconds)
   handles.last_plot_point = handles.file_length_seconds;
   handles.first_plot_point = handles.last_plot_point - handles.sweep_duration;
   set(hObject, 'Value', get(hObject,'Max'))
end

set(handles.graph_axes,'XLim', [handles.first_plot_point handles.last_plot_point])

% Update handles structure
guidata(hObject, handles);

% --- Executes during object creation, after setting all properties.
function view_scrollbar_CreateFcn(hObject, eventdata, handles)
% hObject    handle to view_scrollbar (see GCBO)
% eventdata  reserved - to be defined in a future version of MATLAB
% handles    empty - handles not created until after all CreateFcns called

% Hint: slider controls usually have a light gray background.
if isequal(get(hObject,'BackgroundColor'), get(0,'defaultUicontrolBackgroundColor'))
   set(hObject,'BackgroundColor',[.9 .9 .9]);
end

% --- Executes on button press in pos_up.
function pos_up_Callback(hObject, eventdata, handles)
% hObject    handle to pos_up (see GCBO)
% eventdata  reserved - to be defined in a future version of MATLAB
% handles    structure with handles and user data (see GUIDATA)
switch get(gco,'Tag')
   case 'pos_up1', h_axes = handles.eeg1_axes;
   case 'pos_up2', h_axes = handles.eeg2_axes;
   case 'pos_up3', h_axes = handles.emg_axes;
   case 'pos_up4', h_axes = handles.ekg_axes;
   case 'pos_up5', h_axes = handles.plethy_axes;
end
axes_range = get(h_axes,'YLim');
midpoint = (axes_range(2) - axes_range(1))/2 + axes_range(1);
amplitude = (axes_range(2) - axes_range(1))/2;
midpoint = midpoint - amplitude/2;
set(h_axes,'YLim',[(midpoint-amplitude) (midpoint+amplitude)],'YTick',(midpoint-
amplitude):(2*amplitude/4):(midpoint+amplitude))

% --- Executes on button press in pos_down.
function pos_down_Callback(hObject, eventdata, handles)
% hObject    handle to pos_down (see GCBO)
% eventdata  reserved - to be defined in a future version of MATLAB
% handles    structure with handles and user data (see GUIDATA)
switch get(gco,'Tag')
```

```
    case 'pos_down1', h_axes = handles.eeg1_axes;
    case 'pos_down2', h_axes = handles.eeg2_axes;
    case 'pos_down3', h_axes = handles.emg_axes;
    case 'pos_down4', h_axes = handles.ekg_axes;
    case 'pos_down5', h_axes = handles.plethy_axes;
end
axes_range = get(h_axes,'YLim');
midpoint = (axes_range(2) - axes_range(1))/2 + axes_range(1);
amplitude = (axes_range(2) - axes_range(1))/2;
midpoint = midpoint + amplitude/2;
set(h_axes,'YLim',[(midpoint-amplitude) (midpoint+amplitude)],'YTick',(midpoint-
amplitude):(2*amplitude/4):(midpoint+amplitude))

% --- Executes on button press in mag_up.
function mag_up_Callback(hObject, eventdata, handles)
% hObject    handle to mag_up (see GCBO)
% eventdata  reserved - to be defined in a future version of MATLAB
% handles    structure with handles and user data (see GUIDATA)
switch get(gco,'Tag')
    case 'mag_up1', h_axes = handles.eeg1_axes;
    case 'mag_up2', h_axes = handles.eeg2_axes;
    case 'mag_up3', h_axes = handles.emg_axes;
    case 'mag_up4', h_axes = handles.ekg_axes;
    case 'mag_up5', h_axes = handles.plethy_axes;
end

axes_range = get(h_axes,'YLim');
midpoint = (axes_range(2) - axes_range(1))/2 + axes_range(1);
amplitude = (axes_range(2) - axes_range(1))/2;
amplitude = amplitude/2;
set(h_axes,'YLim',[(midpoint-amplitude) (midpoint+amplitude)],'YTick',(midpoint-
amplitude):(2*amplitude/4):(midpoint+amplitude))

% --- Executes on button press in mag_down.
function mag_down_Callback(hObject, eventdata, handles)
% hObject    handle to mag_down (see GCBO)
% eventdata  reserved - to be defined in a future version of MATLAB
% handles    structure with handles and user data (see GUIDATA)
switch get(gco,'Tag')
    case 'mag_down1', h_axes = handles.eeg1_axes;
    case 'mag_down2', h_axes = handles.eeg2_axes;
    case 'mag_down3', h_axes = handles.emg_axes;
    case 'mag_down4', h_axes = handles.ekg_axes;
    case 'mag_down5', h_axes = handles.plethy_axes;
end

axes_range = get(h_axes,'YLim');
midpoint = (axes_range(2) - axes_range(1))/2 + axes_range(1);
amplitude = (axes_range(2) - axes_range(1))/2;
amplitude = amplitude*2;
```

```
set(h_axes,'YLim',[(midpoint-amplitude) (midpoint+amplitude)],'YTick',(midpoint-
amplitude):(2*amplitude/4):(midpoint+amplitude))

% --- Executes on button press in increase_x.
function increase_x_Callback(hObject, eventdata, handles)
% hObject    handle to increase_x (see GCBO)
% eventdata  reserved - to be defined in a future version of MATLAB
% handles    structure with handles and user data (see GUIDATA)
handles.sweep_index = handles.sweep_index + 1;
   if(handles.sweep_index==8)
     set(handles.increase_x,'enable','off')
   else
      set(handles.increase_x, 'enable', 'on')
   end

   if(strcmp(get(handles.decrease_x,'enable'),'off'))
               set(handles.decrease_x,'enable','on')
   end

   if(handles.sweep_index==numel(handles.sweep_values)+1)
            set(handles.increase_x,'enable','off')
            handles.sweep_index = numel(handles.sweep_values);
            set(handles.view_scrollbar,'enable','off')
            handles.last_plot_point = handles.file_length_seconds;
            set(handles.graph_axes,'XLim',[handles.first_plot_point handles.last_plot_point])
         if(strcmp(get(handles.decrease_x,'enable'),'off'))
               set(handles.decrease_x,'enable','on')
         end

             guidata(handles.Plethy_reading_GUI, handles)
   return
   end

%     handles.first_plot_point = get(handles.view_scrollbar, 'Value');

   handles.sweep_duration = handles.sweep_values(handles.sweep_index);
   set(handles.sweep_duration_label, 'string', num2str(handles.sweep_duration))
   handles.last_plot_point = handles.first_plot_point + handles.sweep_duration;

   if(handles.last_plot_point>handles.file_length_seconds)
      handles.last_plot_point = handles.file_length_seconds;
      handles.first_plot_point = handles.last_plot_point - handles.sweep_duration;
      set(handles.view_scrollbar,'value',handles.first_plot_point)
   end
   set(handles.graph_axes,'XLim',[handles.first_plot_point handles.last_plot_point])

   if(handles.file_length_seconds<handles.sweep_duration)
      set(handles.view_scrollbar,'Max',handles.file_length_seconds)
      set(handles.view_scrollbar,'sliderstep',[0 0])
   else
       set(handles.view_scrollbar,'Max',handles.file_length_seconds-handles.sweep_duration)
```

```
        handles.view_scrollbar_max_min = get(handles.view_scrollbar,'max') -
get(handles.view_scrollbar,'min');
       set(handles.view_scrollbar,'sliderstep',[1/handles.view_scrollbar_max_min
handles.sweep_duration/handles.view_scrollbar_max_min])
   end

   % Update handles structure
   guidata(hObject, handles);

% --- Executes on button press in decrease_x.
function decrease_x_Callback(hObject, eventdata, handles)
% hObject    handle to decrease_x (see GCBO)
% eventdata  reserved - to be defined in a future version of MATLAB
% handles    structure with handles and user data (see GUIDATA)
handles.first_plot_point = get(handles.view_scrollbar, 'Value');
   if(strcmp(get(handles.view_scrollbar,'enable'),'off')==1)
         set(handles.view_scrollbar,'enable','on')
         set(handles.increase_x,'enable','on')

         handles.last_plot_point = handles.first_plot_point + handles.sweep_duration;
         set(handles.graph_axes,'XLim',[handles.first_plot_point handles.last_plot_point])
         guidata(handles.Plethy_reading_GUI, handles)
   return
   end

      handles.sweep_index = handles.sweep_index - 1;
   if(handles.sweep_index==1)
         set(handles.decrease_x,'enable','off')
   else
         set(handles.decrease_x, 'enable', 'on')
   end

   if(strcmp(get(handles.increase_x,'enable'),'off'))
     set(handles.increase_x,'enable','on')
   end

   handles.sweep_duration = handles.sweep_values(handles.sweep_index);
   set(handles.sweep_duration_label, 'string', num2str(handles.sweep_duration))
   handles.last_plot_point = handles.first_plot_point + handles.sweep_duration;

   if(handles.last_plot_point>handles.file_length_seconds)
       handles.last_plot_point = handles.file_length_seconds;
       handles.first_plot_point = handles.last_plot_point - handles.sweep_duration;
      set(handles.view_scrollbar,'value',handles.first_plot_point)
   end
   set(handles.graph_axes,'XLim',[handles.first_plot_point handles.last_plot_point])

   if(handles.file_length_seconds<handles.sweep_duration)
      set(handles.view_scrollbar,'Max',handles.file_length_seconds)
      set(handles.view_scrollbar,'sliderstep',[0 0])
   else
```

```
        set(handles.view_scrollbar,'Max',handles.file_length_seconds-handles.sweep_duration)
        handles.view_scrollbar_max_min = get(handles.view_scrollbar,'max') -
get(handles.view_scrollbar,'min');
        set(handles.view_scrollbar,'sliderstep',[1/handles.view_scrollbar_max_min
handles.sweep_duration/handles.view_scrollbar_max_min])
    end
     % Update handles structure
    guidata(hObject, handles);
```

Graphical User Interface (GUI): 'MouseEMU_single_reading.fig'

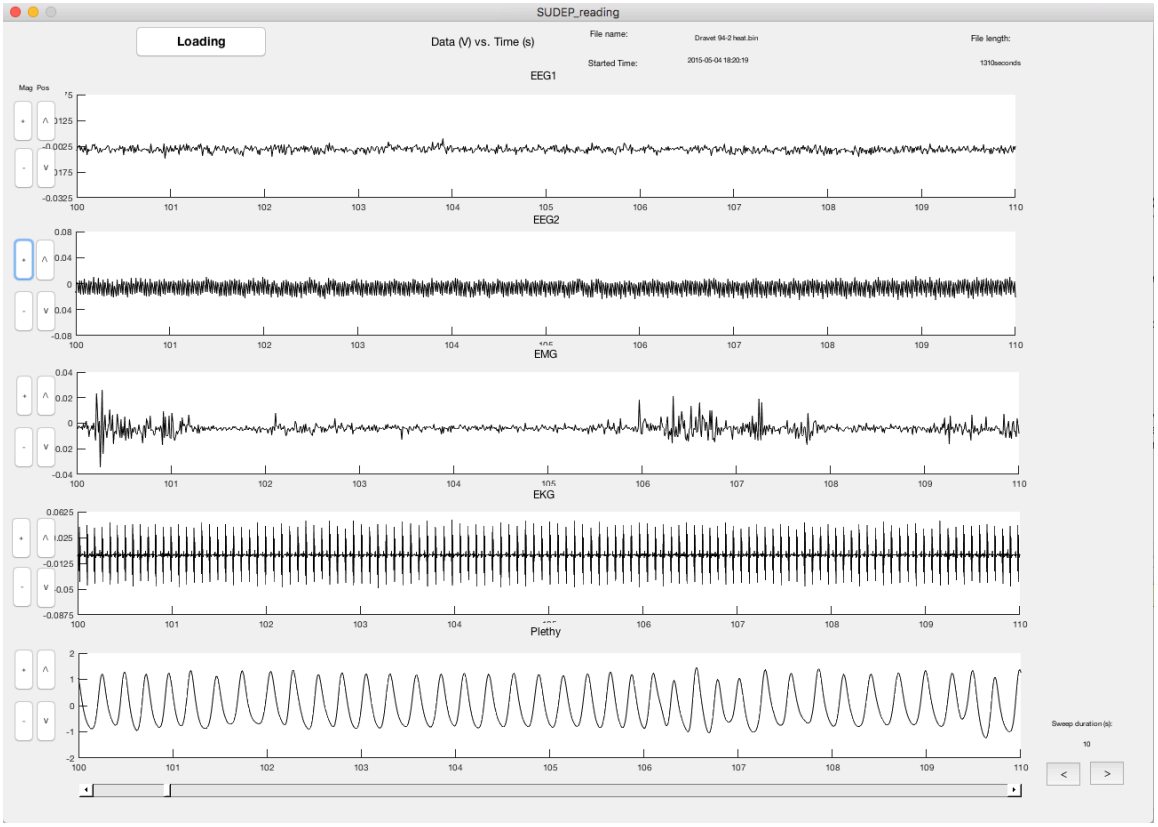

Copyright Permission

Figure 2. used with permission (Devinsky et al., 2016).

Devinsky, O., **Hesdorffer, D. C.**, **Thurman, D. J.**, **Lhatoo, S.**, & **Richerson, G.** (2016). Sudden unexpected death in epilepsy: epidemiology, mechanisms, and prevention. *The Lancet Neurology*, *15*(10), 1075–1088

License Details

This Agreement between YuJaung Kim ("You") and Elsevier ("Elsevier") consists of your license details and the terms and conditions provided by Elsevier and Copyright Clearance Center.

printable details

License Number	4074980116802
License date	Mar 23, 2017
Licensed Content Publisher	Elsevier
Licensed Content Publication	The Lancet Neurology
Licensed Content Title	Sudden unexpected death in epilepsy: epidemiology, mechanisms, and prevention
Licensed Content Author	Orrin Devinsky,Dale C Hesdorffer,David J Thurman,Samden Lhatoo,George Richerson
Licensed Content Date	September 2016
Licensed Content Volume	15
Licensed Content Issue	10
Licensed Content Pages	14
Type of Use	reuse in a thesis/dissertation
Portion	figures/tables/illustrations
Number of figures/tables/illustrations	1
Format	electronic
Are you the author of this Elsevier article?	No
Will you be translating?	No
Order reference number	
Original figure numbers	Figure 2
Title of your thesis/dissertation	Mechanisms and prevention of SUDEP in Dravet Syndrome
Expected completion date	May 2017
Estimated size (number of pages)	1
Elsevier VAT number	GB 494 6272 12
Requestor Location	YuJaung Kim 700 Carriage Hill Apt 6 Iowa City, IA 52246 United States Attn: YuJaung Kim
Publisher Tax ID	98-0397604
Total	**0.00 USD**

Figure 3. used with permission (Löscher, 2011).

Löscher, W. (2011). Critical review of current animal models of seizures and epilepsy used in the discovery and development of new antiepileptic drugs. *Seizure*, *20*(5), 359–368.

License Details

This Agreement between YuJaung Kim ("You") and Elsevier ("Elsevier") consists of your license details and the terms and conditions provided by Elsevier and Copyright Clearance Center.

printable details

License Number	4074850073589
License date	Mar 23, 2017
Licensed Content Publisher	Elsevier
Licensed Content Publication	Seizure
Licensed Content Title	Critical review of current animal models of seizures and epilepsy used in the discovery and development of new antiepileptic drugs
Licensed Content Author	Wolfgang Löscher
Licensed Content Date	June 2011
Licensed Content Volume	20
Licensed Content Issue	5
Licensed Content Pages	10
Type of Use	reuse in a thesis/dissertation
Portion	figures/tables/illustrations
Number of figures/tables/illustrations	1
Format	electronic
Are you the author of this Elsevier article?	No
Will you be translating?	No
Order reference number	
Original figure numbers	Figure 2.
Title of your thesis/dissertation	Mechanisms and prevention of SUDEP in Dravet Syndrome
Expected completion date	May 2017
Estimated size (number of pages)	1
Elsevier VAT number	GB 494 6272 12
Requestor Location	YuJaung Kim 700 Carriage Hill Apt 6 Iowa City, IA 52246 United States Attn: YuJaung Kim
Publisher Tax ID	98-0397604
Total	**0.00 USD**

REFERENCES

Aiba, I., & **Noebels, J. L.** (2015). Spreading depolarization in the brainstem mediates sudden cardiorespiratory arrest in mouse SUDEP models. *Science Translational Medicine*, *7*, 282ra46. https://doi.org/10.1126/scitranslmed.aaa4050

Anderson, J. H., **Bos, J. M.**, **Cascino, G. D.**, & **Ackerman, M. J.** (2014). Prevalence and spectrum of electroencephalogram-identified epileptiform activity among patients with long QT syndrome. *Heart Rhythm : The Official Journal of the Heart Rhythm Society*, *11*(1), 53–7. https://doi.org/10.1016/j.hrthm.2013.10.010

Auerbach, D. S., **Jones, J.**, **Clawson, B. C.**, **Offord, J.**, **Lenk, G. M.**, **Ogiwara, I.**, … **Isom, L. L.** (2013). Altered Cardiac Electrophysiology and SUDEP in a Model of Dravet Syndrome. *PLoS ONE*, *8*(10), 1–15. https://doi.org/10.1371/journal.pone.0077843

Aurlien, D., **Leren, T. P.**, **Taubøll, E.**, & **Gjerstad, L.** (2009). New SCN5A mutation in a SUDEP victim with idiopathic epilepsy. *Seizure*, *18*(2), 158–160. https://doi.org/10.1016/j.seizure.2008.07.008

Avanzini, G., **Spreafico, R.**, **Cipelletti, B.**, **Sancini, G.**, **Frassoni, C.**, **Franceschetti, S.**, … **Simeone, a**. (2000). Synaptic properties of neocortical neurons in epileptic mice lacking the Otx1 gene. *Epilepsia*, *41 Suppl 6*, S200–S205. https://doi.org/10.1111/j.1528-1157.2000.tb01582.x

Avoli, M., **Brancati, A.**, **Pacitti, C.**, & **Barra, P. F. A.** (1982). Neuronal responses to putative neurotransmitters during penicillin epileptogenesis. *Neuroscience*, *7*(8), 1955–1961. https://doi.org/10.1016/0306-4522(82)90010-0

Bachmanov, A. A., **Reed, D. R.**, **Beauchamp, G. K.**, & **Tordoff, M. G.** (2002). Food intake, water intake, and drinking spout side preference of 28 mouse strains. *Behavior Genetics*, *32*(6), 435–443. https://doi.org/10.1023/A:1020884312053

Bateman, L. M., **Li, C. S.**, & **Seyal, M.** (2008). Ictal hypoxemia in localization-related epilepsy: Analysis of incidence, severity and risk factors. *Brain*, *131*(12), 3239–3245. https://doi.org/10.1093/brain/awn277

Bateman, L. M., **Spitz, M.**, & **Seyal, M.** (2010). Ictal hypoventilation contributes to cardiac arrhythmia and SUDEP: report on two deaths in video-EEG-monitored patients. *Epilepsia*, *51*(5), 916–20. https://doi.org/10.1111/j.1528-1167.2009.02513.x

Bear, M. F., **Connors, B. W.**, & **Paradiso, M. A.** (2001). *Neuroscience: Exploring the Brain* (2nd ed.). Lippincott Williams & Wilkins.

Buchanan, G. F., **Murray, N. M.**, **Hajek, M. A.**, & **Richerson, G. B.** (2014). Serotonin neurones have anti-convulsant effects and reduce seizure-induced mortality. *The Journal of Physiology*, *592*(Pt 19), 4395–410. https://doi.org/10.1113/jphysiol.2014.277574

Cao, D., **Ohtani, H.**, **Ogiwara, I.**, **Ohtani, S.**, **Takahashi, Y.**, **Yamakawa, K.**, & **Inoue, Y.** (2012). Efficacy of stiripentol in hyperthermia-induced seizures in a mouse model of Dravet syndrome. *Epilepsia*, *53*(7), 1140–5. https://doi.org/10.1111/j.1528-1167.2012.03497.x

Castel-Branco, M. M., **Alves, G. L.**, **Figueiredo, I. V**, **Falcão, a C.**, & **Caramona, M. M.** (2009). The maximal electroshock seizure (MES) model in the preclinical assessment of potential new antiepileptic drugs. *Methods and Findings in Experimental and Clinical Pharmacology*, *31*(2), 101–106. https://doi.org/10.1358/mf.2009.31.2.1338414

Claes, L., **Del-Favero, J.**, **Ceulemans, B.**, **Lagae, L.**, **Broeckhoven, C. Van**, & **De Jonghe, P.** (2001). De Novo Mutations in the Sodium-Channel Gene SCN1A Cause Severe Myoclonic Epilepsy of Infancy. *Am. J. Hum. Genet*, *68*, 1327–1332. https://doi.org/10.1086/320609

Curia, G., **Longo, D.**, **Biagini, G.**, **Jones, R. S. G.**, & **Avoli, M.** (2008). The pilocarpine model of temporal lobe epilepsy. *Journal of Neuroscience Methods*, *172*(2), 143–157. https://doi.org/10.1016/j.jneumeth.2008.04.019

Daverio, M., **Ciccone, O.**, **Boniver Md, C.**, **De, L.**, **Md, P.**, **Corrado, D.**, & **Vecchi Md, M.** (2016). Supraventricular Tachycardia During Status Epilepticus in Dravet Syndrome: A Link Between Brain and Heart? *Pediatr Neurol*, *56*, 69–71. https://doi.org/10.1016/j.pediatrneurol.2015.12.003

Degiorgio, C. M., **Miller, P.**, **Meymandi, S.**, **Chin, A.**, **Epps, J.**, **Gordon, S.**, … **Harper, R. M.** (2010). RMSSD, a measure of vagus-mediated heart rate variability, is associated with risk factors for SUDEP: The SUDEP-7 Inventory ☆. *Epilepsy & Behavior*, *19*, 78–81. https://doi.org/10.1016/j.yebeh.2010.06.011

Delogu, A. B., **Spinelli, A.**, **Battaglia, D.**, **Dravet, C.**, **De Nisco, A.**, **Saracino, A.**, … **Crea, F.** (2011). Electrical and autonomic cardiac function in patients with Dravet syndrome. *Epilepsia*, *52*(SUPPL. 2), 55–58. https://doi.org/10.1111/j.1528-1167.2011.03003.x

Devinsky, O., **Hesdorffer, D. C.**, **Thurman, D. J.**, **Lhatoo, S.**, & **Richerson, G.** (2016). Sudden unexpected death in epilepsy: epidemiology, mechanisms, and prevention. *The Lancet Neurology*, *15*(10), 1075–1088. https://doi.org/10.1016/S1474-4422(16)30158-2

Dlouhy, B. J., **Gehlbach, B. K.**, **Kreple, C. J.**, **Kawasaki, H.**, **Oya, H.**, **Buzza, C.**, … **Richerson, G. B.** (2015). Breathing Inhibited When Seizures Spread to the Amygdala and upon Amygdala Stimulation. *Journal of Neuroscience*, *35*(28), 10281–9. https://doi.org/10.1523/JNEUROSCI.0888-15.2015

Dravet, C. (2011). The core Dravet syndrome phenotype. *Epilepsia*, *52*(SUPPL. 2), 3–9. https://doi.org/10.1111/j.1528-1167.2011.02994.x

Drorbaugh, J. E., & **Fenn, W. O.** (1955). A BAROMETRIC METHOD FOR MEASURING VENTILATION IN NEWBORN INFANTS. *Pediatrics*, *16*(1), 81–87.

Ergul, Y., **Ekici, B.**, **Tatli, B.**, **Nisli, K.**, & **Ozmen, M.** (2013). QT and P wave dispersion and heart rate variability in patients with Dravet syndrome. *Acta Neurol Belg*, (113), 161–166. https://doi.org/10.1007/s13760-012-0140-z

Espinosa, P. S., & **Tedrow, U. B.** (2009). Clinical / Scientific Notes SUDDEN UNEXPECTED NEAR DEATH IN EPILEPSY : MALIGNANT ARRHYTHMIA FROM, 1702–1705.

Faingold, C. L., & **Randall, M.** (2013). Effects of age, sex, and sertraline administration on seizure-induced respiratory arrest in the DBA/1 mouse model of sudden unexpected death in epilepsy (SUDEP). *Epilepsy and Behavior*, *28*(1), 78–82. https://doi.org/10.1016/j.yebeh.2013.04.003

Faingold, C. L., **Randall, M.**, & **Tupal, S.** (2010). DBA/1 mice exhibit chronic susceptibility to audiogenic seizures followed by sudden death associated with respiratory arrest. *Epilepsy and Behavior*, *17*(4), 436–440. https://doi.org/10.1016/j.yebeh.2010.02.007

Feng, H.-J., & **Faingold, C. L.** (2015). Abnormalities of serotonergic neurotransmission in animal models of SUDEP. *Epilepsy & Behavior*. https://doi.org/10.1016/j.yebeh.2015.06.008

Fisher, R. S., **Van Emde Boas, W.**, **Blume, W.**, **Elger, C.**, **Genton, P.**, **Lee, P.**, & **Engel, J.** (2005). Epileptic seizures and epilepsy: Definitions proposed by the International League Against Epilepsy (ILAE) and the International Bureau for Epilepsy (IBE). *Epilepsia*, *46*(4), 470–472. https://doi.org/10.1111/j.0013-9580.2005.66104.x

Freeman, J. M., **Kossoff, E. H.**, & **Hartman, A. L.** (2007). The ketogenic diet: one decade later. *Pediatrics*, *119*(3), 535–543. https://doi.org/10.1542/peds.2006-2447

Glasscock, E., **Yoo, J. W.**, **Chen, T. T.**, **Klassen, T. L.**, & **Jeffrey, L.** (2010). Kv1.1 potassium channel deficiency reveals brain-driven cardiac dysfunction as a candidate mechanism for sudden unexplained death in epilepsy(SUDEP). *J Neurosci. 2010*, *30*(15), 5167–5175. https://doi.org/10.1523/JNEUROSCI.5591-09.2010.Kv1.1

Goldman, a M., **Glasscock, E.**, **Yoo, J.**, **Chen, T. T.**, **Klassen, T. L.**, & **Noebels, J. L.** (2009). Arrhythmia in heart and brain: KCNQ1 mutations link epilepsy and sudden unexplained death. *Science Translational Medicine*, *1*(2), 2ra6. https://doi.org/10.1126/scitranslmed.3000289

Hahn, T. J., **Halstead, L. R.**, & **DeVivo, D. C.** (1979). Disordered mineral metabolism produced by ketogenic diet therapy. *Calcified Tissue International*, *28*(1), 17–22. https://doi.org/10.1007/BF02441213

Hall, C. S. (1946). Genetic differences in fatal audiogenic seizures. *The Journal of Heredity*.

Hani, A. J., **Mikati, H. M.**, & **Mikati, M. A.** (2015). Genetics of Pediatric Epilepsy. *Pediatric Clinics of North America*. https://doi.org/10.1016/j.pcl.2015.03.013

Hartman, A. L., **Zheng, X.**, **Bergbower, E.**, **Kennedy, M.**, & **Hardwick, J. M.** (2010). Seizure tests distinguish intermittent fasting from the ketogenic diet. *Epilepsia*, *51*(8), 1395–1402. https://doi.org/10.1111/j.1528-1167.2010.02577.x

Hata, Y., **Yoshida, K.**, **Kinoshita, K.**, & **Nishida, N.** (2016). Epilepsy-Related Sudden Unexpected Death: Targeted Molecular Analysis of Inherited Heart Disease Genes using Next-Generation DNA Sequencing. *Brain Pathology (Zurich, Switzerland)*. https://doi.org/10.1111/bpa.12390 [doi]

Hesdorffer, D. C., **Tomson, T.**, **Benn, E.**, **Sander, J. W.**, **Nilsson, L.**, **Langan, Y.**, … **Hauser, A.** (2011). Combined analysis of risk factors for SUDEP. *Epilepsia*, *52*(6), 1150–1159. https://doi.org/10.1111/j.1528-1167.2010.02952.x

Hessel, E. V. S., **Van Gassen, K. L. I.**, **Wolterink-Donselaar, I. G.**, **Stienen, P. J.**, **Fernandes, C.**, **Brakkee, J. H.**, … **De Graan, P. N. E.** (2009). Phenotyping mouse chromosome substitution strains reveal multiple QTLs for febrile seizure susceptibility. *Genes, Brain and Behavior*, *8*(2), 248–255. https://doi.org/10.1111/j.1601-183X.2008.00466.x

Hewertson, J., **Poets, C. F.**, **Samuels, M. P.**, **Boyd, S. G.**, **Neville, B. G.**, & **Southall, D. P.** (1994). Epileptic seizure-induced hypoxemia in infants with apparent life-threatening events. *Pediatrics*, *94*(2 Pt 1), 148–156.

Hitiris, N., **Mohanraj, R.**, **Norrie, J.**, & **Brodie, M. J.** (2007). Mortality in epilepsy. *Epilepsy & Behavior*, *10*(3), 363–376. https://doi.org/10.1016/j.yebeh.2007.01.005

Jacobs, B. L., & **Azmitia, E. C.** (1992). Structure and function of the brain serotonin system. *Physiological Reviews*, *72*(1), 165–229.

Johnson, J. N., **Hofman, N.**, **Haglund, C. M.**, **Cascino, G. D.**, **Wilde, a a M.**, & **Ackerman, M. J.** (2009). Identification of a possible pathogenic link between congenital long QT syndrome and epilepsy. *Neurology*, *72*(3), 224–31. https://doi.org/10.1212/01.wnl.0000335760.02995.ca

Jones, N. A., **Glyn, S. E.**, **Akiyama, S.**, **Hill, T. D. M.**, **Hill, A. J.**, **Weston, S. E.**, … **Williams, C. M.** (2012). Cannabidiol exerts anti-convulsant effects in animal models of temporal lobe and partial seizures. *Seizure*, *21*(5), 344–352. https://doi.org/10.1016/j.seizure.2012.03.001

Kalume, F., **Westenbroek, R. E.**, **Cheah, C. S.**, **Yu, F. H.**, **Oakley, J. C.**, **Scheuer, T.**, & **Catterall, W. A.** (2013). Sudden unexpected death in a mouse model of Dravet syndrome. *J Clin Invest*, *123*(4), 1798–808. https://doi.org/10.1172/JCI66220DS1

Kandel, E., **Schwartz, J.**, **Jessell, T.**, **Siegelbaum, S.**, & **Hudspeth, A.** (2000). *Principles of neural science* (4th ed.). McGraw-Hill.

Kerling, F., **Dütsch, M.**, **Linke, R.**, **Kuwert, T.**, **Stefan, H.**, & **Hilz, M. J.** (2009). Relation between ictal asystole and cardiac sympathetic dysfunction shown by MIBG-SPECT. *Acta Neurologica Scandinavica*, *120*(2), 123–129. https://doi.org/10.1111/j.1600-0404.2008.01135.x

Kloster, R.; Engelskjon, T. (1999). Sudden unexpected death in epilepsy (SUDEP): A clinical perspective and a search for risk factors. *J Neurol Neurosyr Psychiatry*, *67*, 439–444. https://doi.org/10.1016/j.yebeh.2006.11.010

Kossoff, E. H. (2004). More fat and fewer seizures: Dietary therapies for epilepsy. *Lancet Neurology*, *3*(7), 415–420. https://doi.org/10.1016/S1474-4422(04)00807-5

Kossoff, E. H., **Laux, L. C.**, **Blackford, R.**, **Morrison, P. F.**, **Pyzik, P. L.**, **Hamdy, R. M.**, … **Nordli, D. R.** (2008). When do seizures usually improve with the ketogenic diet? *Epilepsia*, *49*(2), 329–333. https://doi.org/10.1111/j.1528-1167.2007.01417.x

Kossoff, E. H., **Rowley, H.**, **Sinha, S. R.**, & **Vining, E. P. G.** (2008). A prospective study of the modified Atkins diet for intractable epilepsy in adults. *Epilepsia*, *49*(2), 316–319. https://doi.org/10.1111/j.1528-1167.2007.01256.x

Kwan, P., & **Sander, J. W.** (2004). The natural history of epilepsy: an epidemiological view. *Journal of Neurology, Neurosurgery, and Psychiatry*, *75*(10), 1376–1381. https://doi.org/10.1136/jnnp.2004.045690

Laffel, L. (1999). Ketone bodies: a review of physiology, pathophysiology and application of monitoring to diabetes. *Diabetes/metabolism Research and Reviews*, *15*(6), 412–426. https://doi.org/10.1002/(SICI)1520-7560(199911/12)15:6<412::AID-DMRR72>3.0.CO;2-8

Langan, Y., **Nashef, L.**, & **Sander, A. S.** (2000). Sudden unexpected death in epilepsy: a series of witnessed deaths. *J Neurol Neurosurg Psychiatry*, *68*, 211–213.

Laux, L., & **Blackford, R.** (2013). The ketogenic diet in Dravet syndrome. *Journal of Child Neurology*, *28*(8), 1041–4. https://doi.org/10.1177/0883073813487599

Lhatoo, S. D., **Faulkner, H. J.**, **Dembny, K.**, **Trippick, K.**, **Johnson, C.**, & **Bird, J. M.** (2010). An electroclinical case-control study of sudden unexpected death in epilepsy. *Annals of Neurology*, *68*(6), 787–96. https://doi.org/10.1002/ana.22101

Löscher, W. (2011). Critical review of current animal models of seizures and epilepsy used in the discovery and development of new antiepileptic drugs. *Seizure*, *20*(5), 359–368. https://doi.org/10.1016/j.seizure.2011.01.003

Lothman, E. W., & **Collins, R. C.** (1981). Kainic acid induced limbic seizures: metabolic, behavioral, electroencephalographic and neuropathological correlates. *Brain Research*, *218*(1), 299–318. https://doi.org/10.1016/0006-8993(81)91308-1

Maier, S. K. G., **Westenbroek, R. E.**, **Yamanushi, T. T.**, **Dobrzynski, H.**, **Boyett, M. R.**, **Catterall, W. A.**, & **Scheuer, T.** (2003). An unexpected requirement for brain-type sodium channels for control of heart rate in the mouse sinoatrial node. *Proceedings of the National Academy of Sciences of the United States of America*, *100*(6), 3507–12. https://doi.org/10.1073/pnas.2627986100

Martin, K., **Cf, J.**, **Rg, L.**, & **Pn, C.** (2016). Ketogenic diet and other dietary treatments for epilepsy (Review) SUMMARY OF FINDINGS FOR THE MAIN COMPARISON, (2). https://doi.org/10.1002/14651858.CD001903.pub3.www.cochranelibrary.com

Massey, C. a, **Sowers, L. P.**, **Dlouhy, B. J.**, & **Richerson, G. B.** (2014). Mechanisms of sudden unexpected death in epilepsy: the pathway to prevention. *Nature Reviews. Neurology*, *10*(5), 271–82. https://doi.org/10.1038/nrneurol.2014.64

McNally, M. A., & **Hartman, A. L.** (2012). Ketone bodies in epilepsy. *Journal of Neurochemistry*, *121*(1), 28–35. https://doi.org/10.1111/j.1471-4159.2012.07670.x

Nakase, K., **Kollmar, R.**, **Lazar, J.**, **Arjomandi, H.**, **Sundaram, K.**, **Silverman, J.**, … **Stewart, M.** (2016). Laryngospasm, central and obstructive apnea during seizures: Defining pathophysiology for sudden death in a rat model. *Epilepsy Research*, *128*, 126–139. https://doi.org/10.1016/j.eplepsyres.2016.08.004

Nashef, L. (1997). Sudden unexpected death in epilepsy: terminology and definitions. *Epilepsia*. https://doi.org/10.1111/j.1528-1157.1997.tb06130.x

Nashef, L., **Walker, F.**, **Allen, P.**, **Sander, J. W.**, **Shorvon, S. D.**, & **Fish, D. R.** (1996). Apnoea and bradycardia during epileptic seizures: relation to sudden death in epilepsy. *Journal of Neurology, Neurosurgery, and Psychiatry*, *60*(3), 297–300. https://doi.org/10.1136/jnnp.60.3.297

Nordli D.R., J., & **De Vivo, D. C.** (1997). The ketogenic diet revisited: Back to the future. *Epilepsia*, *38*(7), 743–749. https://doi.org/10.1111/j.1528-1157.1997.tb01460.x

Oakley, J. C., **Kalume, F.**, **Yu, F. H.**, **Scheuer, T.**, & **Catterall, W. a**. (2009). Temperature- and age-dependent seizures in a mouse model of severe myoclonic epilepsy in infancy. *Proceedings of the National Academy of Sciences of the United States of America*, *106*(10), 3994–9. https://doi.org/10.1073/pnas.0813330106

Ogiwara, I., **Miyamoto, H.**, **Morita, N.**, **Atapour, N.**, **Mazaki, E.**, **Inoue, I.**, … **Yamakawa, K.** (2007). Nav1.1 localizes to axons of parvalbumin-positive inhibitory interneurons: a circuit basis for epileptic seizures in mice carrying an Scn1a gene mutation. *The Journal of Neuroscience : The Official Journal of the Society for Neuroscience*, *27*(22), 5903–14. https://doi.org/10.1523/JNEUROSCI.5270-06.2007

Parihar, R., & **Ganesh, S.** (2013). The SCN1A gene variants and epileptic encephalopathies. *Journal of Human Genetics*, *58*(9), 573–580. https://doi.org/10.1038/jhg.2013.77

Parisi, P., **Oliva, A.**, **Vidal, M. C.**, **Partemi, S.**, **Campuzano, O.**, **Iglesias, A.**, … **Brugada, R.** (2013). Coexistence of epilepsy and Brugada syndrome in a family with SCN5A mutation. *Epilepsy Research*, *105*, 415–418. https://doi.org/10.1016/j.eplepsyres.2013.02.024

Partemi, S., **Vidal, M. C.**, **Striano, P.**, **Campuzano, O.**, **Allegue, C.**, **Pezzella, M.**, … **Brugada, R.** (2015). Genetic and forensic implications in epilepsy and cardiac arrhythmias: a case series. *International Journal of Legal Medicine*, *129*(3), 495–504. https://doi.org/10.1007/s00414-014-1063-4

Patil, N., **Cox, D. R.**, **Bhat, D.**, **Faham, M.**, **Myers, R. M.**, & **Peterson, A. S.** (1995). A potassium channel mutation in weaver mice implicates membrane excitability in granule cell differentiation. *Nature Genetics*, *11*(2), 126–129. https://doi.org/10.1038/ng1095-126

Racine, R., **Okujava, V.**, & **Chipashvili, S.** (1972). Modification of seizure activity by electrical stimulation. 2. Motor Seizure. *Electroencephalography and Clinical Neurophysiology*, *32*, 295–299. https://doi.org/Doi 10.1016/0013-4694(72)90178-2

Ryvlin, P., **Nashef, L.**, **Lhatoo, S. D.**, **Bateman, L. M.**, **Bird, J.**, **Bleasel, A.**, … **Tomson, T.** (2013). Incidence and mechanisms of cardiorespiratory arrests in epilepsy monitoring units (MORTEMUS): a retrospective study. *The Lancet. Neurology*, *12*(10), 966–77. https://doi.org/10.1016/S1474-4422(13)70214-X

Sakauchi, M., **Oguni, H.**, **Kato, I.**, **Osawa, M.**, **Hirose, S.**, **Kaneko, S.**, … **Fujiwara, T.** (2011). Retrospective multiinstitutional study of the prevalence of early death in Dravet syndrome. *Epilepsia*, *52*(6), 1144–1149. https://doi.org/10.1111/j.1528-1167.2011.03053.x

Sarkisian, M. R. (2001). Overview of the Current Animal Models for Human Seizure and Epileptic Disorders. *Epilepsy & Behavior : E&B*, *2*(3), 201–216. https://doi.org/10.1006/ebeh.2001.0193

Seyal, M., **Bateman, L. M.**, **Albertson, T. E.**, **Lin, T. C.**, & **Li, C. S.** (2010). Respiratory changes with seizures in localization-related epilepsy: Analysis of periictal hypercapnia and airflow patterns. *Epilepsia*, *51*(8), 1359–1364. https://doi.org/10.1111/j.1528-1167.2009.02518.x

Shorvon, S., & **Tomson, T.** (2011). Sudden unexpected death in epilepsy. *Lancet*, *378*(9808), 2028–38. https://doi.org/10.1016/S0140-6736(11)60176-1

So, E. L., **Sam, M. C.**, & **Lagerlund, T. L.** (2000). Postictal central apnea as a cause of SUDEP: evidence from near-SUDEP incident. *Epilepsia*, *41*(11), 1494–1497. https://doi.org/10.1111/j.1528-1157.2000.tb00128.x

Surges, R., **Adjei, P.**, **Kallis, C.**, **Erhuero, J.**, **Scott, C. A.**, **Bell, G. S.**, … **Walker, M. C.** (2010). Pathologic cardiac repolarization in pharmacoresistant epilepsy and its potential role in sudden unexpected death in epilepsy: A case-control study. *Epilepsia*, *51*(2), 233–242. https://doi.org/10.1111/j.1528-1167.2009.02330.x

Surges, R., **Henneberger, C.**, **Adjei, P.**, **Scott, C. A.**, **Sander, J. W.**, & **Walker, M. C.** (2009). Do alterations in inter-ictal heart rate variability predict sudden unexpected death in epilepsy? *Epilepsy Research*, *87*. https://doi.org/10.1016/j.eplepsyres.2009.08.008

Surges, R., & **Sander, J. W.** (2012). Sudden unexpected death in epilepsy: mechanisms, prevalence, and prevention. *Current Opinion in Neurology*, *25*(2), 201–7. https://doi.org/10.1097/WCO.0b013e3283506714

Tao, J. X., **Qian, S.**, **Baldwin, M.**, **Chen, X. J.**, **Rose, S.**, **Ebersole, S. H.**, & **Ebersole, J. S.** (2010). SUDEP, suspected positional airway obstruction, and hypoventilation in postictal coma. *Epilepsia*, *51*(11), 2344–2347. https://doi.org/10.1111/j.1528-1167.2010.02719.x

Tecott, L., **Sun, L.**, **Akana, S.**, **Stract, A.**, **Lowenstein, D.**, **Dallman, M.**, & **Julius, D.** (1995). Eating disorder and epilepsy in mice lacking 5-HT2c serotonin receptors. *Nature*, *374*(6), 542–546.

Tedeschi, D. H., **Swinyard, E. A.**, & **Goodman, L. S.** (1956). EFFECTS OF VARIATIONS IN STIMULUS INTENSITY ON MAXIMAL ELECTROSHOCK SEIZURE PATTERN, RECOVERY TIME, AND ANTICONVULSANT POTENCY OF PHENOBARBITAL IN MICE. *JPET*, *116*(1), 107–113.

Téllez-Zenteno, J. F., **Hernández Ronquillo, L.**, & **Wiebe, S.** (2005). Sudden unexpected death in epilepsy: Evidence-based analysis of incidence and risk factors. *Epilepsy Research*, *65*(65), 101–115. https://doi.org/10.1016/j.eplepsyres.2005.05.004

Tiron, C., **Campuzano, O.**, **Pé Rez-Serra, A.**, **Mademont, I.**, **Coll, M.**, **Allegue, C.**, … **Brugada, R.** (2015). Further evidence of the association between LQT syndrome and epilepsy in a family with KCNQ1 pathogenic variant. *Seizure: European Journal of Epilepsy*, *25*, 65–67. https://doi.org/10.1016/j.seizure.2015.01.003

Toman, J. E. P., **Swinyard, E. A.**, & **Goodman, L. S.** (1946). PROPERTIES OF MAXIMAL SEIZURES, AND THEIR ALTERATION BY ANTICONVULSANT DRUGS AND OTHER AGENTS. *J Neurophysiol*, *9*(3), 231–239.

Tomson, T., **Nashef, L.**, & **Ryvlin, P.** (2008). Sudden unexpected death in epilepsy: current knowledge and future directions. *The Lancet. Neurology*, *7*(11), 1021–31. https://doi.org/10.1016/S1474-4422(08)70202-3

Van Der Lende, M., **Surges, R.**, **Sander, J. W.**, & **Thijs, R. D.** (2016). Cardiac arrhythmias during or after epileptic seizures. *J Neurol Neurosurg Psychiatry*, *87*, 69–74. https://doi.org/10.1136/jnnp-2015-310559

van Luijtelaar, G., **Onat, F. Y.**, & **Gallagher, M. J.** (2014). Animal models of absence epilepsies: What do they model and do sex and sex hormones matter? *Neurobiology of Disease*, *72*(PB), 167–179. https://doi.org/10.1016/j.nbd.2014.08.014

Wadhwa, N., **Rubinstein, M.**, **Durand, F.**, & **Freeman, W. T.** (2013). Phase-based video motion processing. *ACM Transactions on Graphics*, *32*(4), 1. https://doi.org/10.1145/2461912.2461966

Wagnon, J. L., & **Meisler, M. H.** (2015). Recurrent and Non-Recurrent Mutations of SCN8A in Epileptic Encephalopathy. *Frontiers in Neurology*, *6*(May), 104. https://doi.org/10.3389/fneur.2015.00104

Walczak, T. S., **Leppik, I. E.**, **D'amelio, M.**, **Rarick, J.**, **So, E.**, **Ahman, P.**, … **Hauser, W. A.** (2001). Incidence and risk factors in sudden unexpected death in epilepsy. *Neurology*, *56*(4), 519.

Zhan, Q., **Buchanan, G. F.**, **Motelow, J. E.**, **Andrews, J.**, **Vitkovskiy, P.**, **Chen, W. C.**, … **Blumenfeld, H.** (2016). Impaired Serotonergic Brainstem Function during and after Seizures. *Journal of Neuroscience*, *36*(9), 2711–2722. https://doi.org/10.1523/JNEUROSCI.4331-15.2016

Zhao, Z.-Q., **Scott, M.**, **Chiechio, S.**, **Wang, J.-S.**, **Renner, K. J.**, **Gereau, R. W.**, … **Chen, Z.-F.** (2006). Lmx1b is required for maintenance of central serotonergic neurons and mice lacking central serotonergic system exhibit normal locomotor activity. *The Journal of Neuroscience : The Official Journal of the Society for Neuroscience*, *26*(49), 12781–8. https://doi.org/10.1523/JNEUROSCI.4143-06.2006